4410-77-X

Report of VESIAC

WASHINGTON CONFERENCE PROCEEDINGS: A REVIEW OF BROADBAND SEISMOGRAPHS TO INCLUDE DIGITAL SEISMOGRAPHS

Edited by
VESIAC Staff

October 1964

NOTICES

Sponsorship. The work reported herein was conducted by the Institute of Science and Technology for the Advanced Research Projects Agency of the Office of the Secretary of Defense under Contract SD-78. Contracts and grants to The University of Michigan for the support of sponsored research by the Institute of Science and Technology are administered through the Office of the Vice-President for Research.

DDC Availability. Qualified requesters may obtain copies of this document from:

> Defense Documentation Center
> Cameron Station
> Alexandria, Virginia

Final Disposition. After this document has served its purpose, it may be destroyed. Please do not return it to the Institute of Science and Technology.

PREFACE

VESIAC, the VELA Seismic Information Analysis Center, is an information collection, analysis, and dissemination facility established at the Institute of Science and Technology of The University of Michigan. The contract is sponsored by the Advanced Research Projects Agency under the Office of the Secretary of Defense.

The purpose of VESIAC is to analyze the research information related to the VELA UNIFORM Program of Project VELA and to function as a central facility for this information. The facility will serve all authorized recipients of VELA UNIFORM research information by issuing subject bibliographies with abstracts and special reports as required. In addition, VESIAC will periodically summarize the progress of the research being conducted.

VESIAC is under the technical direction of the Acoustics and Seismics Laboratory of the Institute. In its operation VESIAC draws upon members of this laboratory and other members of the Institute and University.

CONTENTS

FIGURES

LIST OF ATTENDEES

Dr. S. T. Algermissen	USC & GS
Mr. G. H. Ashley	MIT (Lincoln Obs.)
Dr. C. Bates	ARPA
Lt. Col. W. J. Best, USAF	AFOSR
Mr. R. A. Black	ARPA
Dr. H. Bradner	University of California, San Diego
Mr. C. F. Brown	Southern Methodist University
Mr. T. W. Caless	VESIAC
Mr. D. Clements	ARPA
Mr. J. L. Collins	University of Texas (Defense Research Lab.)
Mr. F. A. Crowley	AFCRL
Dr. W. C. Dean	United ElectroDynamics — DATDC
Dr. J. Cl. De Bremaecker	Rice University
Mr. D. W. Evertson	University of Texas (Defense Research Lab.)
Mr. R. A. Fojek	ARPA
Dr. R. A. Frosch	ARPA
Mr. G. A. Gray, Jr.	Geotechnical Corp.
Mr. J. H. Hamilton	Geotechnical Corp.
Dr. R. A. Haubrich	University of California, San Diego
Dr. E. Herrin	Southern Methodist University
Capt. C. Houston, USAF	AFTAC
Mr. D. P. Johnson	NBS
Mr. J. N Jordan	USC & GS
Dr. S. Kaufman	Shell Development Co.
Dr. E. J. Kelly	MIT (Lincoln Obs.)
Mr. P. S. Klasky	United ElectroDynamics
Mr. H. Lake	Texas Instruments
Maj. H. W. Leaf, USAF	AFOSR
Mr. R. W. Leeder	VESIAC
Mr. R. H. Mansfield	AFTAC
Mr. H. Matheson	NBS
Mr. R. F. McMurray	Geotechnical Corp.
Maj. R. A. Meek, USAF	AFTAC
Mr. Ben S. Melton	AFTAC

Mr. H. R. Myers	ACDA
Mr. J. A. Pfluke	United ElectroDynamics
Mr. S. W. Smith	California Inst. of Tech.
Dr. L. Strickland	Texas Instruments
Dr. L. Van Hemelrick	Lamont Geological Obs.

ABSTRACT

This report publishes a collection of papers presented at a VESIAC Special Study Conference, held 18-19 November 1963, on recent developments in wideband seismic recording. Emphasis is placed on advances in digital recording and problems related to digital recording systems. A related report is included on a pressure-sensitive transducer, known as the "Solion Transducer," applicable to hydroacoustic sensing.

A LUNAR LONG-PERIOD SEISMOMETER AND A LASER-TRANSDUCER SEISMOMETER

L. Van Hemelrick
Lamont Geological Observatory

Seismic instruments whose responses permit measurement of long-period components of earth motion have been and are under development at Lamont Geological Observatory. The two instruments described more particularly hereafter are:

(a) the lunar 4-component seismometer

(b) a laser-transducer seismometer

LUNAR SEISMOMETER

The lunar seismometer (Figure 1-1) has been tested and operated under earth's gravitational field, with a response different from what would be achieved in lunar gravity. The instrument, designed for operation on earth, has been built and will be used for observations on the ocean bottom. In brief, the system consists of the following:

(a) A 3-component, long-period seismometer, with free resonant period of 15 seconds, equipped with displacement transducers (capacitance type) and associated amplifiers having maximum sensitivity of 25-v/μ ground displacement amplitude

(b) A short-period vertical seismometer with free resonant period of 1.3 seconds and equipped with a velocity transducer

(c) A servosystem consisting of two-axis, gimbal, motor-drive circuitry and level sensors, for leveling the 3-component system to within 10 seconds of vertical

(d) A servosystem for recentering of the long-period vertical component

(e) A feedback control circuit to maintain central alignment of the long-period seismometers. Gravity and tilt information is provided by the feedback signal required for recentering.

(f) A calibration system consisting of an accurate current source which is applied to the coil of each component on command

(g) A temperature sensory mounted in the instrument base-plate

The three long-period instruments are similar in design to standard seismometers and together form a matched set, i.e., two horizontal components and one vertical component mounted orthogonally, with uniform natural periods (15 seconds), magnifications, damping, and inertial reactor masses (1.5 kg). The long-period vertical incorporates a LaCoste suspension, modified to permit adjustable passive compensation for changes in period and center position,
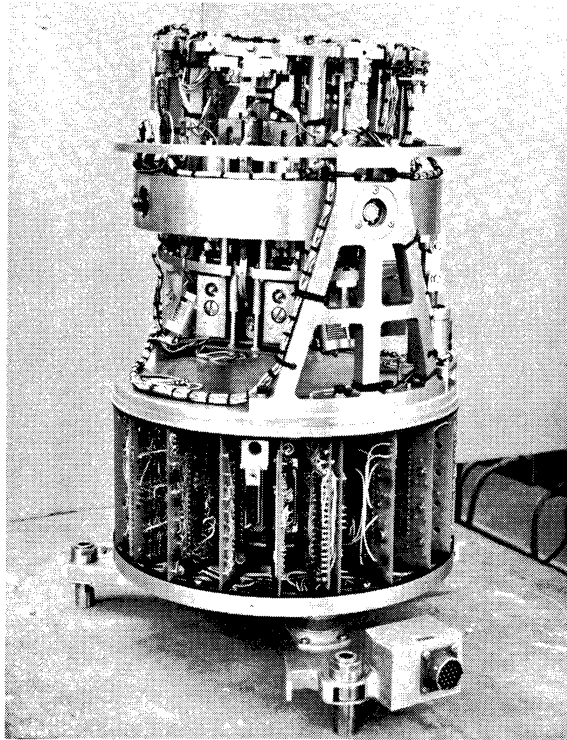
FIGURE 1-1. THE LUNAR SEISMOMETER

which result from the effects of temperature variations. The horizontal instruments are of the swinging gate type, modified to improve their cageability.

Each long-period component is equipped with a differential capacitance transducer and coil-magnet assembly. The coil-magnet assembly serves three purposes:

(a) To provide damping

(b) To provide a motor force by application of feedback current for fine centering of each seismic mass

(c) To transmit a calibration impulse to each seismic mass

In the lunar seismometer, the seismic masses are sectioned so that 5/6 of the mass can be removed for evaluation of parameters essential for accurate prediction of operational characteristics in the lunar environment.

A short-period vertical seismometer (natural period 1.3 seconds), equipped with a coil-magnet transducer, is included. It is adapted to the earth's gravity field by an auxiliary spring which supports 5/6 of the earth weight of the seismic mass, thus permitting prediction of lunar operational characteristics.

The three long-period components are mounted in a gimbaled support frame which is motor driven about two axes parallel to the horizontal seismometers. The gimbal provides leveling resolution of two seconds of arc over a 15° span. The short-period seismometer is contained within a 4- × 4-inch cylinder. The doughnut-shaped space surrounding the short-period component houses the electronics. The electronic circuits are laid out on 20 plug-in modules which are inserted radially into the previously defined space.

The operational values for the important system parameters are as follows:

$$T_o = 15 \text{ seconds}$$

$$T'_o = 1.3 \text{ seconds}$$

$$\beta = 0.7$$

$$F = 50$$

$$M = 1500 \text{ gm}$$

$$M' = 1648 \text{ gm}$$

$$T_f = 2305 \text{ seconds}$$

where T_o = free resonant period of the long-period seismometers

T'_o = free resonant period of the short-period seismometer

β = fraction of critical damping

F = feedback factor, defined as the open-loop boom displacement divided by closed-loop displacement

M = inertial mass of long-period seismometers

M' = inertial mass of short-period seismometers

T_f = corner period of lowpass feedback filter

In the lunar seismograph the hinges are designed to provide a K sufficiently large to supply approximately all of the restoring torque required to obtain the operating period. This is a compromise between the somewhat conflicting requirements of mechanical ruggedness and stability of the operating period. The operating period of a given instrument is obtained by adjusting the hinge tilt angle until the desired period is observed. In order to adjust the long-period instruments for lunar operation at $T_o = 15$ seconds we removed 5/6 of the inertial mass and adjusted the period to $15/\sqrt{6}$ seconds = 6.2 seconds.

The two long-period horizontal seismometers shown in Figure 1-2 ($T_o = 15$ seconds) are oriented parallel to the gimbal axes, permitting relatively independent centering of these components. They are, of course, considerably smaller than standard seismometers. A flat
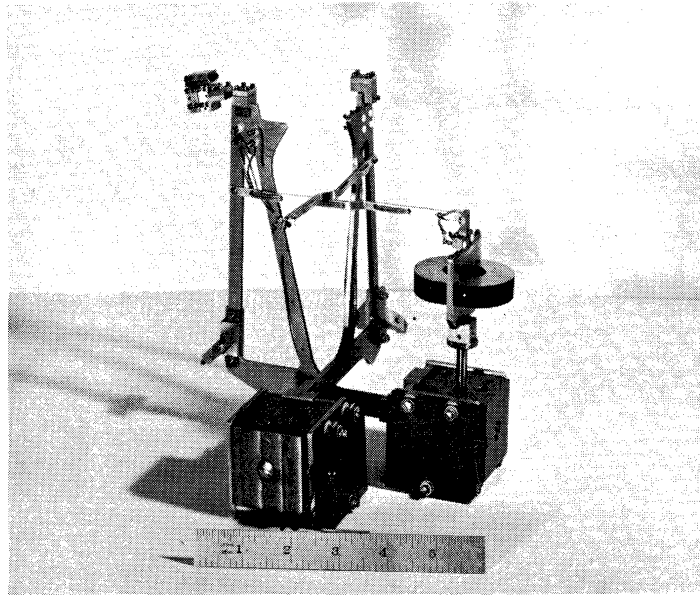
FIGURE 1-2. THE TWO LONG-PERIOD HORIZONTAL SEISMOM-
ETERS

horizontal hinge (0.005 inches thick) is incorporated between the upper hinge and the boom. This

hinge permits the caging system to shift the boom position without applying dangerous shear loads

to the upper hinge. In addition, the horizontal hinge link permits the redistribution of loads

resulting from the difference between earth and lunar gravity fields without introduction of

shear loads of sufficient magnitude to cause buckling at the hinges and consequent nonlinearities

in the seismometer response. The boom end of the lower hinge is attached to a lightweight fix-

ture which is connected to the boom assembly through two small, jeweled pivots. The caging opera-

tion disengages the pivots, permitting the boom to be rigidly held and the hinge unloaded. During

uncaging, the pivots drop into the jewels, and the pivot set behaves as a rigid joint. The tungsten

alloy mass is screwed to an aluminum frame at the outer end of the boom, and is removable for

simulation of lunar-operational load conditions. The choice of tungsten for the mass material

is based on its high density and low magnetic permeability. The two moving capacitor plates are

attached to the mass frame. The fixed capacitor plate is mounted directly on the lower support

plate. Period adjustments for both horizontal components are incorporated into the upper

support-frame plate. Adjustment is made by moving the fixed upper hinge clamp relative to

the upper support-frame plate.

LONG-PERIOD VERTICAL COMPONENT. The long-period vertical seismometer shown in

Figure 1-3 (T_0 = 15 seconds) is a modified LaCoste suspension. A technique has been devised

4
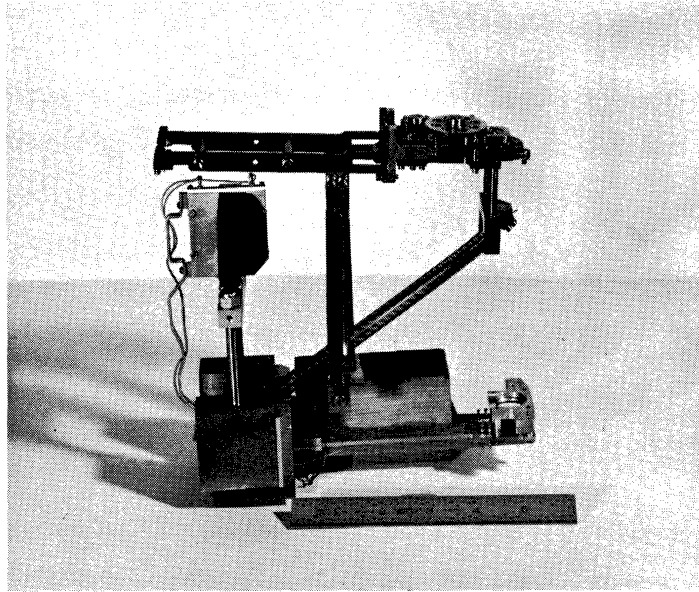
FIGURE 1-3. THE LONG-PERIOD VERTICAL SEISMOMETER

to incorporate compensation for the effect of temperature variation on both period and center position into the basic structure. This technique makes use of the relative differential expansion between invar and aluminum members to compensate for drift and period changes attributable to spring variations and differential expansion of structural members.

The inertial mass, as in the case of the horizontal components, is sectioned to permit removal of 5/6 of the mass for instrument testing. The mass is suspended by a zero length iso-elastic spring. The spring is 1 cm in diameter, with a spring constant of approximately 0.1 lb/in. and a stressed length of 8.5 inches. The fixed capacitor plate is located below the seismic mass, and is supported from the lower support-frame plate by four aluminum shafts. The two moving plates are fixed to the mass frame on the boom. The magnetic circuit consists of a pair of horseshoe magnets pole-to-pole, with a 0.2-inch gap between pole faces. The flux density is approximately 4500 G. The damping and feedback coil, enclosed in an aluminum jacket, is attached to the mass by a structure that also serves as a caging support. Manual period adjustment is provided.

GIMBAL LEVELING SYSTEM. The instrument support frame is trunion-mounted to the central structural plate through a two-axis gimbal. The gimbal is driven about axes parallel to the long-period horizontal components over a range of $\pm 15^\circ$. The leveling drives are geared stepper motors with ratios of approximately 162000:1, providing discrete leveling steps of two seconds of arc.

5

A feedback-controlled seismograph (vertical component) is shown schematically in Figure 1-4. A voltage proportional to the displacement of the seismic mass from its center position is generated by means of the differential capacitor plate assembly and associated circuitry. This signal is amplified, filtered (highpass, 60-second corner), and amplified again to give the direct seismic output.

ANALYSIS OF OPERATION. It is well known that the elastic suspension of a long-period seismograph is subject to long-term drift. Such drift may be ascribed to a combination of the following causes:

(a) Thermal effects: change in spring constants and dimensions of the structural elements with temperature

(b) Mechanical fatigue or creep: inelastic deformation of structural elements with time

(c) Barometric pressure: in general, a change in density of the medium in which the seismograph is immersed

(d) Gravitational effects: changes in zero position of the seismic mass in response to

(1) variations in slope of the local surface caused by passage of the solid tide (affects the horizontal components), and

(2) variations in the magnitude of the vertical component of gravity (affects the vertical component)

Compensation for drift must be provided if the instrument is to remain centered within its operating range for long periods of time. Partial compensation for thermal and barometric variations can be provided by mechanical means. In the present system, residual drift is compensated by feedback control. A portion of the output signal is fed back, through a lowpass filter, to the coil of the coil-magnet assembly that also provides the damping for the seismograph. This way the instrument is held centered to some fraction of its open-loop displacement. We have in effect a force-balance system for long-period signals. If drift proceeds to such an extent that feedback current is no longer able to hold the mass centered within tolerable limits, mechanical recentering is required.

A signal proportional to a long-period acceleration input is available at the point labeled "feedback output" in Figure 1-4. Hence, tidal tilts and changes in the magnitude of the vertical component of gravity can be measured by monitoring this signal under the assumptions that

(a) long-term disturbances resulting from other causes can be minimized, and

(b) tide information can be sorted out from the remaining spurious signal.

6
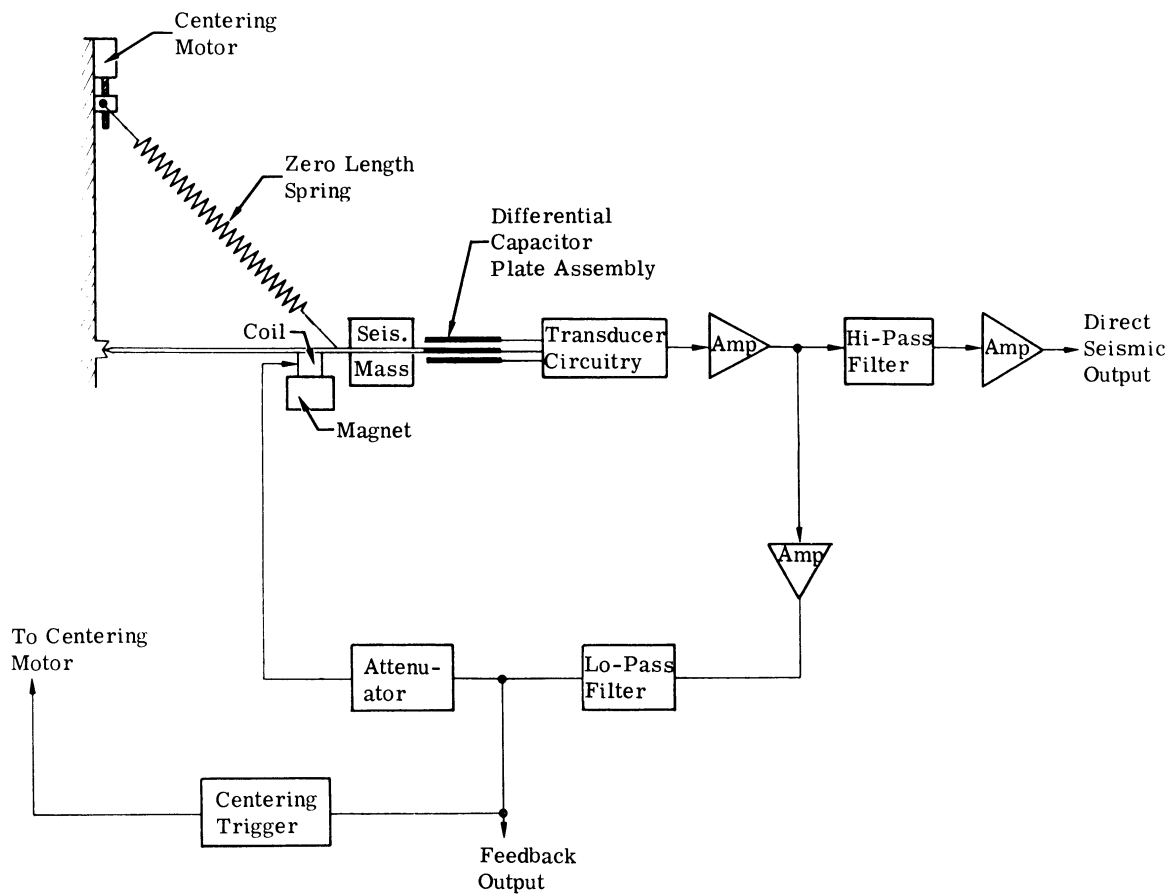
FIGURE 1-4. SCHEMATIC DIAGRAM OF A FEEDBACK-CONTROLLED SEISMOGRAPH (VERTICAL COM-
PONENT)

A theoretical analysis of the feedback-controlled seismograph will be presented next (cf.
Figure 1-5) [1]. For $\omega \ll \omega_{f_2} \ll \omega_0$

$$\left| \frac{V_1}{Y}(j\omega) \right| = K_1 \omega^2/\omega_0^2 + K \qquad (1\text{-}1)$$

$$\left| \frac{V_f}{Y}(j\omega) \right| = K_1 K_2 \omega^2/\omega_0^2 + K \qquad (1\text{-}2)$$

where

$$K = K_1 K_2 K_3 K_4$$

V_0 is zero for very long-period signals because of the highpass output filter F_1.
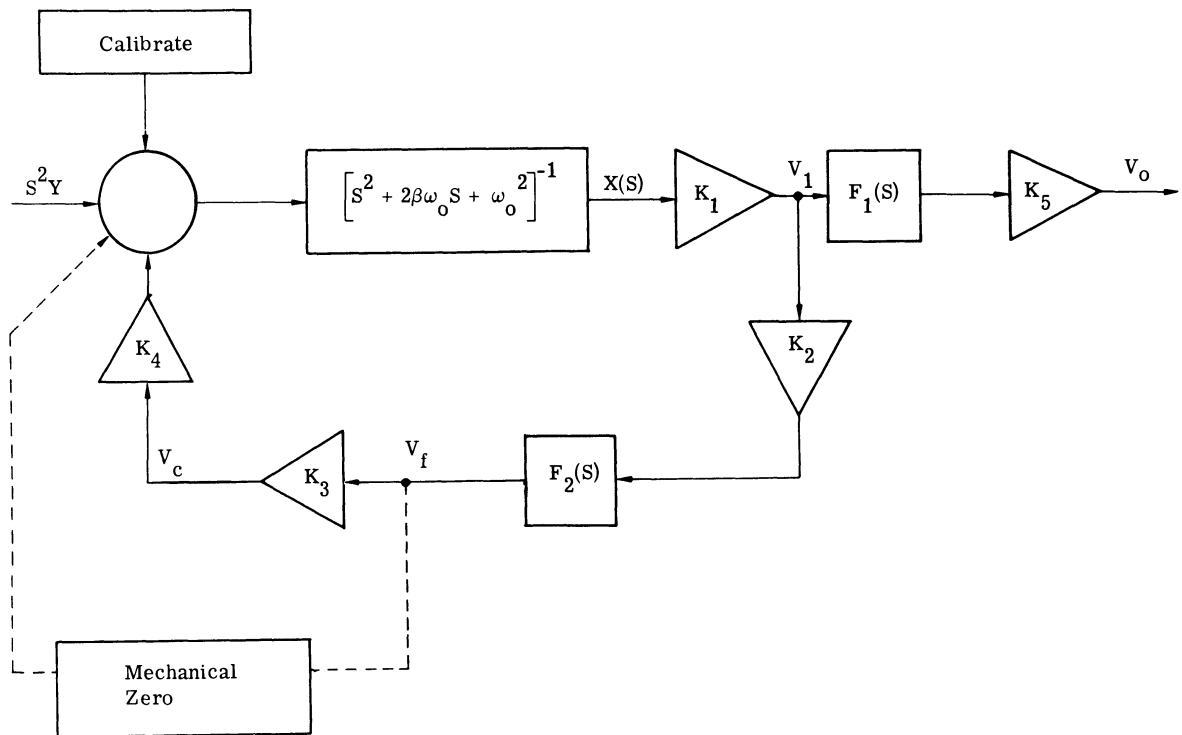
FIGURE 1-5. SCHEMATIC DIAGRAM FOR THE THEORETICAL ANALYSIS OF THE FEEDBACK-CON-
TROLLED SEISMOGRAPH

Acceleration sensitivity, for very long-period signals, can be seen from Equation 1-1
and 1-2 to be

$$\left| \frac{V_1}{\ddot{Y}} (j\omega) \right| = K_1 / \omega_o^2 + K \approx 1/K_2 K_3 K_4 \qquad (1\text{-}3)$$

$$\left| \frac{V_f}{\ddot{Y}} (j\omega) \right| = K_1 K_2 / \omega_o^2 + K \approx 1/K_3 K_4 \qquad (1\text{-}4)$$

for $K \gg \omega_o^2$. Since $V_1 = K_1 X$, we have, from Equation 1-3,

$$\left| \frac{X}{\ddot{Y}} (j\omega) \right| = 1/\omega_o^2 + K \approx 1/K \qquad (1\text{-}5)$$

Since a slowly varying tilt or, in the limit, a constant tilt produces an additional acceleration
on a seismometer, Equation 1-5 represents the displacement of the seismic mass resulting
from a tilt where

$$\ddot{Y} = g\psi$$

8

and $g\psi$ is the gravitational component along the sensitive axis of the seismometer. From Equation 1-5

$$\left| \frac{X}{M\ddot{Y}}(j\omega) \right| = 1/(\omega_0^2 + K)M \tag{1-6}$$

The displacement of the seismic mass, from some initial equilibrium position, caused by an additional force f acting along the sensitive direction of the seismometer is given by

$$X = f/(\omega_0^2 + K)M \tag{1-7}$$

It can be shown [1] that the equivalent expression for a seismometer without feedback is

$$X' = f/\omega_0^2 M \tag{1-8}$$

We define the centering factor F as the ratio of mass displacement with no feedback X' to mass displacement with feedback X (hereafter referred to as open-loop displacement and closed-loop displacement, respectively) caused by some constant off-centering force f. Then, by Equations 1-7 and 1-8, we have

$$F = X'/X = \omega_0^2 + K/\omega_0^2 = 1 + K/\omega_0^2 \tag{1-9}$$

or

$$K = (F - 1)\omega_0^2 \tag{1-10}$$

Thus, by use of degenerative feedback through a lowpass filter, we maintain the seismic mass centered against drift by some factor F which depends upon the loop gain K and the natural period.

It can also be shown [1] that to avoid peaks in the response curve, two conditions must be satisfied:

(a) The damping factor β of the pendulum must be 0.707 or higher

(b) $A_{max} = \dfrac{4\beta + \sqrt{12\beta^2 - 6}}{4\beta^2 + 6}$

$$\tag{1-11}$$

where $A = K\dfrac{\omega_f}{\omega_0}$. For a given β, the maximum value of A for which no peaking will occur in the real frequency domain is determined by Equation 1-11. Assume, for example, $\beta = 0.707$, then the maximum permissible value for A is 0.35. The magnification curves for both direct seismic output and feedback are plotted in Figure 1-6, for A = 0.35, the centering factor F = 15.7,
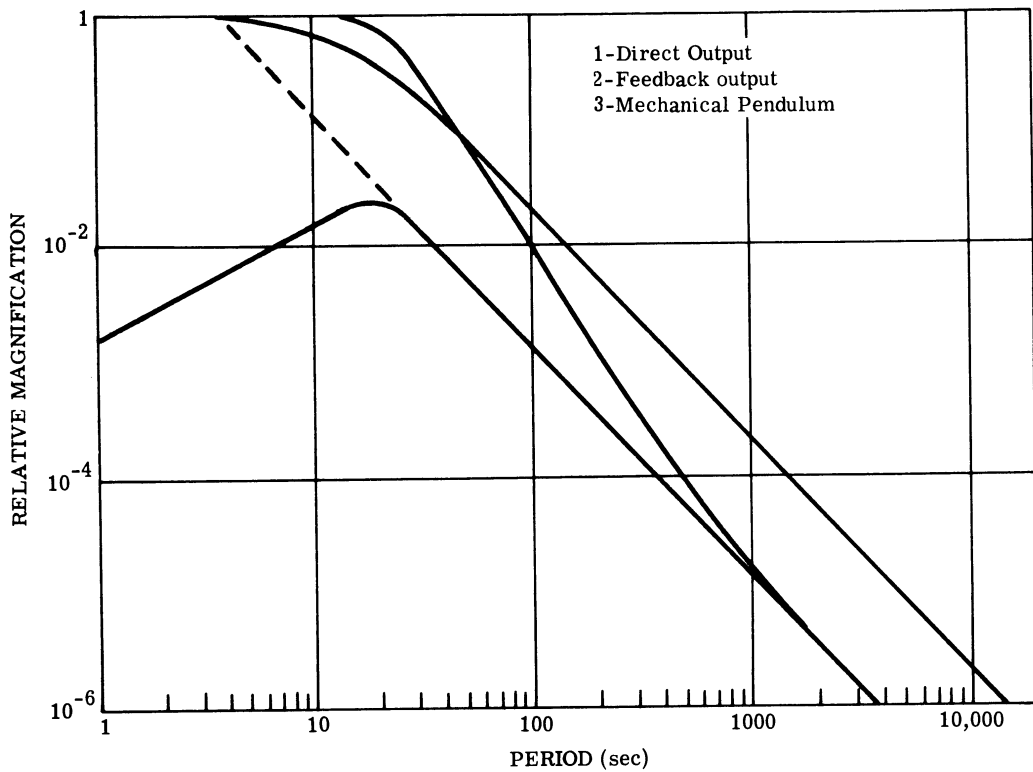
FIGURE 1-6. MAGNIFICATION CURVES FOR DIRECT SEISMIC OUTPUT AND FEEDBACK, AND FOR A MECHANICAL PENDULUM WITHOUT FEEDBACK

$K_2 = 1$, and the filter corner $T_f = 628$ seconds. The response for a simple mechanical pendulum without feedback is shown for comparison. No peaking is observed for this value of A. In Figure 1-6, it should be noted particularly that a line extended through the long-period end of the direct output (dotted line) intersects the short-period end of the curve at $T = 3.8$ seconds. Thus, for long-period signals the instrument behaves as if it were a short-period pendulum.

An accurate method of determining the correct value for $K_3 K_4$ is by direct measurement of this period. The free resonant angular frequency without a lowpass filter in the feedback loop ω'_o is related to the free resonant angular frequency with the filter present by

$$\omega'_o{}^2 = \omega_o{}^2 + K$$

$$\frac{\omega'_o{}^2}{\omega_o{}^2} = 1 + K/\omega_o{}^2 = F$$

$$F = \left(T_o/T_o'\right)^2 \tag{1-12}$$

10

When the free resonant period T_o has been measured, the lowpass filter is removed from the loop and replaced by an equivalent series resistance. If an RC filter is used, removing the capacitor is all that is required. A potentiometer is then placed in the loop and adjusted until the measured period T'_o satisfies Equation 1-12 for the desired value of F. With a free resonant period of 15 seconds, the seismometer is equivalent to a very sensitive galvanometer. Noise generated by the filter within the instrument passband will displace the boom, and cannot be separated from the signal because of ground motion. One has to be careful to keep the feedback circuit noise free if the ultimate sensitivity has to be maintained.

The overall sensitivity of the lunar instrument on maximum gain settings is 25 v/μ. The capacitance transducer has been tested separately because when it is part of a seismic mass, even if it is clamped down, it exhibits a noise level caused by mechanical vibration. The output noise of the transducer alone on maximum gain settings is of the order of 8 mv, and a 1 mμ peak-to-peak displacement input will produce an easily detectable signal. The total linear span of operation is ± 10 μ on low gain, but is limited to ± 0.1 μ on maximum gain by saturation of the final amplifier stages.

The instruments that are derived from this seismometer and used for each operation do not necessarily display the same frequency response characteristics. The response can be modified easily by changing some circuit parameters. The sensitivities required are lower. In the present ocean bottom instrument, the total maximum gain has been reduced by a factor of ten to 2.5 v/μ, and, simultaneously, the linear span has been increased to ± 100 μ. The minimum detectable signal is less than 10 m/μ. The feedback loop output V_f has the same tilt sensitivity and the same total tilt range for both the lunar and the ocean bottom instruments. This total range is ± 10 seconds of arc, or $\pm 50 \times 10^{-6}$ rad, and the sensitivity is 250 mv/sec, or 50 mv for an inclination of 1 part in 10^{-6}. This corresponds to a sensitivity of 50 mv/mgal for the ocean bottom instrument, and to 300 mv/mgal for the lunar seismometer. Earth tide signals of about 0.2-mgal peak-to-peak amplitude, corresponding to 10-mv output, have been recorded successfully by using this circuitry in combination with a pair of conventional long-period horizontal instruments.

Instrument drifts not related to the circuitry but inherent in the mechanical structure of the seismometers are determining the lowest usable signal at present. This is especially true for the vertical instrument. The long-period vertical component is inherently more sensitive to temperature variations than either of the horizontal seismometers or the short-period seismometer. Consequently, study of the thermal characteristics of this component has been emphasized. The long-period vertical shows nonlinear period and center position variations with temperature. The center position of the seismic mass can be adjusted by a vertical motion

of the upper hinge point; the period can be adjusted by a horizontal motion of the upper hinge. Compensation for the variation of center position is provided by the relative thermal expansion of the two vertical members which, by a lever action, produces a vertical motion of the upper hinge. The horizontal motion required for period compensation is provided by the thermal expansion of the upper horizontal member relative to the base.

A model of the prototype long-period vertical has been constructed and placed in an environmental chamber for study. The instrument has been subjected to temperature variations from -20°C to 100°C. Suitable time was provided for stabilizing at each temperature, and the mass was restored to the center of its operating range by feeding d-c current to the damping-feedback coil. The center position and period were observed, and the current and period were noted at each temperature. If the current required for centering the boom is plotted versus temperature, the curves in Figure 1-7 are obtained. The location of the maximum of this curve can be varied by
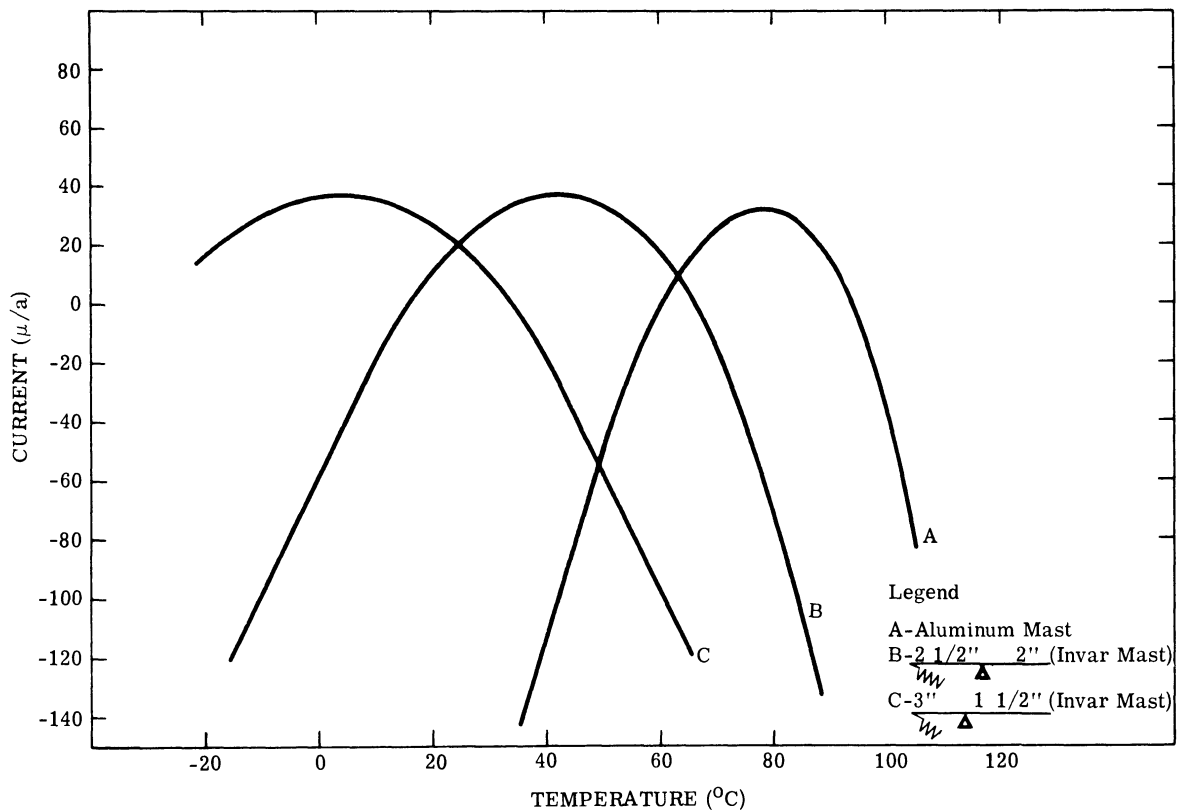
FIGURE 1-7. CURRENT REQUIRED FOR CENTERING VS. TEMPERATURE FOR THE PROTOTYPICAL
LONG-PERIOD VERTICAL COMPONENT

(a) changing the fulcrum position on the horizontal period-compensation bar, or

(b) changing the material used in the adjustable vertical column.

Both of these methods cause a change in the displacement of the upper hinge point, resulting from the relative expansion of the fixed vertical member and adjustable vertical column.

Since the current levels of the centering response curves represent variation in center position of the seismic mass, the region on any one curve where the current variation is a minimum with temperature gives optimum operation. An additional nonlinear effect of the thermal properties of the system causes the spread around the peak of the centering response curve to become narrower for increasing temperature. One particular combination, corresponding to an instrument with an isoelastic spring, mounted into an all-aluminum frame, shows that a zero temperature coefficient can be achieved around $80^{\circ}C$. Above this temperature, the seismic mass will drop with further increase of temperature instead of rising, as it does around ambient temperatures. For different combinations of the spring and frame materials, this zero coefficient can be achieved for other temperatures.

A second step in temperature compensation of a vertical long-period instrument is to compensate for variation of the temperature coefficient with temperature. A small vertical instrument equipped to do so is presently recording tides. These purely passive methods of reducing instrument drifts do not exclude the possibility or usefulness of accurate temperature control as achieved in gravimeters. In the case of the lunar seismometer, an active temperature control did not seem feasible on the basis of the power available.

LASER SEISMOMETER

As a project completely independent from the lunar long-period seismometer, which consists of a relatively small, self-centering instrument package lending itself to temporary installation in the field and long-term remote operation, Lamont Geological Observatory is also exploring the adaptation of laser transducer to observation of seismic motion. A pendulum and a strain seismometer, both with laser transducers, are being designed and constructed. These instruments are expected to have extreme sensitivity over wide period ranges and an extremely large dynamic range. An infrared laser used as a transducer should have a remarkable dynamic range of 10^7 or 140 db.

With this device it will be possible to use one instrument, either a strain or pendulum seismometer, to cover the entire period range of seismic events, from 0.1 second or shorter to earth tidal periods of 40,000 seconds or longer. The output from the transducer will be a varying frequency in the VHF range, linearly proportional to displacement. This type of output

is very convenient for digitization, which will probably be necessary to utilize the large dynamic range of the output signal. The high sensitivity of the laser transducer makes it possible to use a short-period pendulum over the entire period range. The problem of obtaining long-period information is thus reduced to building a good mechanical short-period pendulum rather than the more difficult task of constructing a long-period instrument. Except at the longest periods, the sensitivity of this seismograph would be limited by the thermal noise of the pendulum rather than by the sensitivity of the laser. Laser oscillators at microwave frequencies are characterized by extremely monochromatic radiation.

It is impractical to build standard resonant cavities at infrared frequencies as is done at microwave frequencies. Therefore, multimode cavities are used. The cavity consists essentially of two reflecting plates separated by a distance D. The frequency difference $\delta\nu$ between these modes satisfies the Fabry-Perot condition

$$\delta\nu = \frac{C}{2D}$$

where C is the velocity of light, and D is the distance between the plates. Thus, for a D of one meter, the frequency interval between modes is 150 mc. The line widths of transitions in the infrared range are usually much greater than this, on the order of 1000 mc, so several cavity modes will lie within the resonance. By adjusting the excitation level, only one of these modes will exhibit laser action.

Ultimate frequency shifts in the laser-beam frequency of 1.5×10^{14} cps are expected to be of the order of a few tenths of 1 cps. The fractional change in the oscillation frequency is equal to the fractional change in the distance between the two plates, but directed oppositely. Now, $\delta\nu/\nu_{osc}$ should be measurable to one part in 10^{13} to 10^{14}. This means that with a one-meter laser, a shift of 10^{-4} mμ should be detectable. Presently existing seismograph displacement transducers can measure a shift of only about 10^{-1} mμ.

The actual method of measuring the frequency shift requires two lasers. One provides a reference signal; the second acts as the transducer. The infrared radiation from the two lasers is shown on the photosensitive surface of a photomultiplier tube which is a square-law detector. Thus, the beat frequency between the two lasers is obtained. Variations in the plate distance of the second laser cause a proportional variation in the beat frequency. It is possible to measure beat frequencies from 0 to 500 mc with existing photomultipliers. This places an upper limit on the displacement which the laser can measure. For lasers with D greater than about 20 cm, the value of $\delta\nu$ places a lower upper-limit than this on the displacement, for the frequency can be shifted by only about 1/3 the distance between cavity modes if the oscillation is to be con-

fined to one cavity mode. These considerations yield a dynamic range for the laser of about 10^7 or 140 db, and limit the total displacement to about 0.4 μ for a one-meter laser.

All that has been mentioned about using the infrared laser as a transducer is dependent upon its long-term stability. Instabilities are caused by mechanical noise and by thermal expansion. It is possible to separate visually the effect of mechanical noise from the effect of thermal expansion. Thermal expansion causes a slow drift of the beat note in one direction over a period of several minutes. Mechanical noise causes the beat note to jump back and forth very rapidly.

The lasers to be used would have one of their plates removed from the tube containing the gas. The pendulum seismograph envisaged would consist of a short-period pendulum with one cavity plate of a laser on top of the mass and one on the bottom (or one on either side for horizontal instruments). These plates would be separated from the remaining parts of the two lasers, one on each side of the mass. Rather than one laser being used as a standard as previously described, both lasers would be active and would operate as a push-pull combination. The symmetrical arrangement of the lasers would tend to cancel thermal expansion effects. The two outer fixed plates of the two lasers would be connected through the massive supporting frame. The entire instrument would be placed in a pressure controlled chamber which could be thermally regulated. The pendulum would have a short period because, as mentioned above, it is much easier to construct a rugged, stable, highly symmetrical short-period pendulum than a good mechanical long-period pendulum. It is also easy to remove the spurious resonances of short-period pendulums, but not of long-period pendulums.

If a laser transducer with the expected sensitivities and dynamic range is used to measure displacements of a 2 cps seismometer, the thermal noise of the instrument will be more important than the transducer noise by several orders of magnitude, except for periods longer than 10,000 seconds. At 1 cps the earth noise level at a quiet location is of the order of 1 A^0 (10^{-7} mm). At that frequency, the transducer will have a measuring span of up to 5×10^{-4}-mm equivalent earth motion. The most sensitive long-period instruments now available are peaked over a small period range somewhere between 30 and 100 seconds to detect a minimum earth motion of 3×10^{-5} mm. This laser seismograph would be more sensitive by almost an order of magnitude in this small range of periods, and would compare even more favorably than this over the entire range of 5 to 200 seconds usually covered by long-period seismographs. Still further, its response at periods greater than 200 seconds is orders of magnitude better than that of existing pendulum seismographs. The vertical instrument would react to earth tides as a gravimeter. The change in gravitational acceleration caused by the earth tides is equivalent to an oscillation of about 100 meters amplitude. This instrument would measure the principal earth tides to one part of 10^6.

To obtain most of these goals, it is not even required that the theoretical stability of the laser oscillation is achieved in the actual setup. Considering the tremendous period spreads and dynamic range of the output of these instruments, it would seem best to record the data digitally with a frequency counter, perhaps in combination with several analog outputs over more restricted frequency ranges.

RESULTS TO BE EXPECTED. With present seismographs, there exists a gap between 20 and 60 seconds where noise is not seen. Above 60 seconds there is background observed on special instruments, but whether it is real earth noise, effects of meteorological or other disturbances, or just instrumental noise is not known. The laser seismographs should be about two orders of magnitude more sensitive than existing seismographs for periods less than 60 seconds, and about one order more sensitive for periods slightly longer than 60 seconds. Therefore, it would seem likely that background can be reached in the period range 20 to 60 seconds and that it should be possible to determine the nature of the background above 60 seconds.

As pointed out earlier, one important part of this project will be to build a "perfect" short-period instrument. This can be defined as one in which the relative motion of the mass and the frame depends only on the absolute frame motion along the sensitive axis, and is not influenced by any other factor such as temperature, atmospheric pressure, magnetic fields, time, etc. Usually the different components of an instrument do not behave as "perfect" elements in the sense of performing only the function they are assigned to perform. The mass, for example, instead of reacting by inertia to acceleration only, may also be affected, because of its volume, by the atmospheric pressure, or, because of the magnetic properties of its material, by variations in the exterior magnetic field. Three approaches can be used to reduce the influence of parasitic signals:

(a) The perturbing factor can be minimized by selection of materials and mechanical design, or can be compensated for by a new element whose function is only to "correct" for an unwanted secondary reaction of another component. For example, atmospheric bouyancy of the mass can be reduced by selecting a dense material, or compensated for by an equivalent volume moving in a direction opposite to the mass.

(b) The unwanted reactions can be analyzed and measured, and the relationship between cause and effect found. Subsequent monitoring of the cause allows a parasitic effect to be eliminated from the instrument's output.

(c) The magnitude of perturbing factors can be reduced by, for example, temperature control, pressurization, and shielding.

16

For periods appreciably longer than the natural period, relative motion of the frame and the seismic mass is proportional to the acceleration applied to the frame, and inversely proportional to K, the stiffness of the suspension. In general the temperature coefficients of materials used in an instrument will affect the mass position, also being inversely proportional to the stiffness of the suspension. For similar mechanical structures, the ratio between seismic input and thermal drift is independent of the natural frequency of the pendulum, and this is also true of atmospheric buoyancy and magnetic fields. It can easily be shown that for similar configurations and identical spring materials, the spring weight in an instrument for a given period is inversely proportional to the square of the stress level. "Creep," or slow continuous deformation of a stressed member depends on stress level and on the previous stress history of the considered element. For that reason there probably exists an ideal stress level, different from o, that will provide a maximum stability versus time relation for the suspension.

The general outline for the laser-transducer, short-period seismometer is as follows: The suspension should be designed to minimize relative nonseismic motion of the frame and the mass along the sensitive axis by

(a) using low expansion-coefficient materials;

(b) orienting elements whose coefficient cannot be reduced so that the resultant motion is perpendicular to the sensitive axis;

(c) selecting and treating the spring material to obtain a small thermoelastic coefficient; and

(d) defining the temperature range where the temperature coefficients are smallest, and thermally controlling the instrument.

Operation in a partial vacuum will eliminate atmospheric pressure variations as a direct perturbing factor. Magnetic perturbations will be reduced by shielding, and variations of local magnetism will be monitored.

REFERENCE

1. G. H. Sutton and G. V. Latham, "Analysis of a Feedback Controlled Seismograph," to be published in J. Geophys. Res., Sept. 1964.

2
DYNAMIC RANGE OF BROADBAND SEISMOGRAPHS

Harry R. Lake
Texas Instruments, Inc.

Development of broadband seismograph systems is directed toward increasing the total information content of recorded seismic data. The development of narrowband systems with responses shaped to emphasize particular features of the earth's motion has received a larger portion of seismologists' attention in the past because it was necessary to analyze the data from a visual presentation. However, the advent of high-speed digital computers has made it possible to examine many aspects of the earth's motion and related phenomena that are not evident from a waveform presentation.

Reasons for the immediate need for broader-band seismograph systems are numerous. For instance, the total characteristics of ambient seismic noise can be made available for study and application to array processing if a seismograph system is used that allows wideband noise collection. In addition, broadband arrays will aid in deconvolving crustal effects of the earth by removing reverberations generated near the recording site. Cleaned-up signals would be used to develop deconvolution filters and allow a less complex signal to be observed for identification.

The use of seismic data in such studies makes it necessary to eventually convert the data to digital form for use in high-speed computers. The data can of course be recorded in FM format and later digitized at the convenience of the user. However, present FM systems, with their inherent difficulties such as limited dynamic range, drifting center frequencies, and distortion from wow and flutter, are not adequate to take full advantage of the advanced techniques offered by computer processing. It appears necessary, therefore, to directly digitize the data, with as few intermediate transfers as possible. Two schemes of direct digitization of broadband data have been considered, and advantages and disadvantages of each will be subsequently discussed.

Both displacement and velocity sensing have been considered for broadband recording. Figure 2-1 indicates the dynamic range necessary to record a wideband seismic signal with these two sensing modes. This figure presents the average ambient seismic noise amplitude spectrum published by Brune and Oliver in 1959 [1], with curves for displacement, velocity, and acceleration.
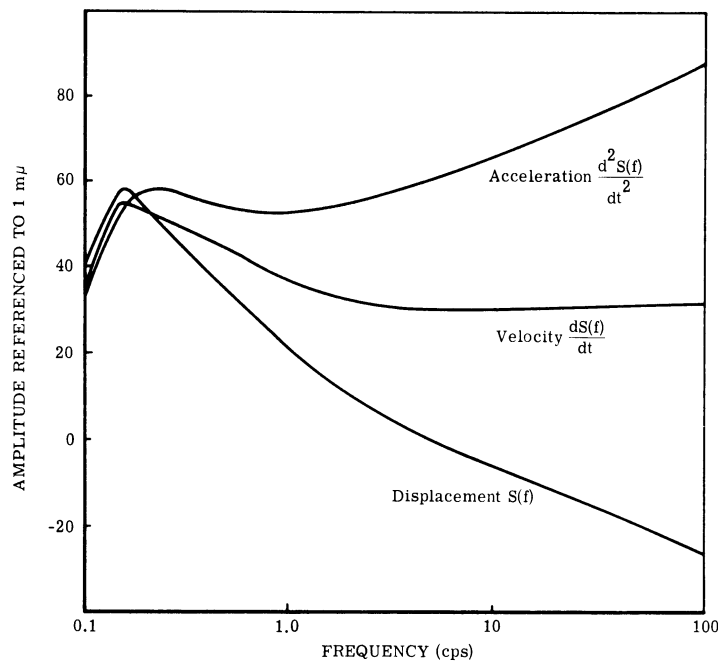
FIGURE 2-1. AVERAGE AMBIENT SEISMIC NOISE AMPLI-
TUDE SPECTRUM [1] REFERENCED TO DISPLACEMENT,
VELOCITY, AND ACCELERATION

If the bandwidth of interest is chosen as 0.1 to 10 cps, the displacement spectrum varies
on the order of 67 db, while the velocity is nearer white and varies only 26 db. Thus, without
further consideration of system response, it will take 41 db more dynamic range to record the
same noise with a displacement-sensing instrument than with one using velocity sensing.

In addition to the dynamic range necessary to simply cover the spectrum of interest, one
must also consider the range necessary to quantize the noise signal so that quantization noise
is negligible with respect to the ambient noise being recorded. Figure 2-2 presents a curve
published by Bennett in his paper on the effects of quantization noise [2]. His work indicated
that, for data having a white spectrum, 8 bits of quantization are sufficient to reduce the quan-
tization noise 42 db below the signal. Thus, in addition to the 67 or 26 db for covering the
spectrum indicated in Figure 2-1, about 40 to 50 db should be allowed for quantizing the smallest
component of interest. One must also consider the necessity of being able to record ambient
noise in the presence of a signal which may be as much as 100 times as large. Thus, the sys-
tem should include as much as 40 db for recording signals.

The dynamic range necessary to record a broadband signal with each of the two sensing
methods mentioned is shown in Figure 2-3. Again, without considering the instrument response,
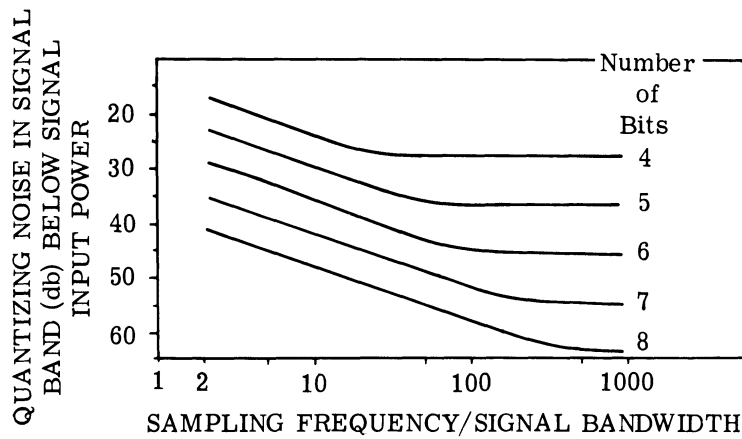
FIGURE 2-2. QUANTIZATION NOISE AS A FUNCTION OF BANDWIDTH
AND QUANTIZATION INTERVAL
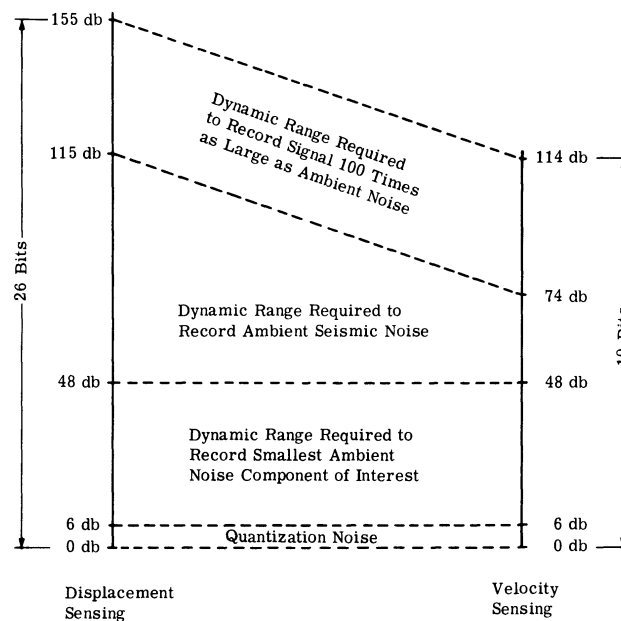
FIGURE 2-3. PARTITIONING OF THE DYNAMIC RANGE FOR DISPLACE-
MENT AND VELOCITY SENSING, RECORDING OVER A BANDWIDTH OF
0.1 TO 10.0 SECONDS

developing a wideband instrument that would record, over the range 0.1 to 10.0 cps, a large
signal and ambient noise simultaneously with sufficient quantization would require a displace-
ment instrument with dynamic range of the order of 155 db and a velocity instrument with one
of the order of 114 db. Clearly, it becomes impractical to record data utilizing these extreme

dynamic ranges and even more impractical to process such data. It would seem, therefore, that pre-whitening of data, by either analog filtering or proper choice of system response, is necessary to record seismic energy of this bandwidth properly.

Work undertaken with broadband seismographs has been done with two systems. The first was developed by Texas Instruments under contract from Air Force Cambridge Research Laboratory; the second was developed from off-the-shelf components. Under the contract administered by AFCRL, a directly digitizing broadband seismograph was developed according to the following specifications:

(a) Broadband recording from 0.1 to 10 cps with flat response to input displacement

(b) Constant resolution

(c) Non-galvometric transducing system

(d) Displacement sensing

(e) Dynamic range of 120 db (20 bits)

(f) Total recording range of 0.2 mμ to 200 μ

Displacement sensing was chosen in this case in order to record earth motion with as small a change as possible; also, this type of sensing offered a possible non-galvometric transducing system.

The choice of dynamic range, of course, was also influenced by the decision to record displacement. Since state-of-the-art analog-to-digital converters afford only on the order of 80- to 90-db dynamic range for constant resolution, an FM-to-digital scheme such as that most recently used by De Bremaecker et al. [3] was employed. This system, shown in Figure 2-4, consists of two oscillators connected to opposite sides of the seismometer boom. As the boom is displaced, air capacitors connected to either side of the boom change the capacitance in the tank circuits of the two oscillators. Boom displacement in one direction causes one oscillator to increase in frequency while the other decreases, and the frequency difference is then developed in the mixer and amplified to a usable level. The two oscillators have center frequencies of 420 and 441.8 Mc respectively; so when the boom is centered the difference in frequency is 21.8 Mc. As the boom moves $\pm 100 \mu$, frequencies of the two oscillators vary ± 10.9 Mc, and the difference in frequency varies from 0 to 43.6 Mc. From the mixer the signal is introduced into a frequency counter which counts for 24 milliseconds (less 4 μsec for readout into digital circuits). The theoretically least detectable boom motion in this system is then one cycle change per sampling period, and corresponds to 0.2 mμ. After counting for one sampling period is completed, counter contents are gated into a buffer which connects the binary word to the output. For the research evaluation of this seismometer, output was made
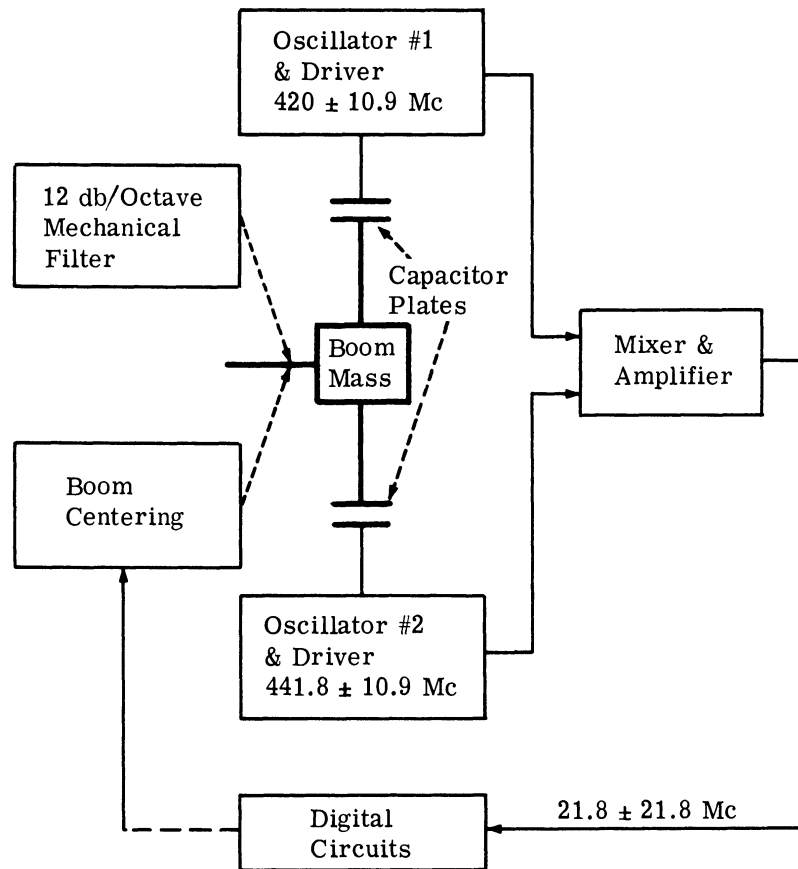
FIGURE 2-4. SYSTEM FOR DIRECTLY DIGITIZING DISPLACEMENT
SENSING DATA

compatible with that from one of Texas Instruments' special purpose computers. However, it
can also be made compatible with such machines as the IBM 7090 or CDC 1604.

A significant problem in designing a system of this type is the need for incorporating
aliasing filters. Unlike in conventional systems, filtering cannot be regarded as a separate
component after the seismometer since the seismometer transducer yields binary numbers.
Sampling theory shows that all energy at frequencies above one-half the sampling frequency
will be folded back into the Nyquist band of the system, as indicated in Figure 2-5. Therefore,
one would want, ideally, a filtering system that reduced the energy 120 db at frequencies above
20.8 cps. Such a filtering system is obviously impossible to design, but, since the displace-
ment spectrum drops off so rapidly at higher frequencies, one can get by with a much smaller
reduction. The present seismometer has two filters. First, there is a 6-db/octave filter for
the continuous counting during the sampling period. In addition, a mechanical spring dash-pot

23
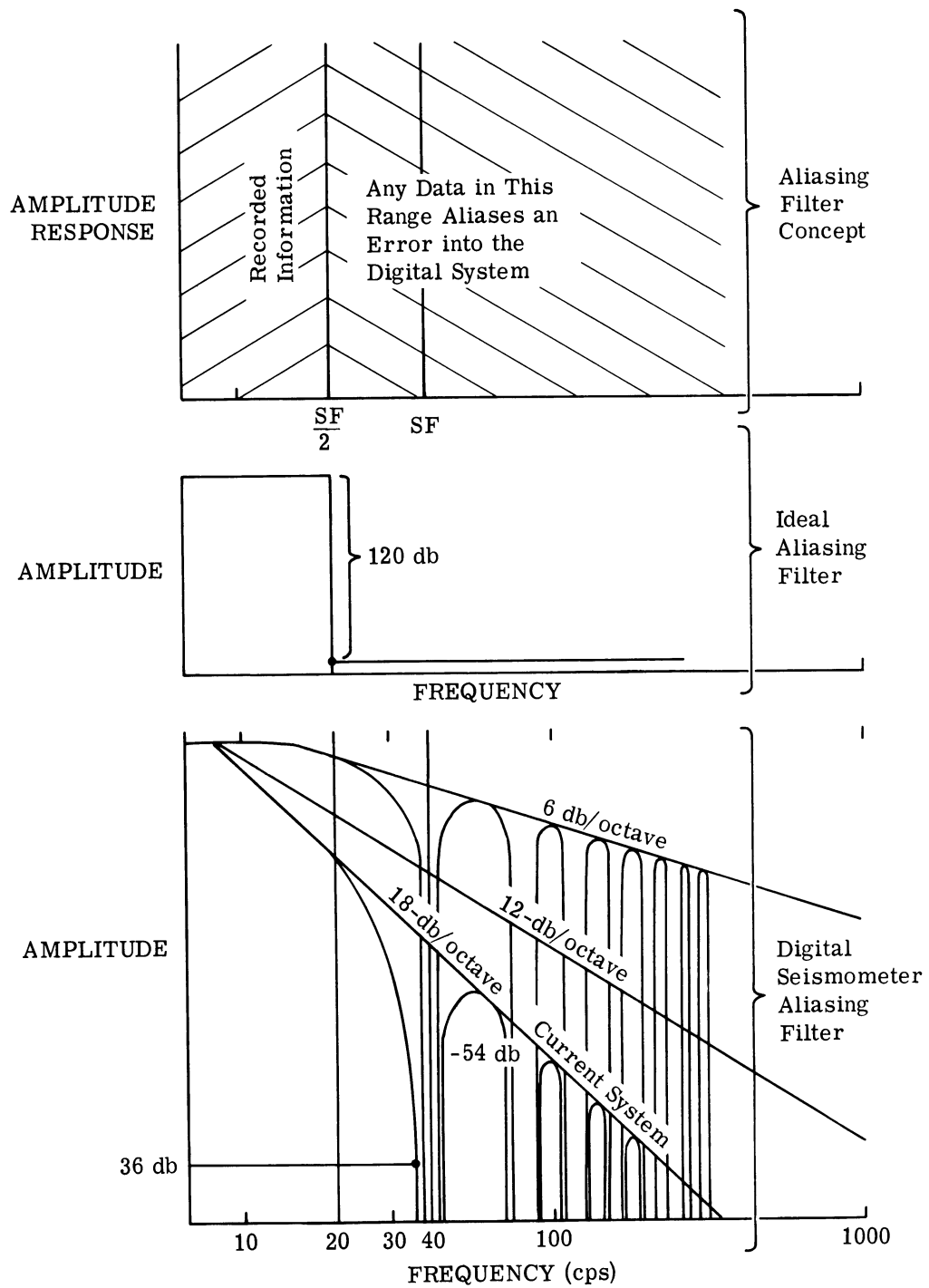
FIGURE 2-5. ALIASING FILTERS

filter is used between the earth and seismometer to obtain another 12-db/octave reduction above 10 cps. Thus, a total of 18-db/octave reduction can be realized.

After a review of the seismometers available it was decided to use a Press-Ewing vertical and to build horizontal seismometers using the Romberg suspension. The Romberg suspension, shown in Figure 2-6, appeared especially applicable because of its insensitivity to tilt and possibility for compact construction. Romberg suspension consists of a simple pendulum whose restoring force is partially balanced by a spring, thereby lengthening the period. Figure 2-7 shows one of the horizontals and the modified Press-Ewing vertical.
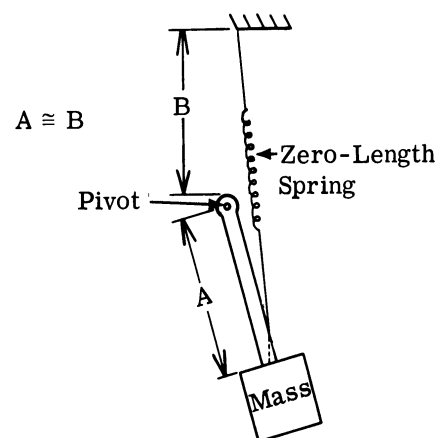
FIGURE 2-6. ROMBERG SUSPENSION SYSTEM. For long periods, spring force $\cong$ 2 x weight of the mass; so resultant force on the pivots is upward; approximately equal to the weight of the mass.

A unique feature of the displacement recording system is the possibility of determining the static linearity of the transducing system by moving the boom through the sensor field in known increments, and recording the digital output at each position. Figure 2-8 shows the results of making such measurements for the present system. The ordinate corresponds to movement of the boom from one maximum position to the other, a distance of 0.008 inch or 200 μ, and the abscissa is digital output. As the boom moves 200 μ, the output varies from -50 $\times$ 10^4 to +50 $\times$ 10^4. Many readings were taken, and the maximum variation at each point is indicated by a bar on the curve. These data were then used to fit a least-mean-square cubic curve. A linear regression analysis was performed to determine whether the cubic and quadratic terms were significant, and this indicated that both were significant when the total dynamic range is used. However, when only half the range was used, neither of the higher-order
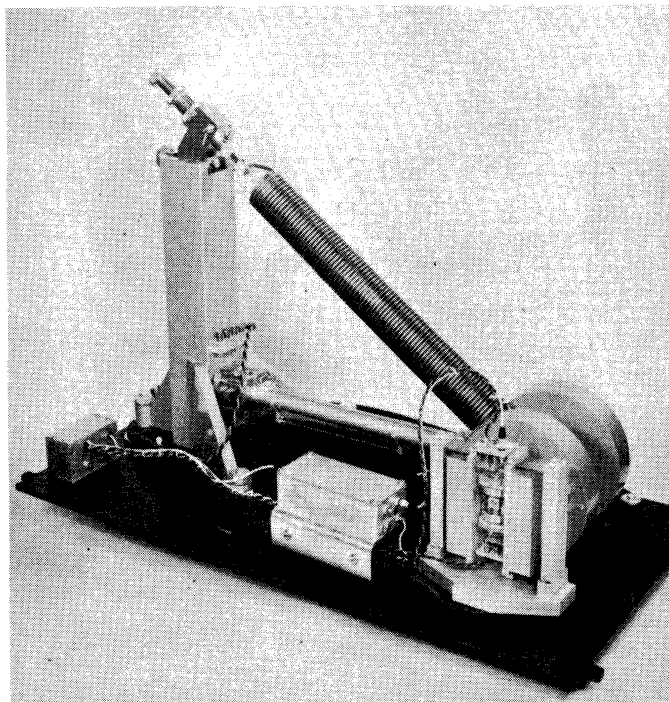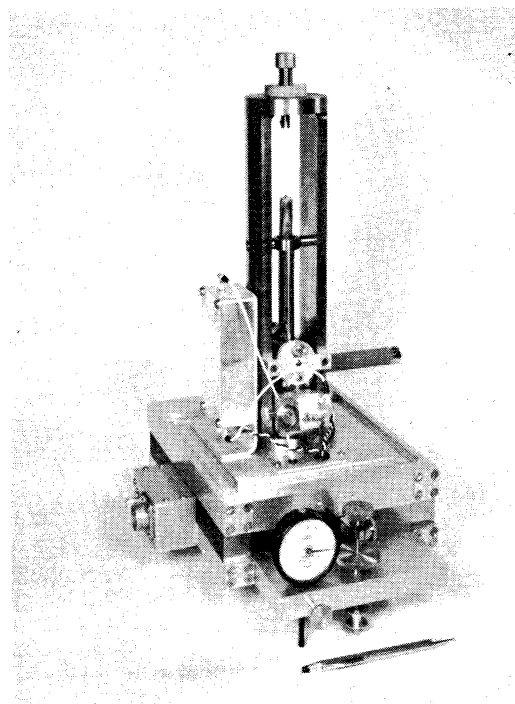
(a)   (b)

FIGURE 2-7. TWO OF THE SEISMOMETERS USED. (a) Press-Ewing vertical. (b) Millis-Romberg
horizontal.
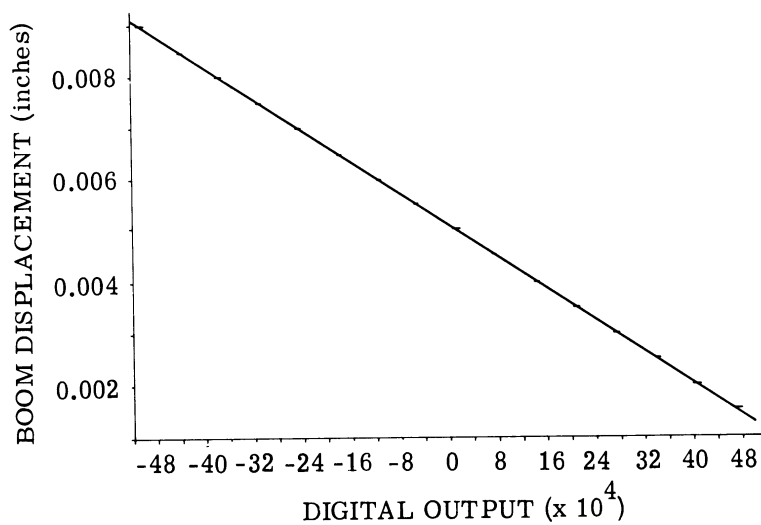
FIGURE 2-8. STATIC RESPONSE OF THE TRANSDUCING SYSTEM

terms was statistically significant. Where the higher order terms were significant, the equation for the curve was used to compute harmonic distortion. Second-order harmonic distortion was found to be 0.75%, third-order distortion was 0.43%, and total harmonic distortion less than 1%.

The second system used with broadband seismographs was put together with off-the-shelf components. In this system, conventional velocity sensing was used. Figure 2-9 presents a block diagram of the major components. For horizontal instruments, long-period Sprengnethers set at 10-second periods were used. These seismometers were followed by short-period photo-tube amplifiers with 5-cps galvonometers. Since these instruments were to be used in comparison with the displacement seismograph system, the same sampling rate (24 milliseconds) was used. To insure that energy above 20.8 cps was not folded back into the passband, the PTA was followed by a 10-cps low-pass filter. The filtered signal was then introduced into an analog-to-digital converter where it was quantized into 14 binary bits for recording on magnetic tape. The only difference in the vertical seismograph system was the use of a Melton vertical. Figure 2-10 illustrates the asymptotic response to input displacement of a composite system of this type. Response falls off at 18 db/octave below the resonance frequency and increases at 6 db/octave above the resonance frequency until the short-period PTA takes effect. From 5 to 10 cps, system response falls off at 6 db/octave because of the combined effect of the pendulum and PTA. Above 10 cps, the low-pass filter takes effect and rapidly attenuates all energy.

To determine the usefulness of broadband instruments, data was recorded with the two three-component broadband systems just described, a short-period Benioff three-component system and a long-period Sprengnether three-component system. All instruments were set up
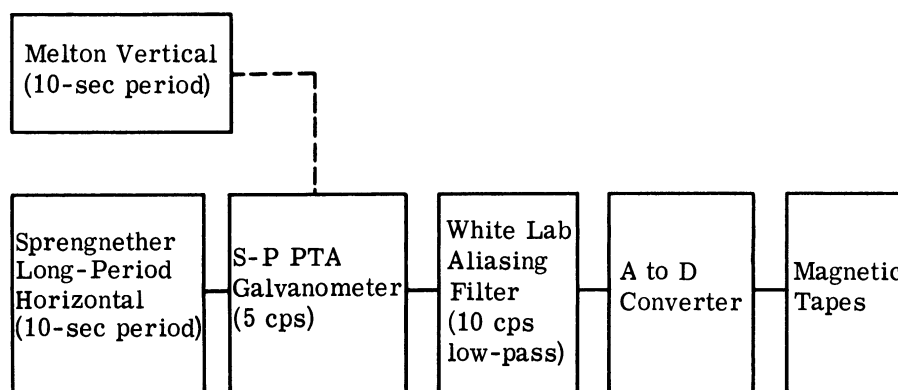
FIGURE 2-9. BROADBAND VELOCITY SYSTEM
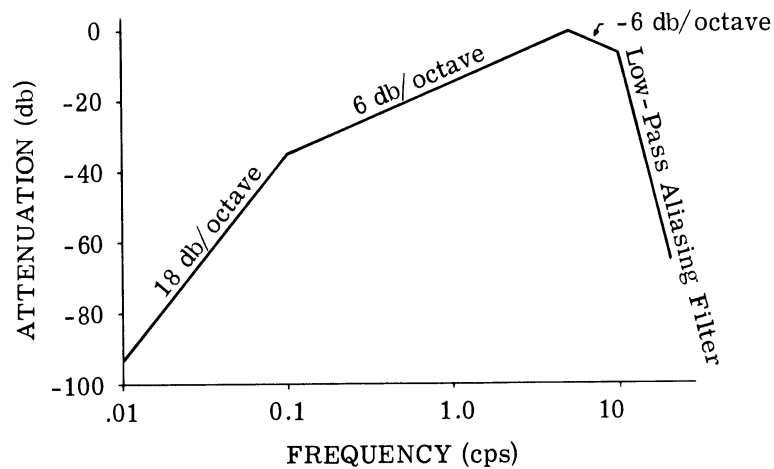
FIGURE 2-10. RESPONSE OF THE BROADBAND VELOCITY SYSTEM
TO INPUT DISPLACEMENT

on the same concrete floor in a cave at the USC & GS installation near Albuquerque. Data from all instruments were recorded on the same magnetic tape with the same sampling rate (24 milliseconds). Several studies were carried out with this data in an attempt to determine its usefulness; two of these studies will be described here.

One method of evaluating information content of a signal recorded on a broadband instrument is to determine if that signal can be filtered with a convolution operator so that it resembles the same signal recorded on a second instrument of different response. A useful tool in the studies carried out is the method used to develop such convolution operators. While a number of criteria can be chosen to judge how well one trace can be filtered to resemble another, Norbert Wiener [4] has shown that the filter which minimizes the mean square error between the two is especially useful in statistical communication theory mathematics. In his work optimum filters are usually developed to minimize the error in the frequency domain. This method has the disadvantage, however, of minimizing the error equally well over the entire Nyquist bandwidth rather than just where the signal resides. However, Norman Levinson [5, 6] extended the use of the minimum mean square error criteria to the development of convolution operators in the time domain, thus minimizing the error in only those parts of the frequency band containing energy.

The convolution operators used in the studies to be described were computed by a modified version of Levinson's technique. Figure 2-11 will help clarify this computation. Let us assume that one has two signals, S_1 and S_2, and desires to develop a convolution operator, h(t), to map S_1 into S_2. The Levinson process allows development of the N-point operator that

28
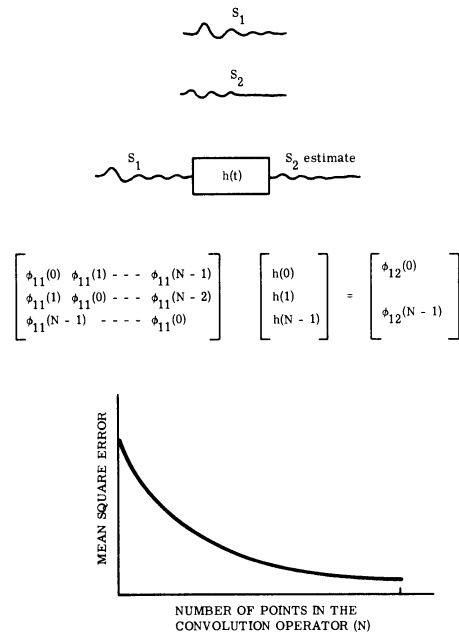
FIGURE 2.11. SCHEME OF THE DEVELOP-
MENT OF CONVOLUTION OPERATORS IN
THE TIME DOMAIN

will minimize the error between the signal S_2 and the estimate S_2. This technique is an iterative procedure; so once the N-point least mean square error filter is solved for, the results can be used to solve for the N + 1-point optimum filter. Moreover, this process also yields the mean square error that will exist between the estimate and the signal being estimated. This variable is a monotonic function which decreases as the number of points in the filter increases. A plot of the error is very useful in determining what length of filter should be used and in comparing how well several individual signals can be mapped into a single reference trace.

To demonstrate that wide dynamic range of a broadband system is necessary for the sole purpose of increasing sensitivity of the instrument while maintaining the ability to record very large signals, a study was designed to show that the increased quantization obtained by a wide dynamic range system does not appreciably increase the information content of large signals. In this study, an event was chosen that used a large part of the dynamic range of the displacement seismometer, one that used 16 bits of the dynamic range of the vertical seismometer. Figure 2-12 shows a surface wave from the large event. To demonstrate the effect of quantization, the signal of the vertical seismometer was divided by 2, 4, 8, and 16. Each division by 2, or discarding of the least significant bit, effectively doubled the size of a quantization width.

29

Broadband Displacement (Horizontal)

Broadband Displacement (Vertical)
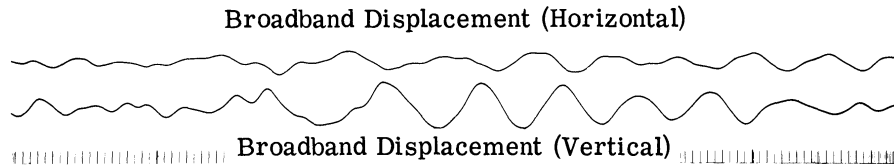
FIGURE 2-12. LARGE-AMPLITUDE SURFACE WAVE

Convolution filters were then developed to map the original vertical trace and each of the less highly quantized signals into the east-west horizontal signal. The filters developed were 363 points long. Each doubling of the quantization width increased the predicted error by only 0.001% of the maximum possible error. (The maximum possible error is the power in the reference trace.) Additionally, spectra of the traces of varying quantizations were computed, and again no appreciable difference could be noted. The point to be made again here is that the only reason to include wide dynamic range as one of the specifications of a broadband system is to give sufficient sensitivity to record a small signal at higher frequencies, in the presence of a much larger long-period information.

To determine how well the broadband systems could record large amplitude long-period energy and smaller amplitude short-period energy simultaneously, 500-point convolution filters were developed to map the two vertical broadband instruments into a vertical short-period Benioff. Additionally, to further compare the amount of information contained in the broadband instruments, convolution filters were developed to map each broadband instrument into the other. The data sample chosen for this test was a P-phase from a local event arriving during the long-period Rayleigh waves of a teleseismic earthquake (see Figure 2-13). It therefore contained energy at both ends of the normal earthquake spectrum. The approximate maximum amplitude of the P-wave was 15 mμ. The epicenter of this magnitude 5.3 earthquake was in the Kermadec Islands region, at approximately 93 degrees.

Short-Period Benioff (Vertical)

Broadband Velocity (Vertical)

Broadband Displacement (Vertical)
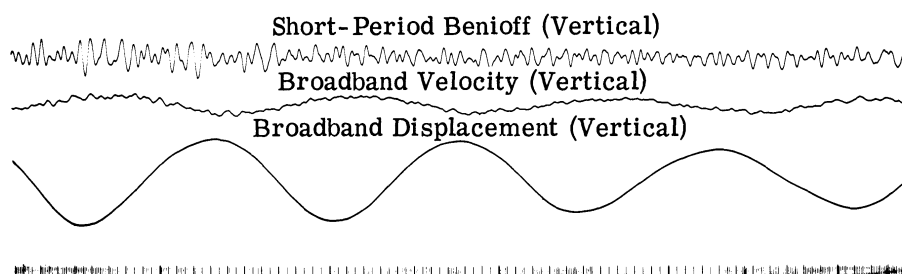
FIGURE 2-13. LOCAL P WAVE ARRIVING SIMULTANEOUSLY WITH LARGE-
AMPLITUDE LONG-PERIOD RAYLEIGH WAVES

To develop the convolution filters, it was necessary to compute all combinations of cross-correlation functions. These functions, shown in Figure 2-14, indicate the period of the information contained in each of the traces. The cross-correlation between the velocity instrument and the short-period Benioff indicates that both the long- and short-period energy is present on the broadband velocity instrument. However, the cross-correlation between the displacement instrument and the short-period Benioff does not reveal much short-period energy. In fact, the only energy of significant magnitude was the 18-second Rayleigh wave that is clearly evident in the original traces.
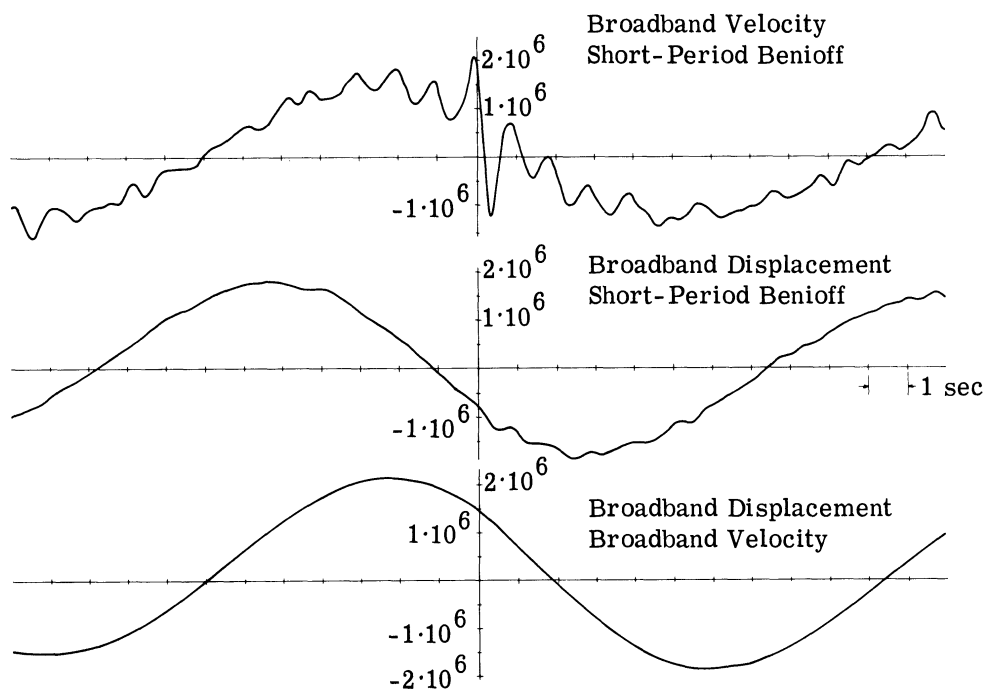
FIGURE 2-14. CROSS-CORRELATION FUNCTIONS FOR THE THREE INSTRUMENTS
USED

The convolution operators were applied; Figure 2-15 presents the results. The four groups shown are formed by mapping the two broadband vertical traces into the vertical short-period trace and each of the broadband instruments into the other. The three traces in each of these groups are the filtered estimate, the reference trace, and the error between the two. In the first group the broadband velocity instrument was mapped into the short-period signal, and the results are exceptionally good, even in fine detail. It might be well to emphasize again that the convolution operator being applied is not a simple bandpass filter, but a much more complex filter designed to correct for both phase and amplitude differences between the two in-

Short-Period Benioff
(Vertical)

Broadband Velocity
(Vertical)

Broadband Displacement
(Vertical)

Broadband Velocity
→ Short-Period Benioff
Short-Period Benioff

Error

Broadband Displacement
→ Short-Period Benioff
Short-Period Benioff

Error

Broadband Velocity →
Broadband Displacement
Broadband Displacement

Error

Broadband Displacement
→ Broadband Velocity
Broadband Velocity

Error

FIGURE 2-15. RESULTS OF APPLICATION OF THE CONVOLUTION OPERATORS TO THE THREE INSTRUMENTS

struments. It is also of interest to note that by using one broadband system which properly covers the bandwidth of interest, one could use filters of this type to obtain the output of any conventional or non-conventional instrument desired. The second group in Figure 2-15 is the result of mapping the displacement instrument into the short-period instrument. The largest mean square error that a convolution filter developed by the Levinson process will allow is the power in the reference trace. Thus, in the worst case, the filter would simply shut the seismometer off, and it can be seen that this is nearly the case with the displacement instrument. The filtered result contains a low amplitude long-period signal, and the error trace is nearly idential to the reference. The next group represents mapping the broadband velocity seismograph into the displacement instrument. The long-period component is nearly perfectly reproduced, but a small amount of short-period energy remains. This can be attributed to the fact that the Levinson method produces a filter that emphasizes that part of the bandwidth where the most energy resides. Since most of the power in these two signals is in the 18-second period component, the filter concentrates on making these parts of the spectrum alike and does not place as much emphasis on the short-period energy. The final group is for the case of mapping the displacement instrument into the velocity seismometer. Here the 18-second component is reproduced almost exactly, but not the higher-frequency energy, again indicating the lack of high-frequency energy in the displacement instrument.

To determine over what part of the spectra the convolution operators were performing best, the power density spectra of the error trace and the reference trace were computed for each of the four cases. Figure 2-16 presents the reference spectra and the ratio of the error spectra to the reference spectra. Where the filtering was able to do a good job, the ratio falls far below 0 db, and where it did not do so well, the ratio is approximately 1, or 0 db. Figure 2-16a represents mapping the broadband displacement and velocity instruments into the short-period Benioff. The upper curve is the spectrum of the short-period signal, and the lower two curves are the ratios of the error spectra to the reference spectrum. As can be seen in the reference spectrum, the major portion of the energy is in a band from 0.25 cps to 2.5 cps. There is an additional contribution at 4.75 cps from the ambient seismic noise, which is nearly sinusoidal and is well polarized in the east-west direction. The ratio for the broadband velocity error spectrum is well down below 0 db (or a ratio of 1) throughout the portion of the short-period spectrum that contains the most energy. In the portion of the spectrum where there is not much energy (2.5 to 4.5 cps) the error increases because of the Levinson filter's weighting the larger part of the spectrum more heavily. At the 4.75-cps noise peak, this ratio again drops sharply, indicating that a respectable job of filtering is possible. It is noticeable that the error-to-reference ratio resulting from mapping the displacement instrument into the
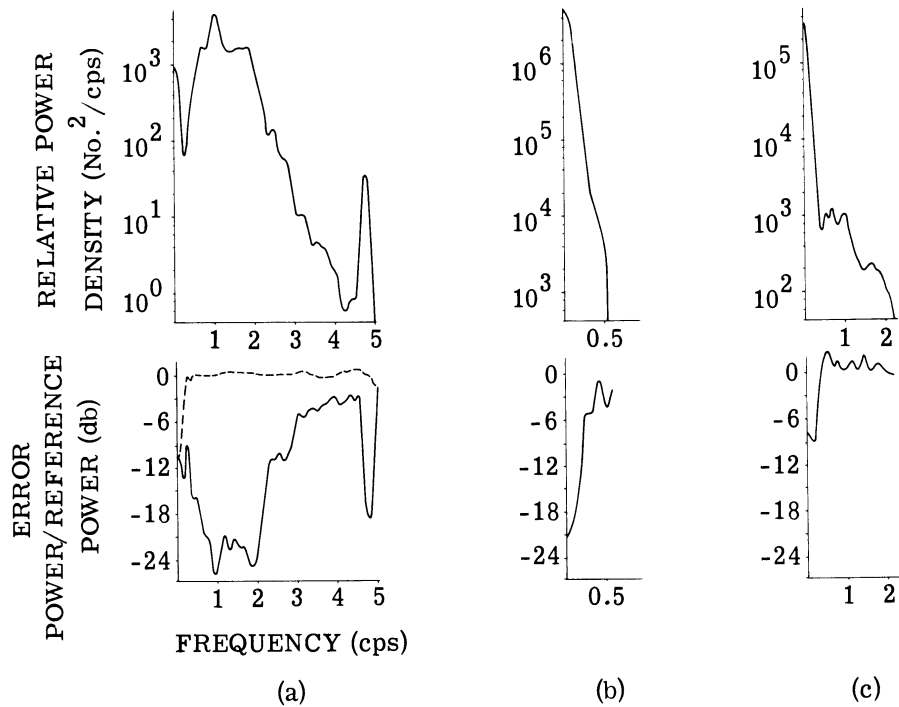
FIGURE 2-16. POWER DENSITY SPECTRA OF THE REFERENCE TRACES AND NORMALIZED ERROR SPECTRA. (a) Top: spectrum of short-period Benioff signal. Bottom: estimation error with displacement sensing (- - -) and estimation error with velocity sensing (——). (b) Top: spectrum of broadband displacement signal. Bottom: estimation error with velocity sensing. (c) Top: spectrum of broadband velocity signal. Bottom: estimation error with displacement sensing.

short-period Benioff holds up reasonably well for the long-period portion, but indicates that essentially no energy above 0.25 cps is available for mapping. In both remaining cases (Figure 16b and c), where the broadband velocity instrument was mapped into the displacement instrument, and the displacement instrument into the velocity instrument, results were nearly the same. The major portion of the energy was of about an 18-second period, and both instruments did a reasonably good job of mapping in this region. Thus, for the example chosen, velocity sensing was superior to displacement sensing in recording a broadband signal.

In conclusion, some of the advantages and disadvantages of the two broadband systems considered may be listed. First, the advantages for the directly digitizing displacement instrument are:

(a) Its output contains a minimum change from true ground motion, displacement in and displacement out.

(b) The displacement sensing scheme offers a means of obtaining a much wider dynamic range with low distortion than conventional analog-to-digital converter systems.

(c) There is no necessity for an intermediate wide dynamic range amplifier.

(d) It is a good strong-motion instrument.

However, it does have several disadvantages:

(a) The response of the displacement instrument is not optimum for broadband recording. Even if sufficient dynamic range is used to cover the spectrum of the input signal, the data will be so large that expensive double- or triple-precision arithmetic will be necessary to use it in many computer processes.

(b) There is difficulty in providing aliasing filters for this system. Since transducer output is digital numbers, it is not possible to prevent aliasing by filtering the seismometer output. Mechanical filters and integration filters help, but are probably not sufficient in all cases.

(c) It is difficult to obtain sufficient sensitivity to record the higher-frequency end of the spectrum. This can be accomplished by using higher oscillator center frequencies, but there is some design difficulty in doing so.

The advantages and disadvantages of the velocity transducing system are of course closely related to those of the displacement instrument. It offers the following advantages:

(a) It pre-whitens the earth's natural spectrum, and thus requires much less dynamic range than other systems to do the same job.

(b) Conventional analog aliasing filters can be used so that aliasing is not a problem.

(c) State-of-the-art components are available, and it is, therefore, less expensive to build.

Its major disadvantage is that it does require a high-gain intermediate amplifier such as the PTA. However, if nongalvometric transducing systems are desired, it is possible to use a low-noise parametric amplifier. The total dynamic range of this system will probably be limited by the dynamic range of the amplifier used.

REFERENCES

1. J. Brune and J. Oliver, "Seismic Noise of the Earth's Surface," Bull. Seism. Soc. Am., 1959, Vol. 49, pp. 349-354.

2. W. R. Bennett, "Spectra of Quantized Signals," Bell System Tech. J., 1948, Vol. 27, No. 3.

3. J. Cl. De Bremaecker et al., "The Rice Digital Seismograph System," J. Geophys. Res., 1963, Vol. 68, pp. 5029-5034.

4. N. Wiener, Extrapolation, Interpolation and Smoothing of Stationary Time Series, The Technology Press of MIT, Cambridge, Mass., and John Wiley and Sons, Inc., New York, N. Y., 1946.

5. N. Levinson, "The Wiener RMS Error Criterion and Filter Design and Prediction," J. Math. Phys., 1947, Vol. 25, pp. 261-278.

6. N. Levinson, "A Heuristic Exposition of Wiener's Mathematical Theory of Predictions and Filtering," J. Math. Phys., 1947, Vol. 26, pp. 110-119.

3

OPERATIONAL EVALUATION OF BROADBAND SEISMOGRAPHS[1]

George A. Gray, Jr.
The Geotechnical Corporation

The broadband three-component seismograph at the Wichita Mountains Seismological Observatory (WMO) was designed in accordance with recommendations of the Geneva Conference of Experts. The specific requirement for the broadband response characteristics was constant magnification of 1.0 to 2.0×10^3 over the period range 0.1 to 10 seconds. Seismographs with these approximate response characteristics, known as the Kirnos System, SVK (vertical) and SGK (horizontal) seismographs, had been in general use at USSR seismological stations [1]. The computed relative frequency response of the SVK seismograph with close coupling and loose coupling is shown in Figure 3-1. In the figure, f_s and f_g are the natural frequencies of the seismometer and galvanometer, respectively; λ_s and λ_g are ratios of actual damping to
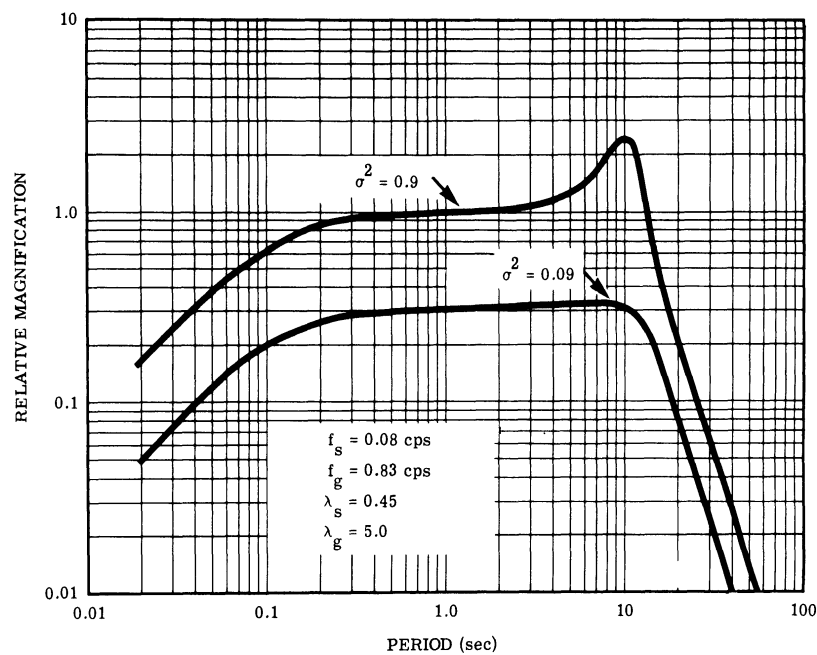
FIGURE 3-1. RELATIVE MAGNIFICATION OF THE SVK SEISMOGRAPH

critical damping for the seismometer and galvanometer, respectively; and σ^2 is the coupling factor. The phase shift corresponding to these amplitude responses is plotted on a linear scale as a function of frequency to help indicate the degree of phase distortion which may be expected (see Figure 3-2). The closely coupled condition is shown because relatively close coupling is normally required with the vertical seismograph for operating magnifications of around 1000. The value 0.9 for σ^2, the coupling factor, in the response computations may be higher than any value actually used, but a value of 0.6 is frequently used for the vertical component [2].
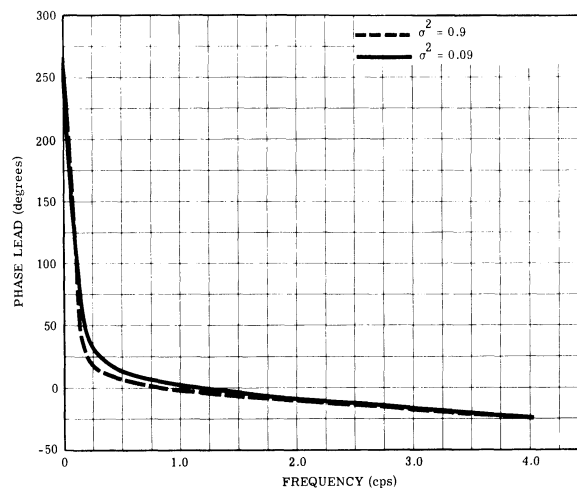
FIGURE 3-2. PHASE SHIFT OF THE SVK SEISMO-
GRAPH AS A FUNCTION OF FREQUENCY

The WMO broadband seismographs were designed to have a somewhat flatter response than the SGK seismograph (see Figure 3-3). The 7-kg mass of the Press-Ewing vertical seismometer allows the use of loose coupling. Resolution is based on the noise level under favorable conditions, and is within 3 to 6 db of the thermal noise level, approximately. M_s in the figure is the effective mass of the seismometer, and K_g is the moment of inertia of the galvanometer. Phase shift of the WMO broadband seismographs as a function of frequency (see Figure 3-4) is slightly more linear than that of the SGK seismograph; however, phase distortion is evident for both in the lower frequency portion of the passband (below 0.5 cps).

Preliminary evaluation of the detection capability of the broadband seismograph indicated that the broadband system added very little to the total seismic signal detection capability of WMO. During a period of 2 and 1/2 months, 93% of all earthquakes detected by WMO could not be detected by viewing only the broadband traces. Use of more than one recording speed would have made some improvement in the broadband detection capability, but only one rela-
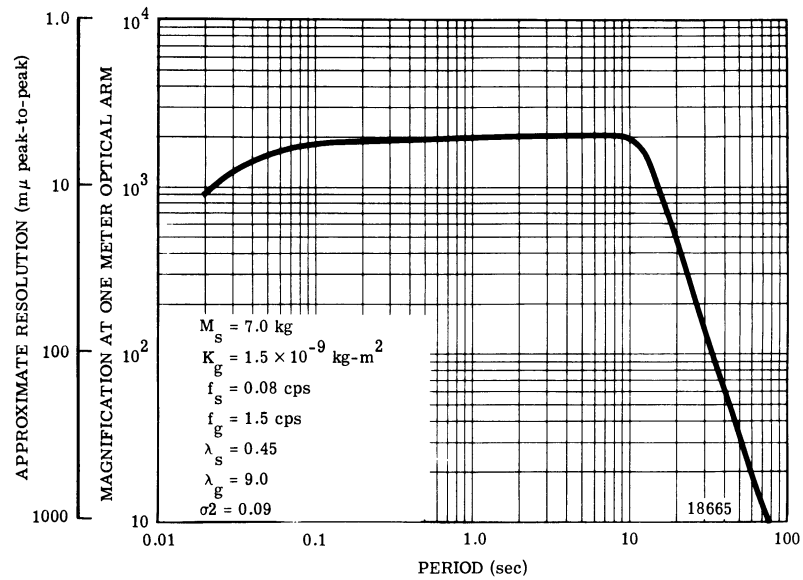
FIGURE 3-3. MAGNIFICATION AND RESOLUTION OF THE WMO BROAD-
BAND SEISMOGRAPH
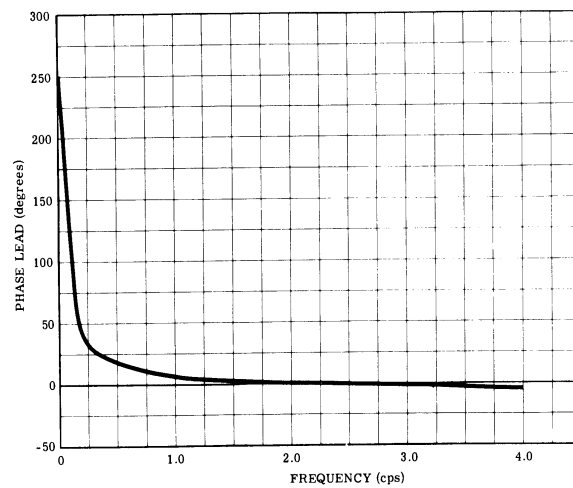
FIGURE 3-4. PHASE SHIFT OF THE WMO BROADBAND
SEISMOGRAPH AS A FUNCTION OF FREQUENCY

tively slow speed was used (1.0 mm/sec as normally viewed). The identification of earthquake
phases, especially for large regional earthquakes, seemed to be the only area in which the
broadband visual presentation was often superior to the other systems (see Figure 3-5). BZ,
BN, and BE are used in the margins of the seismogram illustrations to identify the broadband
vertical, north-south, and east-west components, respectively. SP is short period, LP is long
period, IB is intermediate band, and S indicates the summation of several short-period seis-
mographs. Figure 3-6 shows the frequency response of all these systems. Magnifications are
at 1 cps for all systems except the long period, which has magnifications at a 25-second period.
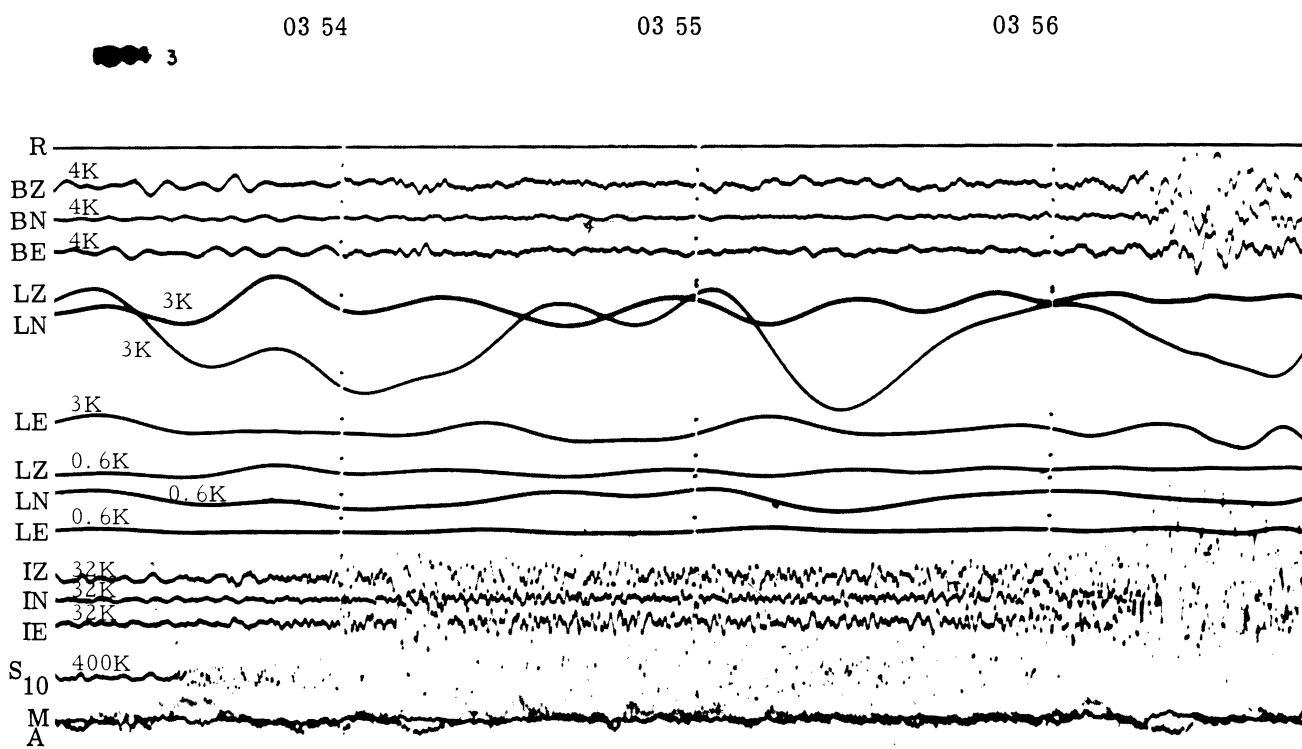
FIGURE 3-5. RECORDINGS OF A REGIONAL EARTHQUAKE AT A DISTANCE OF $12°$. The figure shows
the usefulness of the broadband seismographs for showing directly the ground motion produced by differ-
ent phases at different periods between 0.3 and 10 seconds. Note: The seismograph magnifications given
in the margin should be reduced by 25% to correspond to reduction in size of the figure for printing.

The magnification and resolution of the broadband seismograph are limited by the amplitude
of the predominant microseisms within the passband and by the recorder's dynamic range. The
noise spectrum at WMO (Figure 3-7) covers a minimum of about 50 db within the passband of
the broadband seismograph. Under certain conditions, the range of the noise spectrum can be
as large as 74 db, as shown in Figure 3-8. These spectra were obtained with 1/3-octave band-
pass filters spaced 1/3 octave apart.
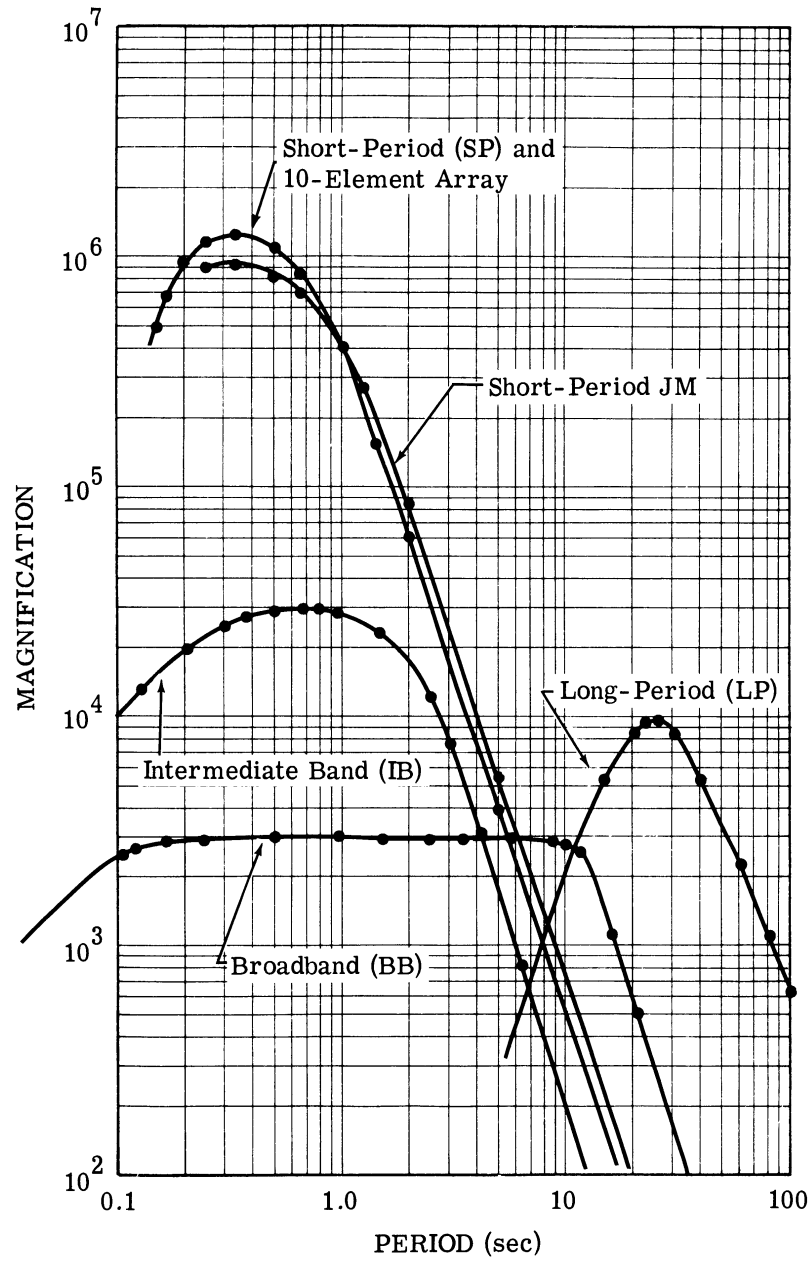
FIGURE 3-6. RESPONSE CHARACTERISTICS OF SEISMOGRAPHS
CONSIDERED IN FIGURE 3-5
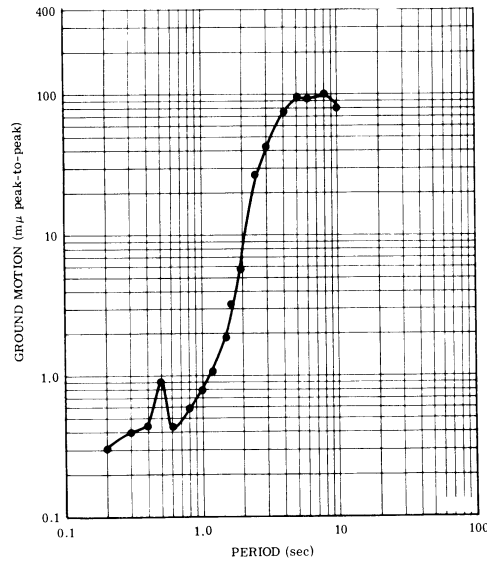
FIGURE 3-7. WMO NOISE SPECTRUM. This
is a composite of short-period and broadband
data for July and August 1961, exclusive of
storms.
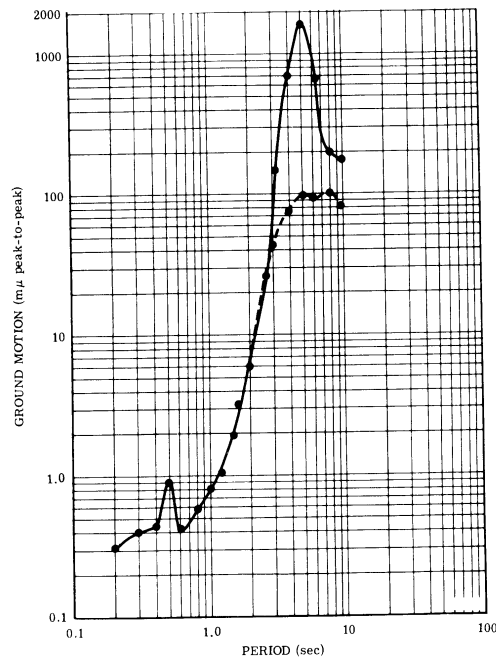
FIGURE 3-8. WMO NOISE SPECTRUM MEASURED FROM THE VERTICAL
BROADBAND SEISMOGRAPH. The dotted line indicates the average noise
spectrum exclusive of storms. Data are for a 2-minute interval when
Hurricane Carla was in the Gulf of Mexico.

The broadband vertical seismograph was also operated at a higher speed for several months in an effort to further evaluate its detection capabilities. Magnification was increased to approximately 3 times the magnification which seemed best for the slower speed recording, and the coupling factor was increased to about 0.09. The trace was positioned closer to the center of the film, and trace intensity was adjusted to provide as much dynamic range as possible. The seismograms which resulted also provide information by which to evaluate the other narrowband seismographs. Figure 3-9 shows the recording of a relatively small P-wave signal by the broadband, short-period, and array summation traces (Σ). The traces marked EP are low-gain short-period traces. Figure 3-10 shows the recording of a somewhat larger P-wave signal by these traces. One of the advantages of the broadband visual presentation is that a more accurate picture of ground displacement for large signals is obtained than can usually be reconstructed from a number of narrowband seismograms. Figures 3-11 and 3-12 illustrate the response of the broadband vertical seismograph to large signals.

By adding a slightly underdamped, 5-cps galvanometer to the broadband seismometer circuit, a flat-velocity broadband seismograph was obtained. Figure 3-13 shows the flat-velocity (BBV) and the flat-amplitude (BBZ) seismographs responding to the same earthquake P wave.
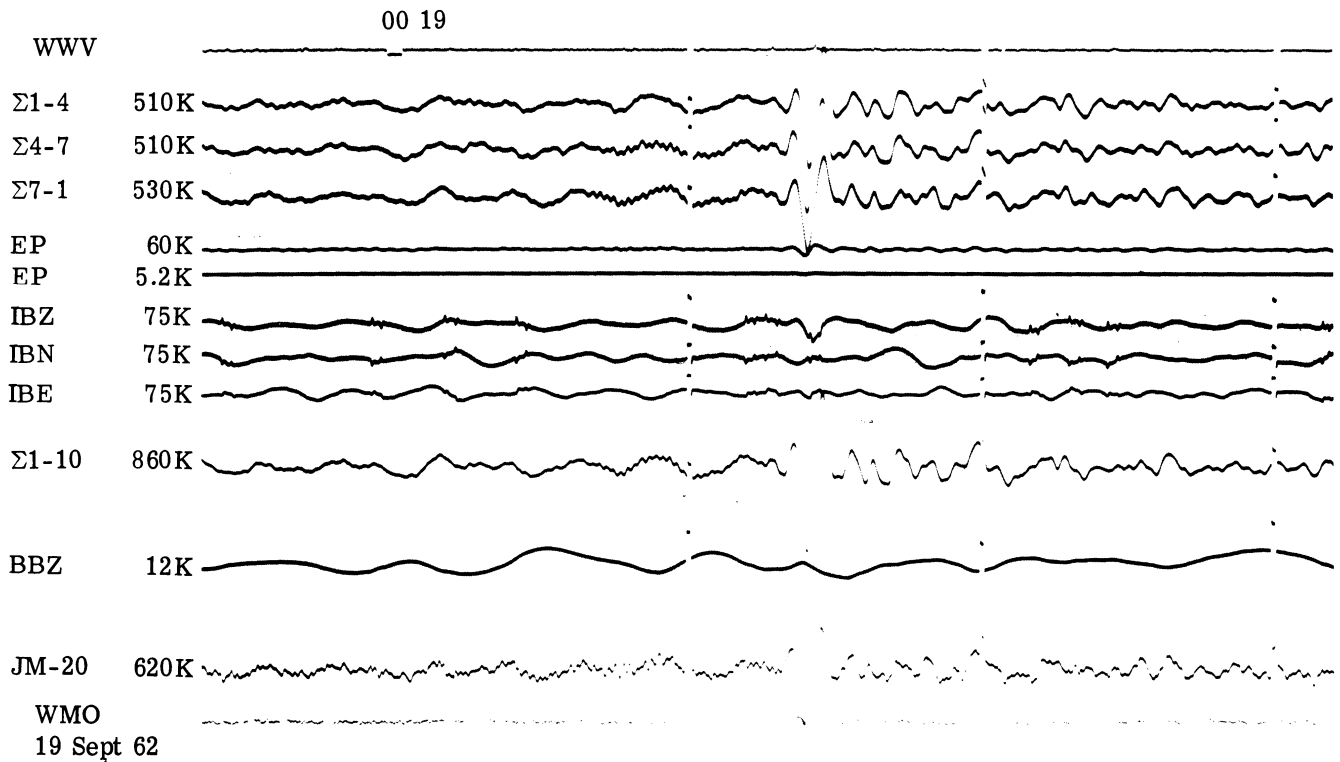
FIGURE 3-9. RECORDINGS OF A P WAVE FROM AN EARTHQUAKE WITH EPICENTER IN THE SEA OF JAPAN. $\Delta = 90°$, $h \simeq 436$ km, $O = 00:06:58.7$. Note: The seismograph magnifications given in the margin should be reduced by 25% to correspond to the reduction in size of the figure for printing.

01 32

WWV

Σ1-4	510K	
Σ4-7	510K	
Σ7-1	530K	
EP	60K	
EP	5.2K	
IBZ	75K	
IBN	75K	
IBE	75K	
Σ1-10	860K	
BBZ	12K	
JM-20	620K	

WMO
10 Sept 62

FIGURE 3-10. P-WAVE ARRIVAL FROM THE ANDREANOF ISLANDS. $\Delta = 53°$, $h \simeq 33$ km, O = 01:22:35.5.
Note: The seismograph magnifications given in the margin should be reduced by 25% to correspond to reduction in size of the figure for printing.

44

05 40

WWV

Σ1-4   480K

Σ4-7   570K

Σ7-1   630K

EP   60K

EP   5.2K

IBZ   75K

IBE   75K

IBN   75K

Σ1-10   840K

BBZ   12K

JM-20   540K

WMO
16 Sept 62

FIGURE 3-11. P-WAVE ARRIVAL FROM KERN COUNTY CALIFORNIA. Δ = 16°; h $\simeq$ 10 km; O = 0.5:36:15.7;
magnitude = 4.75-5.0 (PAS), 5.5-5.75 (BRK). Note: The seismograph magnifications given in the margin
should be reduced by 25% to correspond to reduction in size of the figure for printing.

Σ1-4	480K	
Σ4-7	570K	
Σ7-1	630K	
EP	60K	
EP	5.2K	
IBZ	75K	
IBN	75K	
IBE	75K	
Σ1-10	840K	
BBZ	12K	
JM-20	540K	

WMO
15 Sept 62

FIGURE 3-12. P-WAVE ARRIVAL FROM THE KURILE ISLANDS. $\Delta = 72.5^{\circ}$; O = 22:50:46.3; magnitude
= 6.5 (PAS), 6.0 (PAL). Note: The seismograph magnifications given in the margin should be reduced by
25% to correspond to reduction in size of the figure for printing.

46
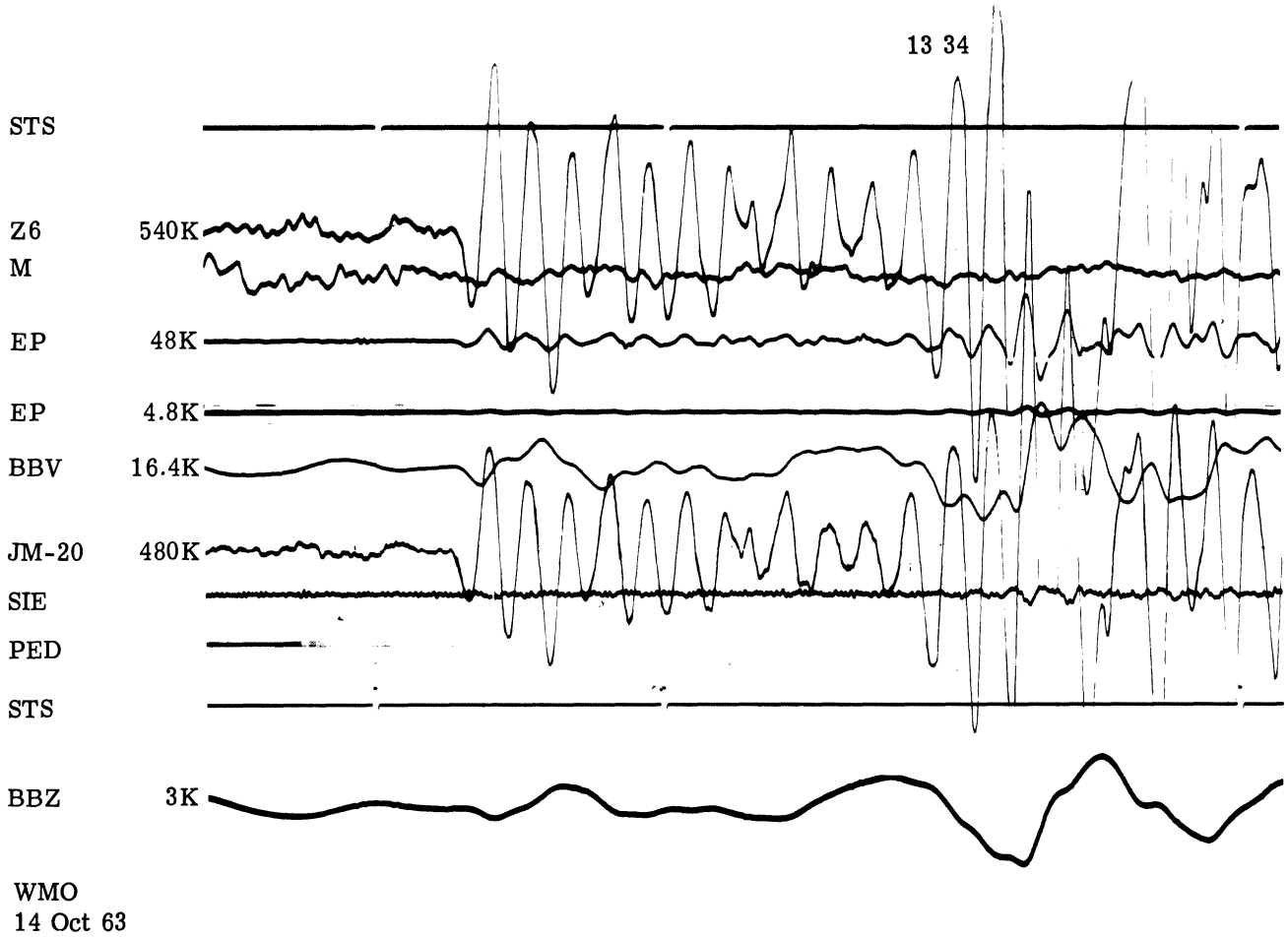
FIGURE 3-13. P-WAVE ARRIVAL FROM THE KURILE ISLANDS. $\Delta \simeq 78°$, $h \simeq 60$ km, $O = 13:21:45.2$, CGS magnitude = 5.9. Note: The seismograph magnifications given in the margin should be reduced by 25% to correspond to reduction in size of the figure for printing.

We have reason to believe that flat-velocity broadband seismographs will be useful in magnitude studies. Body-wave magnitudes are calculated from the ratio of the amplitude to the period of the ground motion by using the maximum amplitude-to-period ratio within a given interval after the phase arrival. Many body waves contain a wide range of frequency components which undergo such a large degree of relative attenuation and phase distortion when recorded on narrowband instruments that accurate determination of the maximum velocity component is impossible. Figure 3-14 shows the difference in the magnitude obtained from using the flat-velocity broadband seismograph in one isolated case.

Another seismograph in use at WMO also has a flat-velocity broadband response, but the flat-velocity band covers a higher range of frequencies. It uses a Johnson-Matheson seismometer and a directly coupled 20-cps galvanometer (JM-20). The amplitude and resolution of the JM-20 seismograph as a function of period is shown in Figure 3-15, and the phase re-
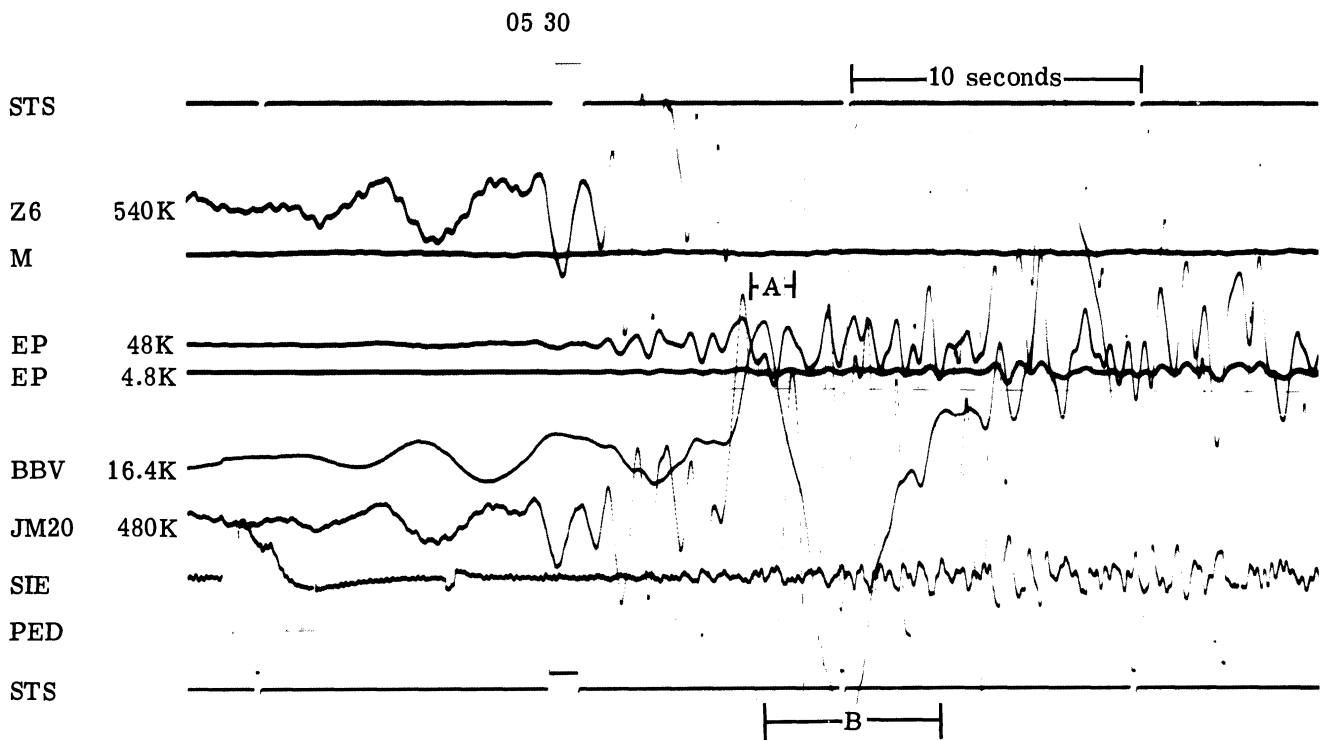
FIGURE 3-14. WMO RECORDING OF A P WAVE FROM A LARGE KURILE ISLANDS EVENT. Assumed $\Delta \simeq 75^\circ$, $h \simeq 50$ km. Short-period magnitude calculated from pulse A $\simeq$ 6.1; flat-velocity magnitude calculated from pulse B $\simeq$ 6.9. Note: The seismograph magnifications given in the margin should be reduced by 25% to correspond to reduction in size of the figure for printing.
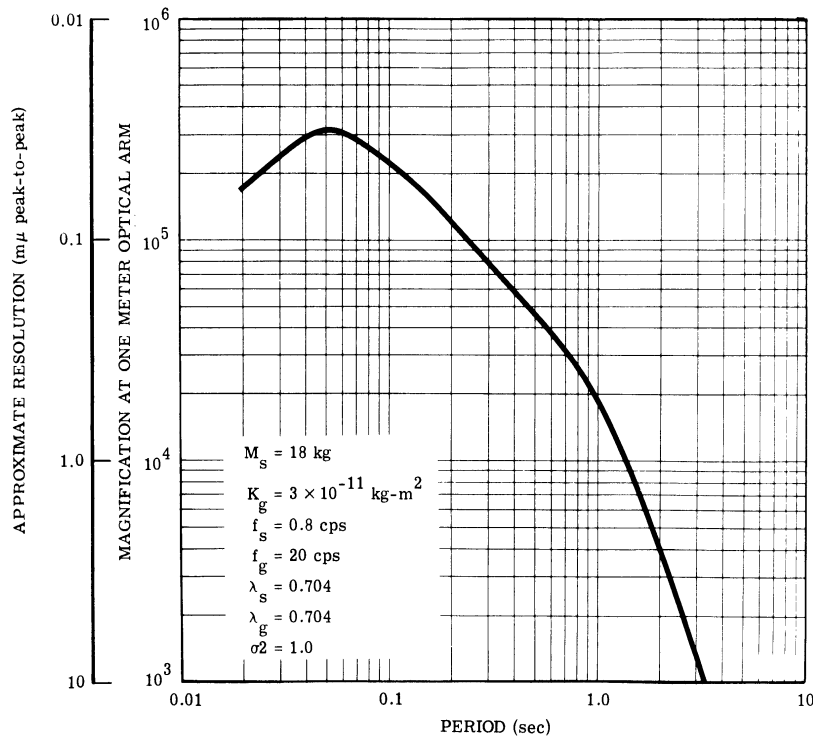
FIGURE 3-15. MAGNIFICATION AND RESOLUTION OF THE JM-20
SEISMOGRAPH

sponse is shown in Figure 3-16. The response of the JM-20 is more nearly the inverse of the WMO noise spectrum in the range 1.0 to 10 cps than is the response of the standard short-period seismographs. The P phases of near-regional and local events are often recorded with greater amplitude and clarity on the JM-20 trace (see Figure 3-17); but teleseismic signals are recorded equally well on the standard short-period seismographs because they contain little or no frequency higher than about 3 to 4 cps.

To exemplify the maximum resolution which may be obtained in a practical flat-amplitude broadband seismograph using existing instrumentation, a computation was made based on the characteristics of a Geotech long-period seismometer (model 7505A) and system parameters which can be maintained fairly easily (see Figure 3-18). A maximum approximate resolution of slightly less than 1.0 $m\mu$ over the flat portion of the response resulted. The phase shift associated with the amplitude response is shown in Figure 3-19. The resolution is limited primarily by the effective mass of the seismometer; the moment of inertia of the galvanometer does not matter if its rotation can be measured with sufficient resolution.
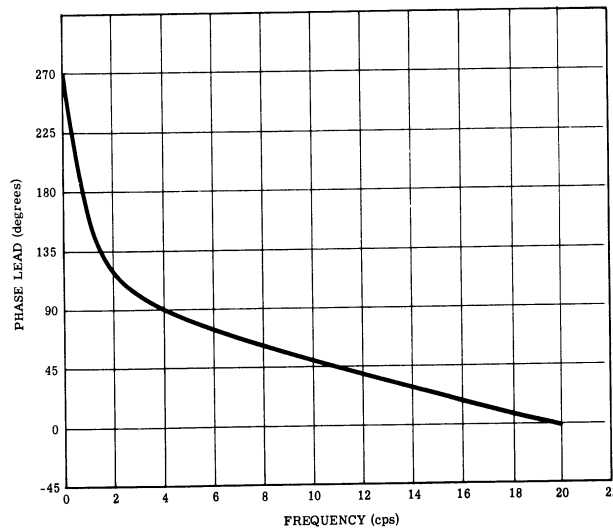
FIGURE 3-16. PHASE SHIFT OF THE JM-20 SEISMOGRAPH
AS A FUNCTION OF FREQUENCY
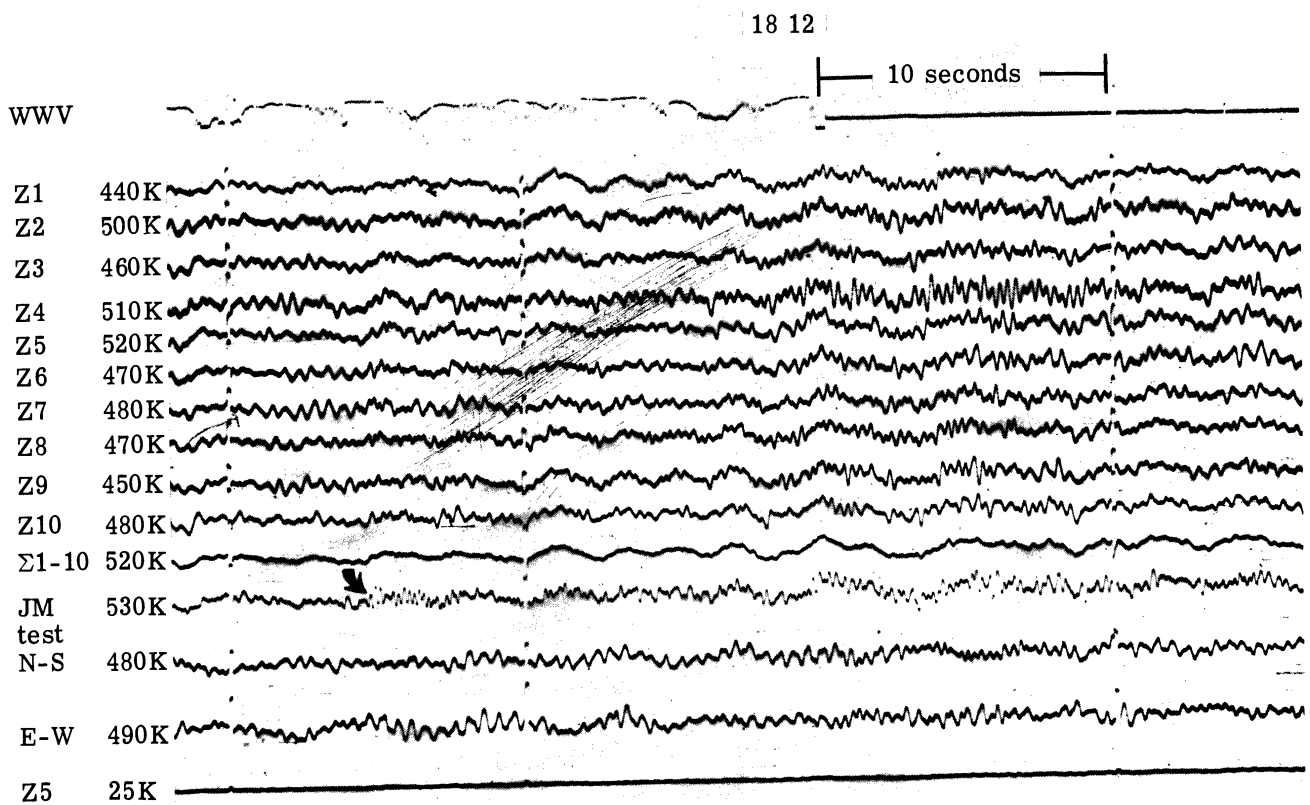
FIGURE 3-17. WMO RECORDING OF A WEAK QUARRY BLAST. The arrow indicates P as detected by the
JM-20 seismograph. Note: The seismograph magnifications given in the margin should be reduced by 25%
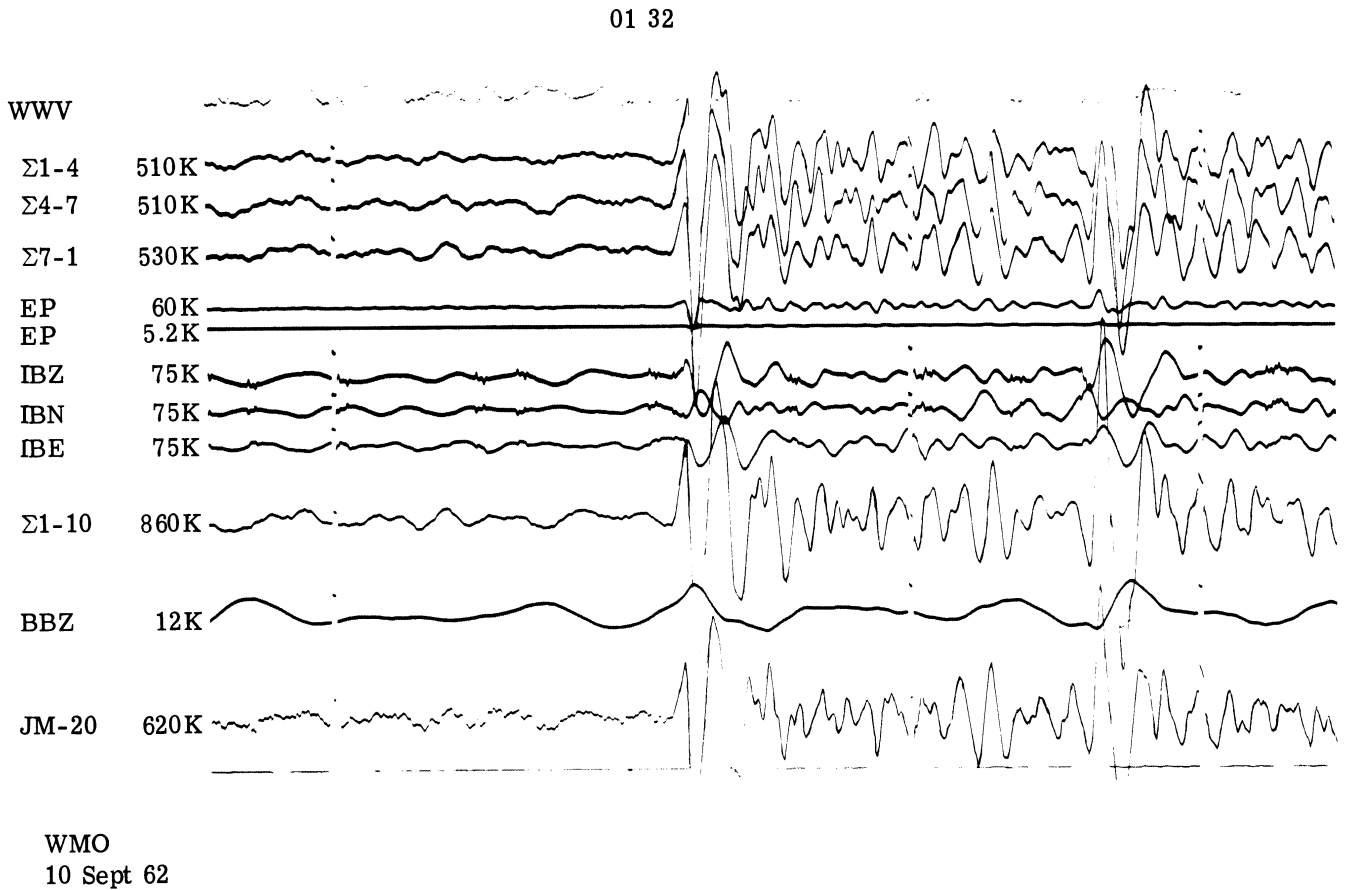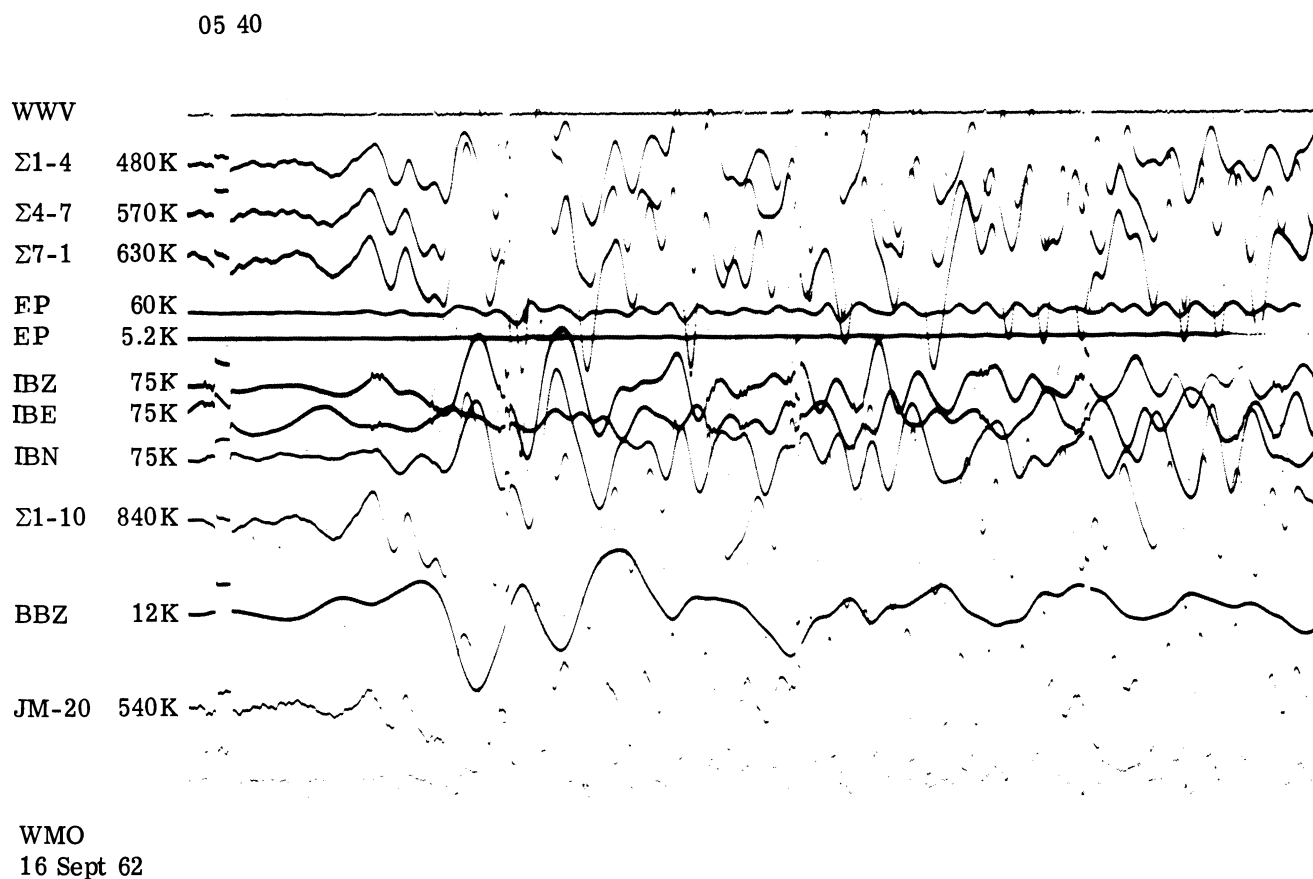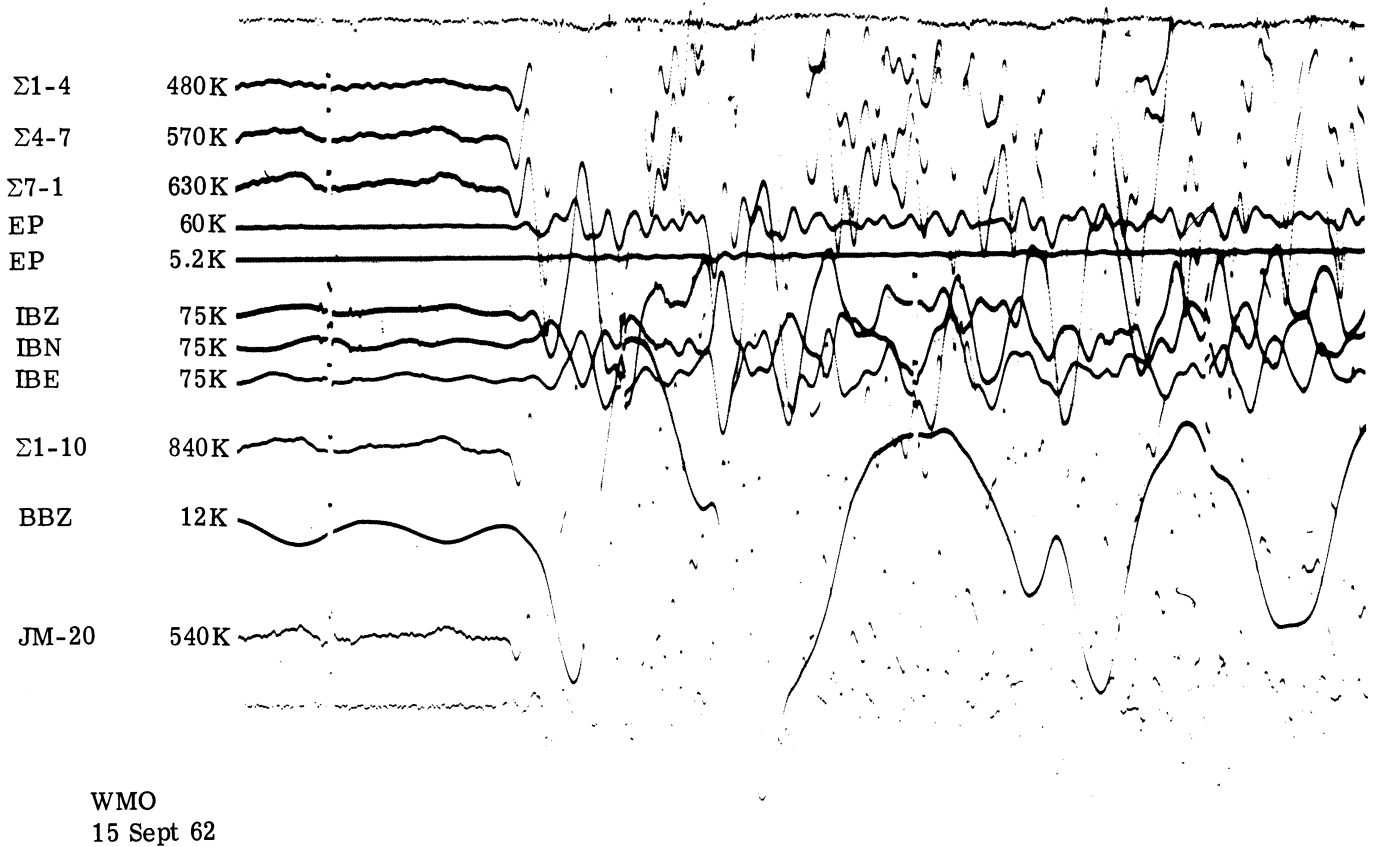to correspond to reduction in size of the figure for printing.
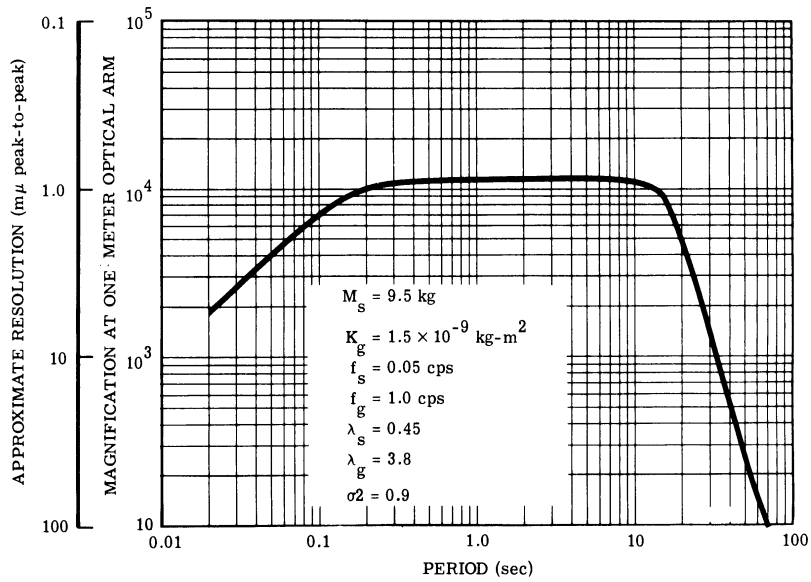
FIGURE 3-18. MAGNIFICATION AND RESOLUTION OF A CLOSELY
COUPLED BROADBAND SEISMOGRAPH
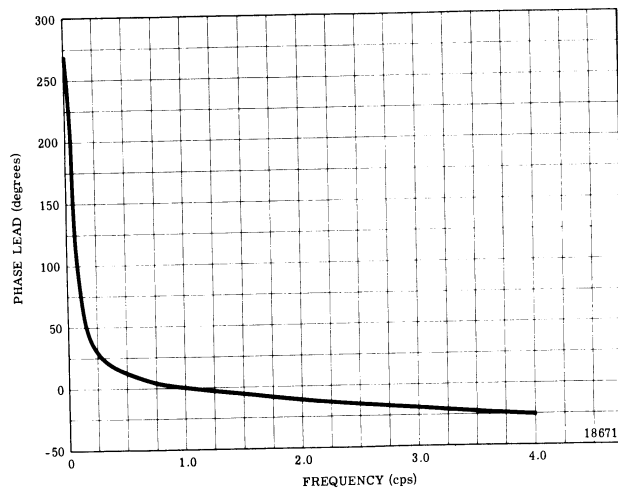
FIGURE 3-19. PHASE SHIFT OF THE CLOSELY COUPLED
BROADBAND SEISMOGRAPH AS A FUNCTION OF FRE-
QUENCY

51

A technique which has been tested at Geotech uses a single seismometer and two galvanometers to yield an approximately flat-velocity broadband response with a notch at the 6-second period (see Figure 3-20). A Melton seismometer set at 6-second free period drives both a short-period and a long-period phototube amplifier. The outputs of the amplifiers are 180° out of phase at the free period of the seismometer, resulting in a notch at the 6-second period when the two outputs are summed. The solid lines in Figure 3-20 show the response before summing, and the broken line is the response after summing the amplifier outputs.
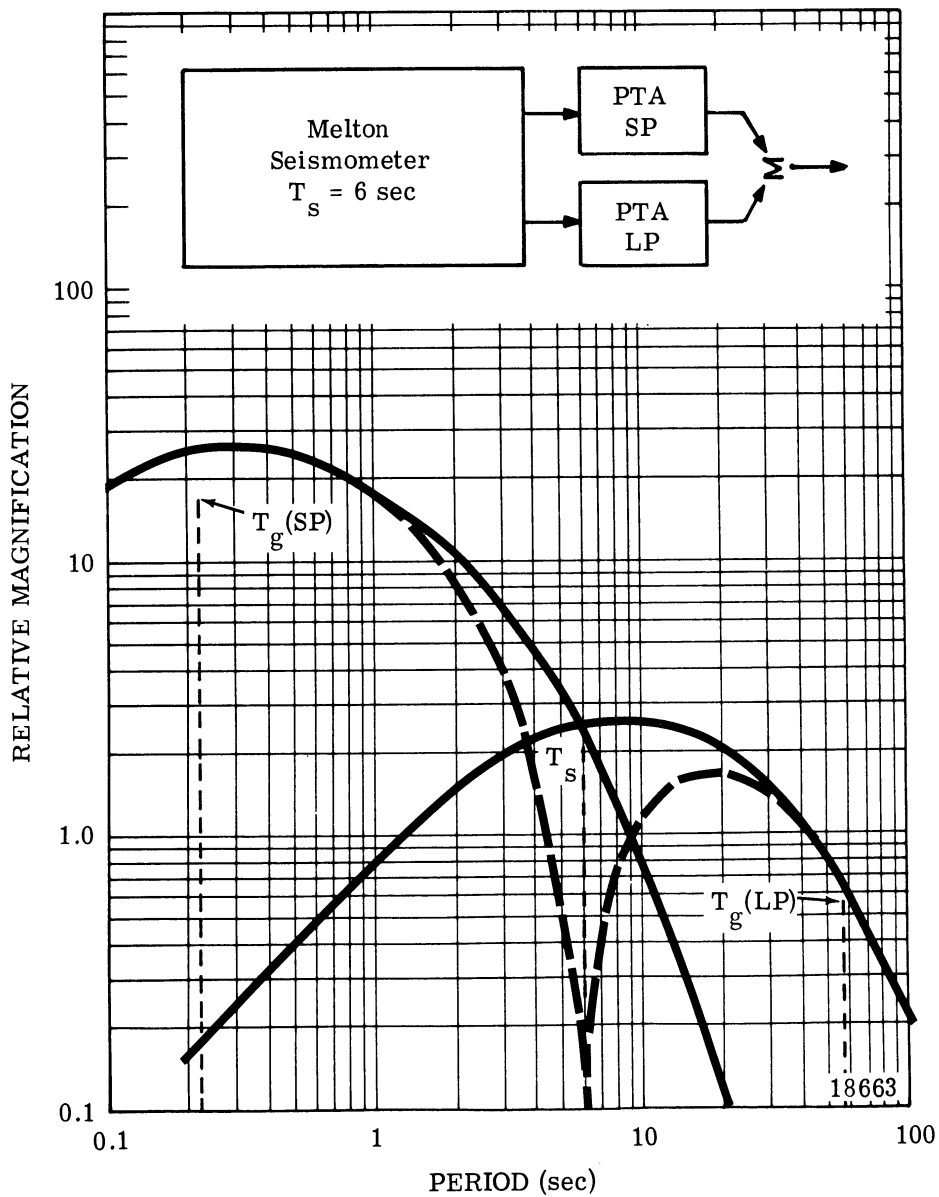
FIGURE 3-20. USE OF A MELTON SEISMOMETER IN A DUAL-GALVANOMETER
SEISMOGRAPH

REFERENCES

1. I. P. Passechnik and N. E. Fedoseenko, "Modernization of the SVK and SGK Type Seis-
   mographs," Bull. Acad. Sci. USSR, Geophys. Ser., 1959, No. 12, pp. 1294-1298.

2. D. P. Kirnos and N. V. Kondorskaya, "Computation of the True Value of the First Amplitude
   of Ground Particle Motion at the Arrival of a Seismic Wave," Bull. Acad. Sci. USSR, Geophys.
   Ser., 1958, No. 12, pp. 840-844.

BIBLIOGRAPHY

Geotechnical Corporation (Staff), Wichita Mountains Seismological Observatory: Report on
   Phase II, Technical Rep. No. 61-2, Contr. No. AF 33(600)-41318, The Geotechnical Corp.,
   Garland, Texas, 1961.

Geotechnical Corporation (Staff), Wichita Mountains Seismological Observatory: Report on
   Phase III, Technical Rep. No. 63-8, Contr. No. AF 33(600)-41318, The Geotechnical Corp.,
   Garland, Texas, 1962.

4
POSSIBILITIES AND LIMITATIONS OF THE DIRECT FM SEISMOGRAPHS

J. Cl. De Bremaecker
Rice University

INTRODUCTION

In the present paper we shall examine the advantages and limitations of each component of the direct FM system. We shall also give a typical example of the use of this system. Beforehand it is necessary to review briefly the scheme used (see Figure 4-1): it is the familiar push-pull capacitor transducers method. The heterodyned frequency is counted and constitutes the digital output. It also is converted into a voltage which drives two feedback circuits, one which greatly attenuates the very low frequencies, and one which does the same thing for the
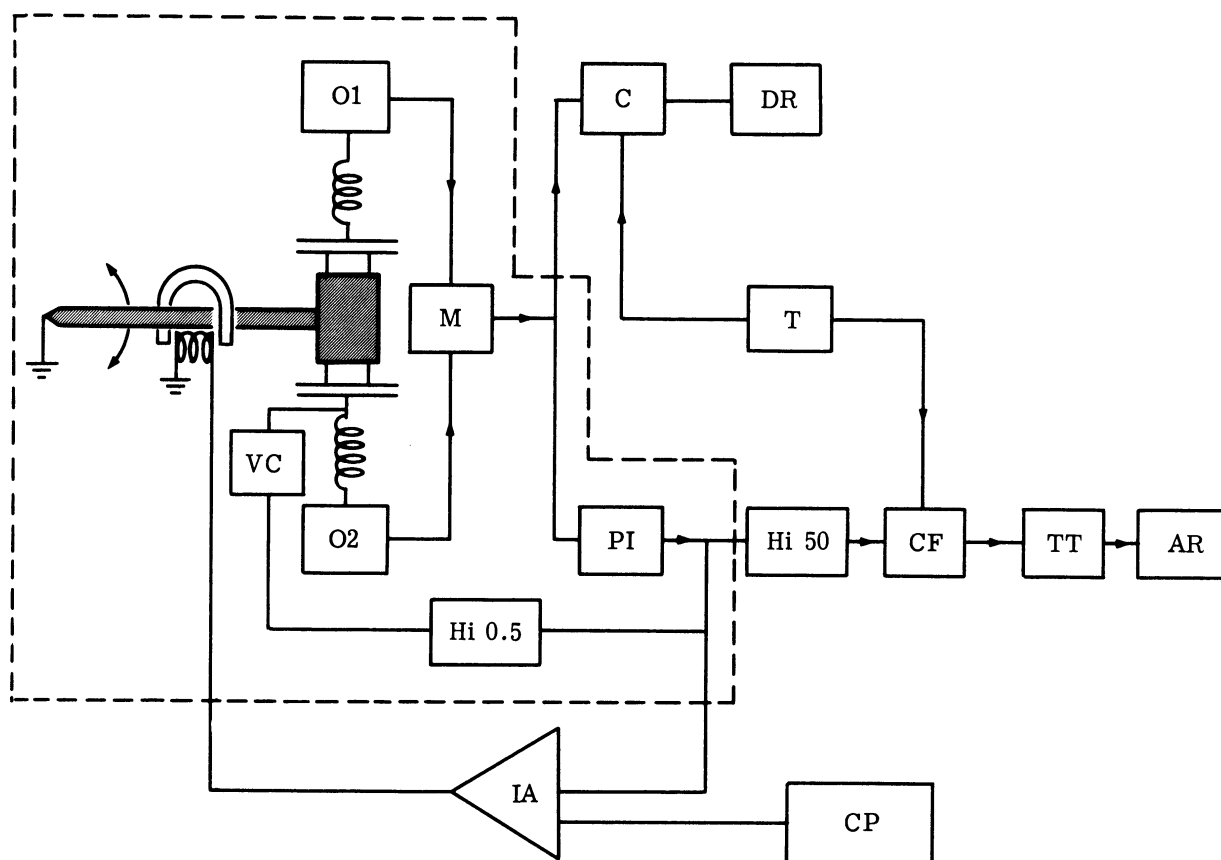
FIGURE 4-1. DIAGRAM OF ONE SEISMOGRAPH. O 1 and O 2, oscillators; M, mixer; VC, voltage variable capacitor; C, counter; DR, digital recorder; T, timing system; PI, pulse integrator; Hi 50, high-pass filter with time constant ~ 50 seconds; CF, cathode follower; TT, adjustable twin-T filter; AR, analog recorder; Hi 0.5, high-pass filter with time constant ~ 0.5 seconds; IA, integrating amplifier; CP, calibrating pulses generator.

very high ones. The first one is an amplifier with an RC network having a very long time constant; the other one is another amplifier and a high-pass filter. The latter drives a voltage variable capacitor (vari-cap) which opposes the short-period fluctuations of the instrument. This second filter was suggested by Mr. Miller from Texas Instruments.

THE COMPONENTS OF THE SYSTEM

(1) Seismometers

Because high frequencies are attenuated only by the vari-cap and by the counting scheme, parasitic vibrations of the instrument are more undesirable than in other systems. So far we have not noticed any undesirable effects. It is, of course, true that one cannot detect these effects subsequent to recording, but it is encouraging to find that the spectrum decreases to the detectable minimum near 8 to 9 cps. As there is no reason to believe that there is another increase in the spectrum at higher frequencies, the system appears not to suffer greatly from high-frequency problems. Better seismometers are nevertheless desirable. Willmore, in England, claims to have a vertical instrument of very long period (30 seconds), which uses leaf springs instead of coil springs and which has very few parasitic vibrations.[1]

(2) Transducers

The linearity of the transducers in the worst case is about 4%. A better linearity may be attained with more care, since one of our instruments is linear to less than 1%. This matter necessitates the trial and error method because of the parasitic capacitances etc., involved. It may be mentioned that this nonlinear behavior is probably present on many instruments equipped with velocity transducers, but cannot be easily detected on them, while our displacement transducers enable us to measure this phenomenon very easily, at least to the limit of the accuracy of the micrometers. At present the range of the transducers is set to ±0.3 mm. We had thought that this would be adequate, but we have recently found that it will be desirable to increase the range and decrease the sensitivity. This will enable us to read larger shocks without hitting the stops, and will be more suitable for our high background noise.

(3) Oscillators (O1 and O2 in Figure 4-1)

The stability of the heterodyned frequency was measured at the operating frequency, both by replacing the transducers with high quality ceramic capacitors and by resting the boom on supports (blocking it is not satisfactory). The peak-to-peak noise is of the order of 10 and the variance is below 1. This is higher than we would wish, and may be due in part to the noise

---

[1]As of January 14, 1964, it appears that this instrument may be manufactured and sold by Hilger and Watts at a later date.

associated with the vari-cap scheme. On the other hand, since we record 20 times per second and are normally interested in periods of say 1 second or longer, this noise is not as detrimental as it might first appear. It could be further decreased by appropriate redesigning of the circuits of the oscillators. All the preceding concerns the short-term noise. The drift over several days was very slow, about 400 cps around the heterodyned frequency of 500 kc. Since this drift is normally reduced by the feedback by a factor of 100, it is not important. Moreover, it may be pointed out that the same circuit has long been used in the Humble underwater gravimeter and is now used in the Lamont tidal gravimeter. Together, these factors give one a great deal of confidence in the long-term possibilities of the method. I might mention here that the seismographs are covered with styrofoam and are all in a thermostated enclosure (the dashed line in Figure 4-1).

(4) Pulse Integrator (PI in Figure 4-1)

This particular circuit is as linear as can be detected for about 0.9 of the total displacement and is about 5% off at the low end of the range. It is practically insensitive to fluctuations in the supply voltage, and the latter is held quite stable by trickle charging a battery through a magnetic voltage regulator which eliminates the sudden transients. It would be possible to use a digital-to-analog converter, but this would increase the cost without any certain benefits.

(5) Feedback Amplifiers (Integrating Amplifiers, IA in Figure 4-1)

These are a relatively delicate part of the circuit. We require a very long time constant in the feedback circuit, which means a high resistance (100 MΩ), necessitating here a high front-to-back resistance. On the other hand, if the characteristics of these amplifiers vary slowly (over several days, weeks, or months), this is not likely to be critical because they are in a feedback circuit rather than in a direct output configuration. We first used Philbrick USA-3's with satisfactory results. After about two years of continuous use these amplifiers deteriorated because of the high temperature generated by the vacuum tubes. They were still working, but their effective front-to-back resistance was well below 100 MΩ. They were thus unsatisfactory for this application, and we have replaced them with a transistorized Philbrick P-2 and P-5 (in series). Since these remain cool, they should last a very long time. The results with them are highly satisfactory.

In addition, a milliammeter located on a front panel enables us to monitor the feedback current in any component. When this gets excessively high we re-center the instruments by hand. This is very rarely necessary with the vertical (every six months at the most), but more frequently necessary with the horizontals because of the strong tilts characteristic of our very unstable location. The time constant in the feedback loop is 300 seconds, and the drift reduction is 100.

We have investigated the stability of this system, and it is easy to show that it satisfies the Hurwitz stability criteria even for much shorter time constants. Consequently it is expected to be stable, and this is confirmed by our experience.

(6) Damping

We use eddy-current damping and a copper vane. Coils with an adjustable resistance would clearly be preferable, but were not practical because of the design of the instruments we have used. As it is the system is satisfactory though not optimum.

(7) Calibration (CP in Figure 4-1)

We use the second input of the feedback amplifiers (these are differential amplifiers), and calibrate by sending first an exactly rectangular pulse 0.1 second long, then, after 4 minutes, another rectangular pulse 4 minutes long. While the short pulse theoretically yields the complete system response, it is advantageous in practice to have an input with more low-frequency energy to calibrate the feedback system, and this is the reason for the second (the long) pulse.

(8) Timing (T in Figure 4-1)

For analog purposes and for starting the digital system we use a tuning-fork Times Chronometer. The accuracy is satisfactory, but the contacts are not. We have replaced them with microswitches which are much more satisfactory. The master oscillator for the digital system is a Times tuning fork built to our specified frequency and is entirely satisfactory.

(9) Analog Recorders (AR in Figure 4-1)

After passing through a succession of filters to reduce the microseisms and the drift, the signals activate three Varian G-10 recorders. While these instruments are apparently the only ones suitable for this application at present, they are not adequate. They suffer from a number of faults, one of which is that they need to be operated without cover to keep them at a suitable temperature. Much more serious is the erratic behavior of their slide-wire potentiometers, which may cause "spikes," etc., but may, unaccountably, improve with age. A better recorder using a glass-type potentiometer (or a "stranducer" like Honeywell) and a transistorized circuit is very much needed.

We have successfully experimented with pens and now use a very fine stainless steel tube (ca. 3.3 mil i.d. to 5 mil o.d.) soldered into a larger tube. This is connected by a thin plastic tube to a reservoir and is fed by gravity flow. The ink supply is adequate for many months. Cleaning may be done with an appropriate thin wire if suction or compression is not successful.

(10) Frequency counters (C in Figure 4-1)

The counters for the seismographs are straight binary counters, 16 bits each, of which the least important one is not used at present. Instead, to fill the computer word of 54 bits, we use

a 9-bit frequency counter for the microbarograph. This instrument promises to be very valuable for our purposes.

(11) Associated Circuitry (DR in Figure 4-1)

Regardless of the digitization scheme, there are elements to perform the necessary logical operations. The gates to our main buffer memory are of a very special experimental type, prepared as an educational endeavor. They consist of small neon bulbs which are ionized and thus made conductive by an rf pulse. Experience has shown that this is not a satisfactory system because of the aging of the bulbs and their sensitivity to location in the rf field and to light. We plan to change to diode gates as soon as possible. The buffer itself consists of capacitors. The rest of the logic is trouble free.

(12) Tape Transport

We use a Honeywell 3160 tape transport adapted for 3/4-inch tape and 0.4 in./sec. The speed is very precise and the head is perfectly aligned in both azimuth and position. All this is important since we record at 400 bits/in./channel. We noticed after 6 months, however, that a certain amount of skew suddenly appeared, which made the records useless. It appears likely that the change in the surface properties of the magnetic tape caused by repeated use is partly responsible for this. The remedy is simply to change the threading of the tape to provide better guidance. It is not sufficient to have the tape pass on the top wheel equipped with a flywheel. Since this flywheel is useless at these slow speeds, nothing will be lost by the change.

(13) Checks

When changing tapes it is possible to turn a switch which checks the operation of almost all the elements of the system and turns on a red light if one element fails. So far the gates have been the only elements which have failed.

(14) Barograph

This consists of a microbarographic capsule made by Geotech according to NBS specifications. We have installed a transistorized Clapp oscillator on it and bring the rf down by coaxial cable. An analog recording similar to the seismographic record is obtained.

(15) Tape Format

The tape format is nonstandard, but it presents such advantages that it should be briefly discussed. The tape contains ten tracks of which two are clock tracks. The writing is done in the phase-modulation method. The clock tracks are normally 180° out of phase, but are put in phase during one word every 30 seconds. We refer to these 30-second periods as "blocks," and the phase relationship is sensed by the computer when it searches for a block. This method has two main advantages:

(a) No gaps are necessary on the recording; the tape is directly acceptable by the computer, which can start reading at any place. After reading and stopping, it can return to the beginning of the block and read again.

(b) If the recording is imperfect in one spot the computer will not get completely out of step. It will read either 30 seconds (or multiples of 30 seconds) too early or too late, but it always reads exact words, not part of one and part of another. This is extremely important in a continuous data acquisition system, and accounts in part for our low number of errors. It is possible to make the blocks 1 minute long by turning a switch, but this is not desirable at present because of the memory limitations of the machine.

SOME ADVANTAGES AND LIMITATIONS OF THE SYSTEM

(1) Counters and Voltmeters

It appears that counters are inherently simpler than digital voltmeters, since time appears easier to measure than volts. Binary counters are of course the simplest variety. These are inherently stable and precise, and never need calibration, unlike most high-precision voltmeters. On the other hand, the high frequencies cannot be filtered as sharply as a voltage output.

(2) Low-Frequency Response

It is clear that displacement transducers have an advantage over velocity transducers at low frequency. This is indicated in Figure 4-2, Curve 6. The necessity of using feedback decreases this advantage, however (cf. Figure 4-2, Curve 5). It has been mentioned that we need to reduce the drift by 100 because of our very unstable location. This is by far the largest reduction that has been attempted while maintaining a good low-frequency response. It is possible to use less feedback on the vertical instrument, but we generally prefer a nearly matched set of instruments. Naturally, as the drift reduction decreases, the time constant of the feedback loop may increase proportionately, thereby passing longer and longer periods.

As an extreme example, Figure 4-3 shows an analog recording made without using feedback, but by using the amplifier and low-pass filter to drive a recorder. One clearly sees the lunisolar attraction. An earthquake in Mexico, $M = 7.25$, is visible both on this record and on our more conventional analog record (Figure 4-4). The digital record may of course be filtered to give either of these. More recently the Kurile Island shock gave us the record shown in Figure 4-5, obtained by filtering the digital output. In this case the boom hit the stops rather frequently, so that the precision of the record is uncertain.

(3) High-Frequency Response

The high-frequency response is limited by the folding frequency of 10 cps and by the attenuation in high frequencies resulting from both the counting and the vari-cap scheme. With

60
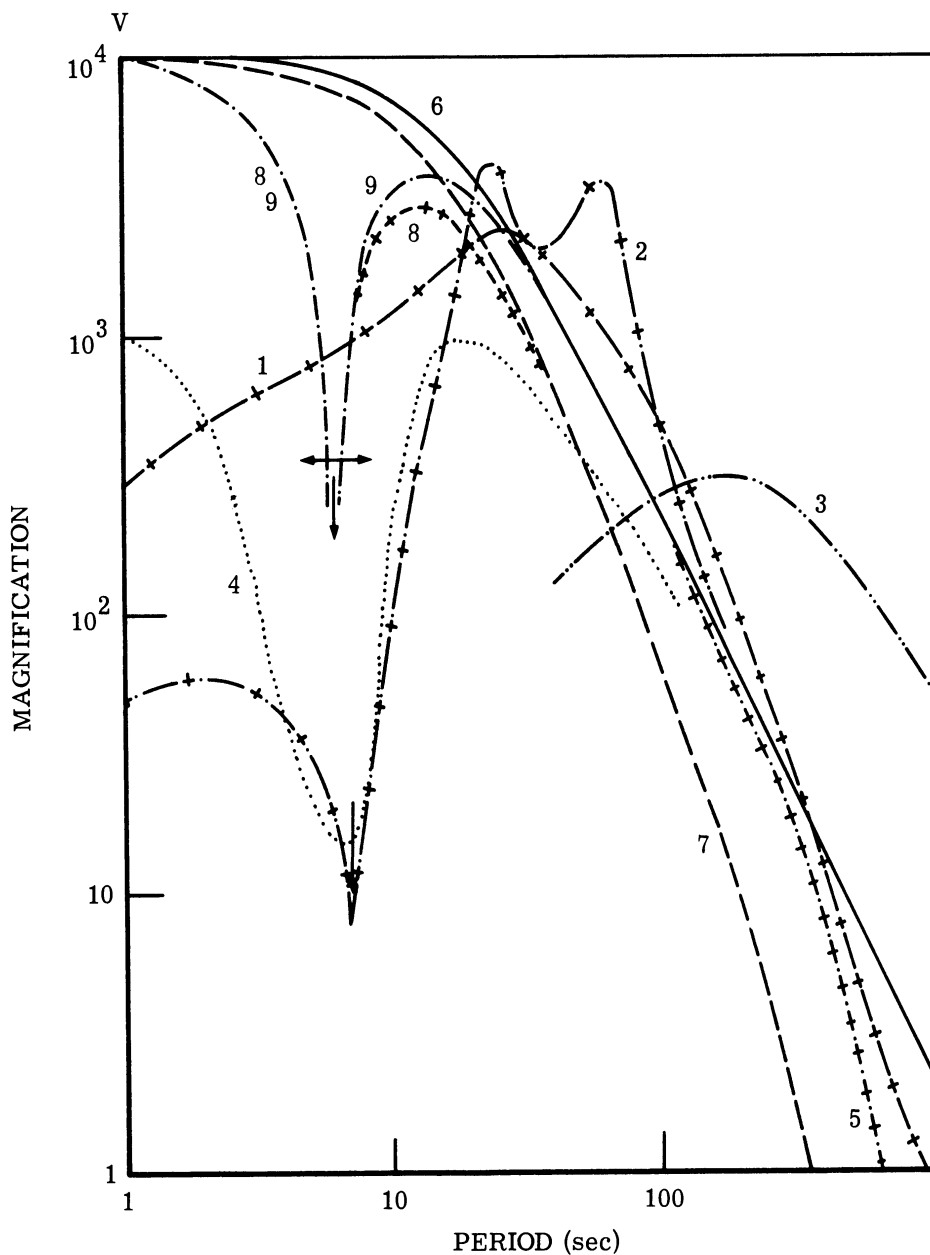
FIGURE 4-2. MAGNIFICATION CURVES FOR VARIOUS INSTRUMENTS. (1) 30-second pendulum, 90-second galvanometer (after Gilman, 1960). (2) 30-second pendulum, 100-second galvanometer, 6.7-second filter galvanometer (Pomeroy and Sutton, 1960). Only the relative magnification is correct; the absolute magnification was not given. (3) 60-second pendulum, 480-second galvanometer, 200-second low-pass filter (after Gilman, 1960). (4) Inverse of the noise (after Brune and Oliver, 1959). (5) Digital output of the Rice seismograph with feedback. Drift reduction 100; 400 cps/μ correspond to V = 10,000, 40 cps/μ to V = 1000, etc. (6) Digital output of the Rice seismograph without feedback (same scale as 5). (7) Analog output of the Rice seismograph with high-pass filter only. V_0 is taken as 10,000. (8) Analog output of the Rice seismograph with high-pass filter and twin-T filter. V_0 is taken as 10,000. The notch can be moved from about 1 second to about 6.3 seconds. (9) Analog output of the Rice seismograph with only twin-T filter. Curves 8 and 9 are virtually identical to the left of the notch.
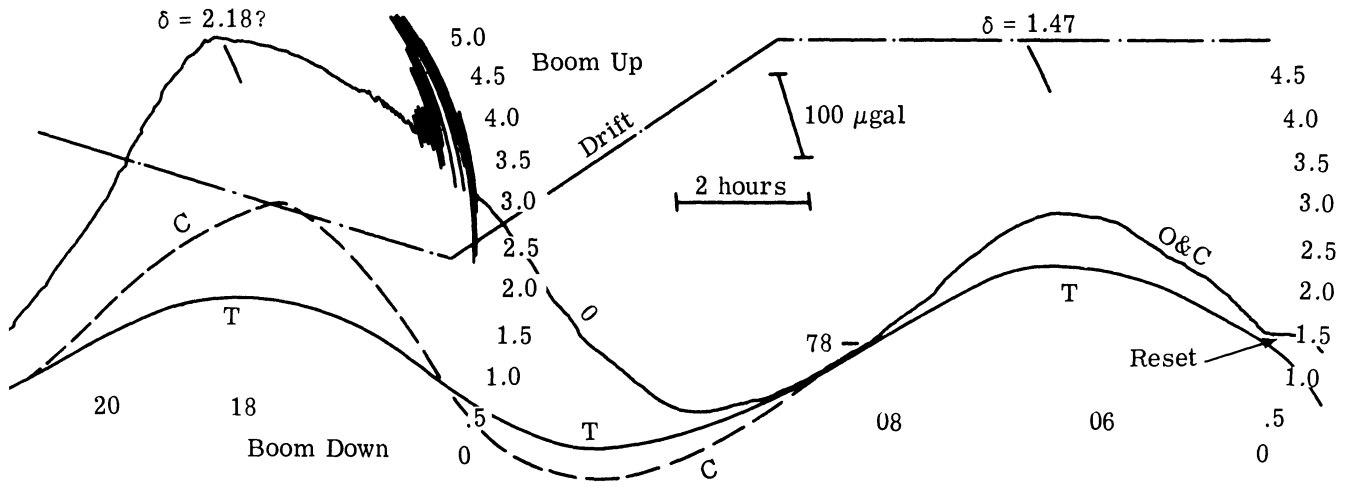
FIGURE 4-3. RECORD SHOWING THE LUNISOLAR ATTRACTION OF A RICE VERTICAL SEISMOGRAPH. The prominent disturbance is a Mexican earthquake on May 19, 1962, M = 7 to 7.5. O, observed tides; T, theoretical tides for a solid earth; C, curve O corrected for drift; δ, ratio of C to T at the maximum. The drift curve is approximate.
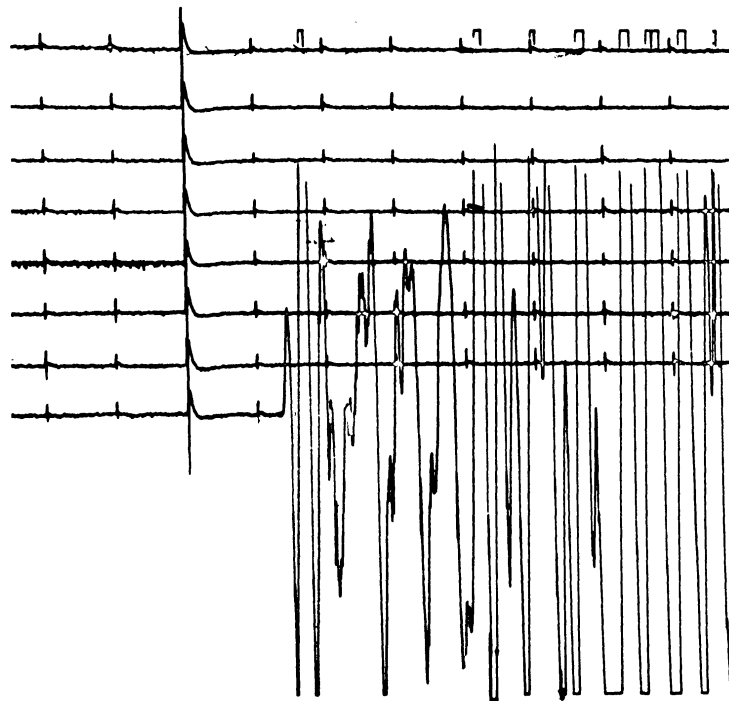
FIGURE 4.4. ANALOG RECORD OF THE VERTICAL SEISMOGRAPH FOR THE MEXICAN EARTHQUAKE, M = 7.25.
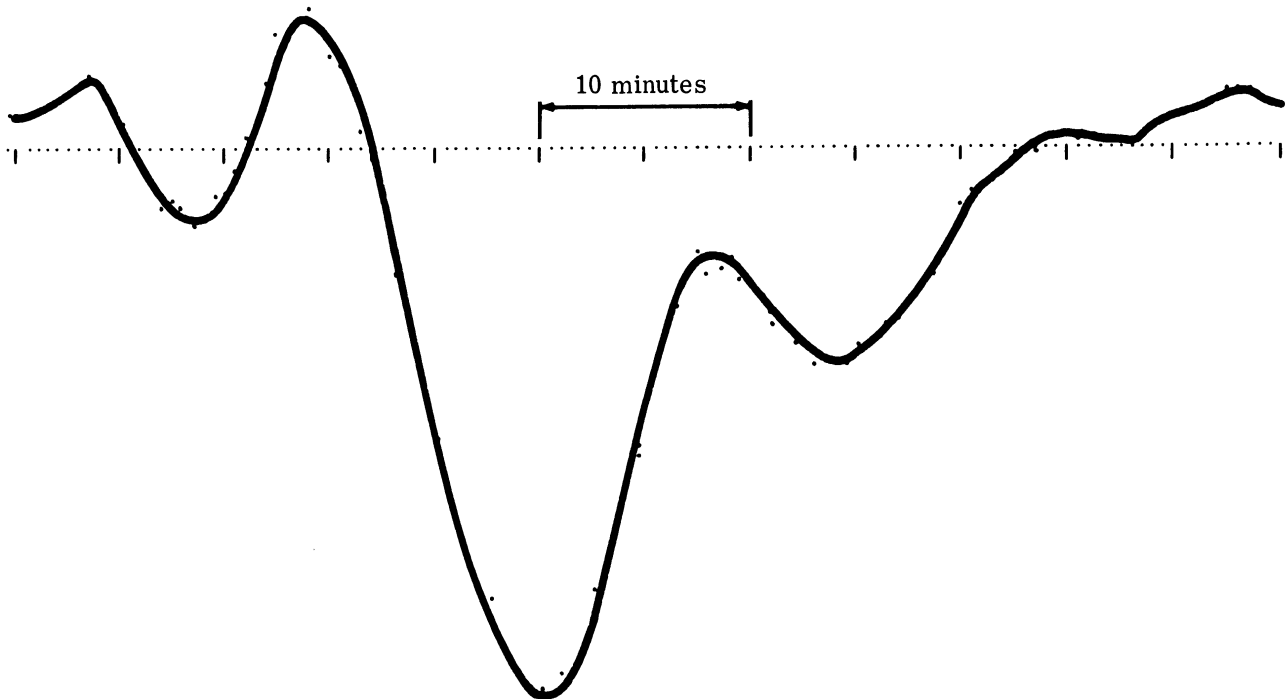
FIGURE 4.5. FILTERED DIGITAL RECORD OF THE VERTICAL SEISMOGRAPH FOR A KURILE ISLANDS
EARTHQUAKE: ULTRA-LONG-PERIOD RAYLEIGH WAVES

earthquakes, the limitations do not appear to be serious. For instance, Figure 4-6 shows our
analog records and the higher and lower frequencies recorded digitally. The ground amplitude
was about 300 mμ; so it is clear that amplitudes a good deal smaller than 100 mμ can be re-
corded quite clearly.

(4) Data Handling

We have already mentioned advantages of our recording format. It should be added here
that the possibility of automatic correction of errors in recording is a very substantial advan-
tage of digital operation. In analog recording a spurious signal, caused by, for instance, flaws
in the magnetic tape, may seriously compromise a part of the record. We have found our cor-
rection scheme fast and efficient, and it is an integral part of our reading subroutine. Reading,
checking, and correcting four minutes of data takes about 10 seconds per component.

The advantages of filtering without phase shift are fairly obvious. This, of course, is also
possible with the analog format. Indeed, it is done routinely in the oil industry, though it is
somewhat laborious. It is very simple digitally. However, the computer time is approximately
proportional to the periods desired, and this creates serious problems even if one uses Cheby-
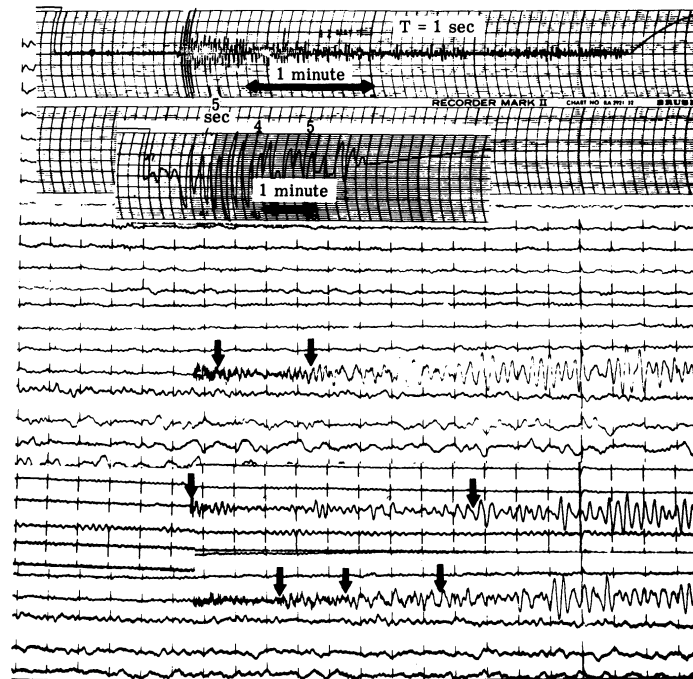
FIGURE 4.6. ANALOG RECORDS (BOTTOM) AND DIGITAL RE-
CORDS OF THE HIGHER AND LOWER FREQUENCIES (TOP) FOR
AN EARTHQUAKE OF MAY 13, 1962

shev filters which are optimal for a given length. For this reason we often use double or mul-
tiple summation filters. These multiply the speed by at least 50 for three reasons: (a) they
can use fixed-point arithmetic; (b) they use additions rather than multiplications; and (c) they
reduce the number of operations. One makes the long summation just once, and then adds ele-
ments at the "tail" and subtracts elements from the "head." Thus, the time used in filtering
becomes independent of the periods desired. In practice we filter and decimate simultaneously.
The summations are of slightly different lengths to reduce the sidelobes. In this way, with a
machine whose speed is between that of an IBM 709 and a 7090, we can filter four minutes of
data in about 10 seconds. It is clear that high-pass filters can be constructed in the same man-
ner. We sum by about 10 K, while decimating by $\sqrt{K}$; then, we sum the decimated data by about
12 $\sqrt{K}$ while decimating again by $\sqrt{K}$. This appears satisfactory, but other decimations factors
might be equally good.

(5) Automatic Reading of First Arrivals

Taking the first differences between successive points, we multiply the spectrum by the
frequency. It appears, at present, that a judicious use of the lengths and number of summations
followed by differencing can produce a filter reasonably close to the inverse of the recorded

64

noise for frequencies below the microseismic maximum. These operations are thus more or less similar to optimum filtering, and we have used them successfully for the automatic detection of first arrivals.

We have also attempted to construct a logical scheme which reads the whole seismogram. At present this scheme is about as satisfactory as an inexperienced human observer, which is not too bad a beginning. The idea is to detect arrivals which follow a reasonably long quiet period, but what is "reasonably long" is not very clear. The problem is complex, as shown even by the fact that "experience" is needed by a human observer.

CONCLUSIONS

One point should probably be emphasized in concluding: recording continuously on magnetic tape is much more difficult than doing it only when everything is ready. Many things can go wrong which one cannot possibly foresee, from tape skewness to fuse blowouts, from relay failures to overheating. Many of these problems depend little on the mode of recording, but the direct FM scheme appears to minimize the number of avoidable problems.

5
METHODS OF DIGITIZING EARTH MOTION[1]

R. F. McMurray
The Geotechnical Corporation

INTRODUCTION

When observed with seismographs available today, the particle motion resulting from events at large epicentral distances can be described by continuous mathematical functions. Even though modern narrowband seismographs are capable of resolving earth motion on the order of 10^{-10} meter, no natural quantized motion appears to be involved. While the term "digital seismograph" has been used, examination of any instrument so named has shown a mechanical device and some type of converter to change the mechanical motion of the instrument into a digital output. Desirable as they may be, truly digital seismographs have not yet been devised.

To use the language of computer men, "analog" will here refer to both the continuous mechanical motion of the instruments and the electrical signals that represent it. In this context, analog-to-digital (A/D) converters, or encoders, will be discussed. A/D converters will be classified in two groups, mechanical and electrical. The mechanical group is composed of converters which depend on a mechanical standard for comparison. The usual standards are code discs or plates that convert rotation or translation into discrete numerical values, and incremental encoders that convert motion into incremental stops which can be counted by auxiliary means. Converters in the electrical group change electrical voltage or frequency analog signals into discrete numerical values. Incremental transducers that produce electrical pulses by interferometer techniques are also placed in this group, but could just as well be classified as mechanical.

MECHANICAL CONVERTERS

Let us first consider the mechanical group, exemplified in Figure 5-1. Typically, we have a seismometer and low-level amplifier sending a control signal to a servomechanism. The servomotor shaft turns a code disc in a direction commanded by the control signal. The mechanical layout of the pattern on the code disc represents a desired code, with numerical value being a function of shaft angle. Reading the pattern optically or electrically at discrete times provides a digital output. To complete the loop, a digital-to-analog (D/A) converter provides a feedback signal to null the input signal when the proper position on the code disc is reached.

---

[1]Tech. Rep. No. 63-113, The Geotechnical Corp., Garland, Texas, 1963.
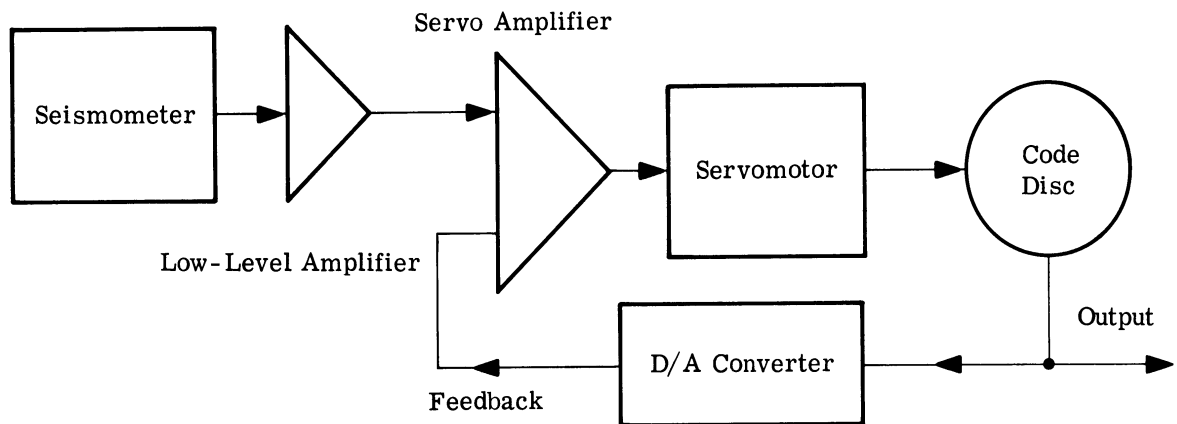
FIGURE 5-1. SIMPLIFIED TYPICAL SERVOMECHANISM CODE-DISC CONVERTER

Feedback from a linear potentiometer can be used instead of that from the D/A converter to reduce cost.

The servomechanism converter can have very high accuracy or resolution, depending on the code disc and servomechanism used, and has been used in long-period systems. Code discs (see Figure 5-2) with an 18-bit resolution have been reported by the Baldwin Piano Company of Cincinnati. A disc with this resolution will have 1/4 million divisions on its outside ring. Various codes with almost any lesser resolution can be provided on the discs. Code plates are the linear equivalents of the discs, and their applications are similar in principle.

(a)   (b)
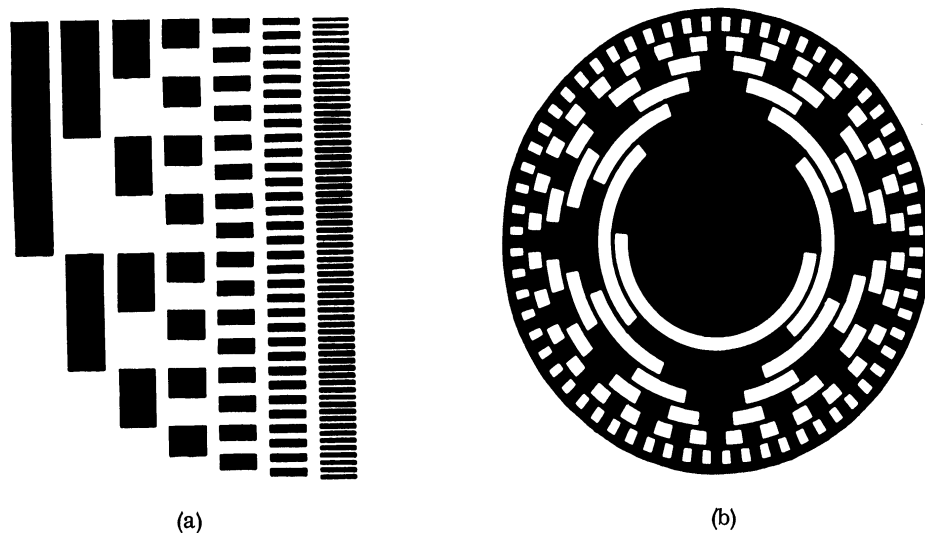
FIGURE 5-2. (a) TYPICAL SPATIAL CODING MASK LAID OUT ON A
FLAT RECTANGULAR SURFACE. (b) SEGMENT OF A SPATIAL BINARY
CODING MASK LAID OUT RADIALLY ON A WHEEL [1].

The disadvantages of this system are its slowness in operation compared to electrical techniques, its relative expensiveness, and its probable unsuitability for short-period use.

The incremental shaft-angle encoder divides rotational motion into steps, which are determined by a variety of methods as the trade names of the devices (e.g., Optisyn, Inductosyn) suggest. Figure 5-3 is a simplified block diagram of a typical incremental converter. The input to the encoder can be driven by a servomechanism as previously described. For simplicity, feedback of shaft position to the servoamplifier is assumed to come from a potentiometer-type control connected to the motor shaft, but other means can probably also be employed.

Incremental Encoder
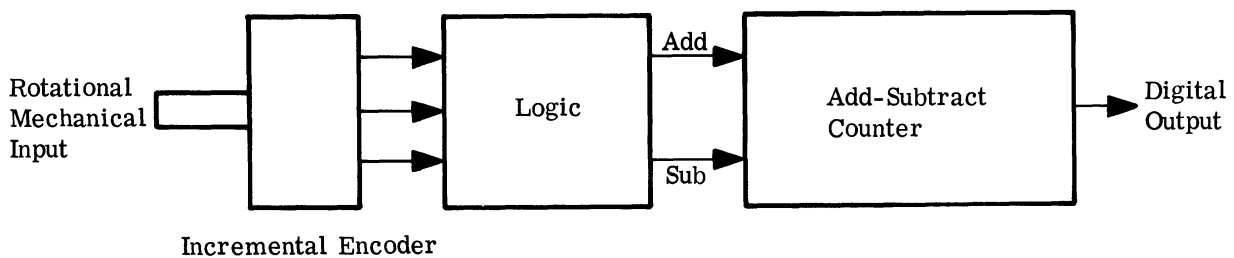
FIGURE 5-3. SIMPLIFIED TYPICAL INCREMENTAL DIGITIZER

ELECTRICAL CONVERTERS

When one looks at electrical A/D converters, which are the more prevalent in use, one finds a variety of systematic methods. Only the most common will be touched on briefly here; the serious investigator is referred to the Bibliography for additional information. The method considered by the author as most straightforward and easily understood is illustrated by Figure 5-4. In this arrangement, the sample-and-hold amplifier takes a sample of the analog signal on command and stores it, usually in a capacitor. The time for this act should be insignificant (1 μsec is typical) when compared to the period of the highest data frequency. While the amplifier holds the voltage sample and waits for the next command, the A/D converter produces a number proportional to the sample voltage in some desired code. The whole process may consume less than 100 μsec in a typical case. Where it is desired to digitize multiple analog signals, time sharing of some of the equipment is possible (see Figure 5-5). While the control logic becomes more complex, time sharing often saves enough to permit use of high-accuracy, high-speed equipment. The selector switches are usually high-speed solid-state circuits in modern systems. If it is important to the data collector to have all channels sampled simultaneously, a separate sample-and-hold amplifier will be required for each input, but the A/D converter can still be time shared.
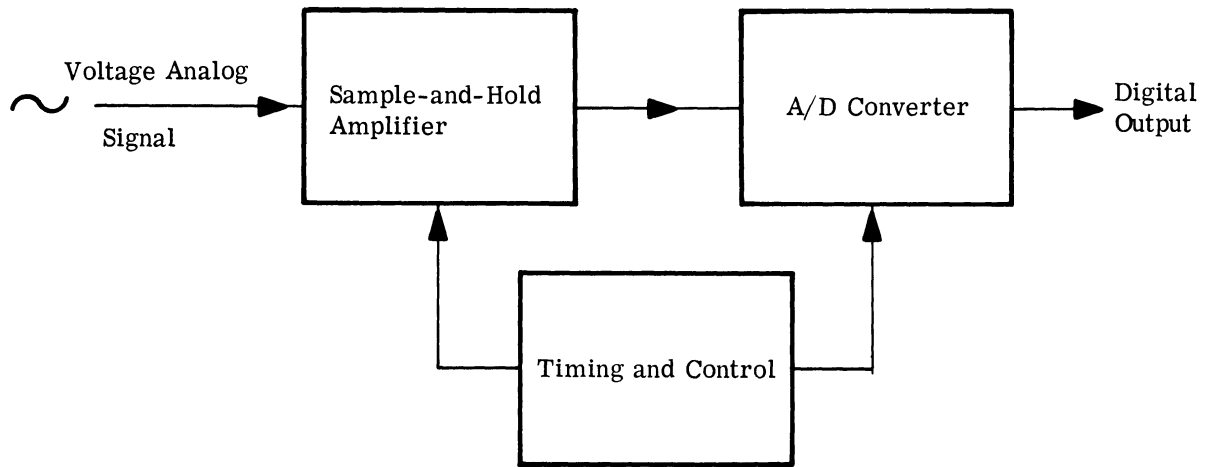
FIGURE 5-4. TYPICAL ELECTRICAL A/D CONVERTER WITH SAMPLE-AND-HOLD AMPLIFIER
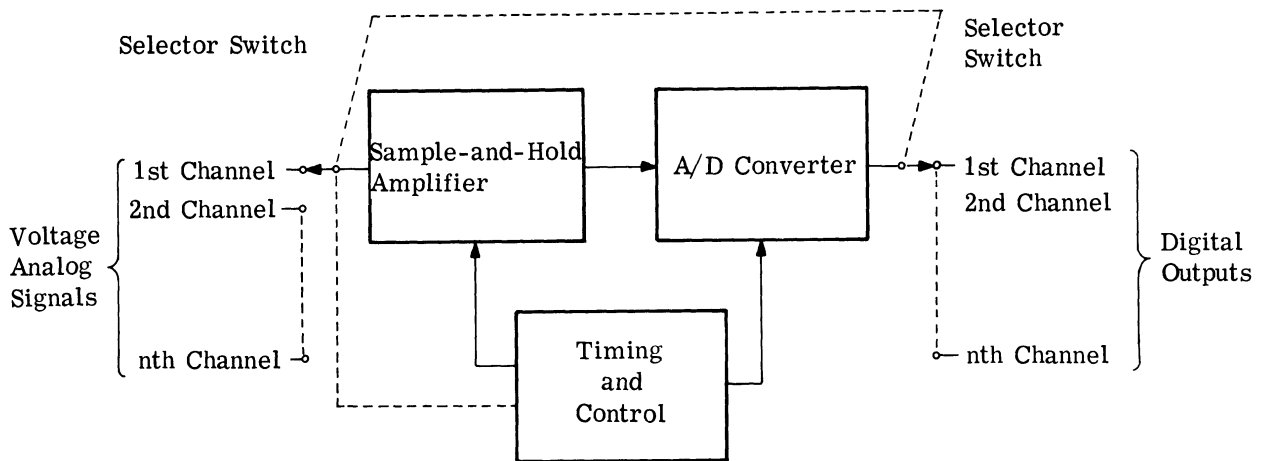
FIGURE 5-5. SIMPLIFIED TYPICAL ELECTRICAL A/D CONVERTER WITH SAMPLE-AND-HOLD
AMPLIFIER AND WITH TIME SHARING

One of the most common methods of converting a voltage analog to a numerical value is to use a voltage waveform whose amplitude changes linearly with time (a ramp) in combination with a precision frequency as a standard of comparison (see Figure 5-6). The voltage analog is applied to a comparison amplifier. On command of the control, the linear ramp is started and the counter gate opened. When the ramp voltage equals the voltage analog, a stop pulse closes the counter gate, and a number proportional to the analog is in the counter. After the number is read out by means not shown in the diagram, the control resets the counter to zero, and the process is repeated. The method is relatively straightforward and easily instrumented.
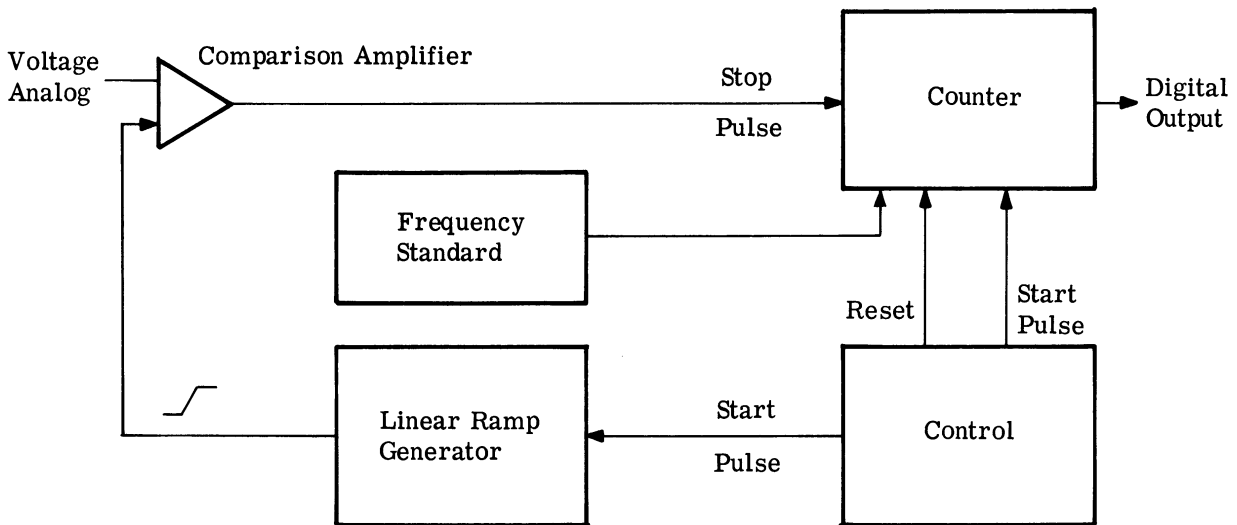
FIGURE 5-6. TYPICAL ELECTRICAL A/D CONVERTER USING A LINEAR VOLTAGE WAVEFORM AND A
PRECISION FREQUENCY AS A COMPARISON STANDARD

Conversion accuracy depends on the linearity of the ramp waveform and the stability of the fre-
quency standard. Conversion time is relatively long.

Figure 5-7 shows a variation of the method, using a precision power supply, a precision
attenuator, and precision switches to form a D/A converter, or decoder. The D/A converter
output is used as the standard of comparison. The significant difference between this method
and the one just described is that the linear ramp generator in the latter has been replaced by
a D/A converter that generates a staircase waveform as the count accumulates in the counter.
The accuracy of this converter is established by the comparison standard, and the conversion
time is the same as for the previous method. It is interesting to note that a precision frequency
is not required in this method, nor need the staircase be linear. The only requirement is that
for each count of the oscillator frequency, a precision amplitude step be produced.

The method diagrammed in Figure 5-8 is usually called the "successive approximation"
method. The timing and control logic block is the significant component. First it puts a "one"
in the most significant position in the register, causing a voltage equal to half of full-scale to
appear at the output of the D/A converter. If the voltage analog is less than half of full-scale,
a negative output is obtained from the comparison amplifier; if the voltage analog is greater
than half of full-scale, a positive output occurs. The control circuit logic then senses this pos-
itive or negative output and makes a decision. If the output is negative, it replaces the "one"
in the most significant bit with a "zero;" if it is positive, it leaves the "one." In either case,
it puts a "one" in the second most significant bit position. This bit represents the one-fourth
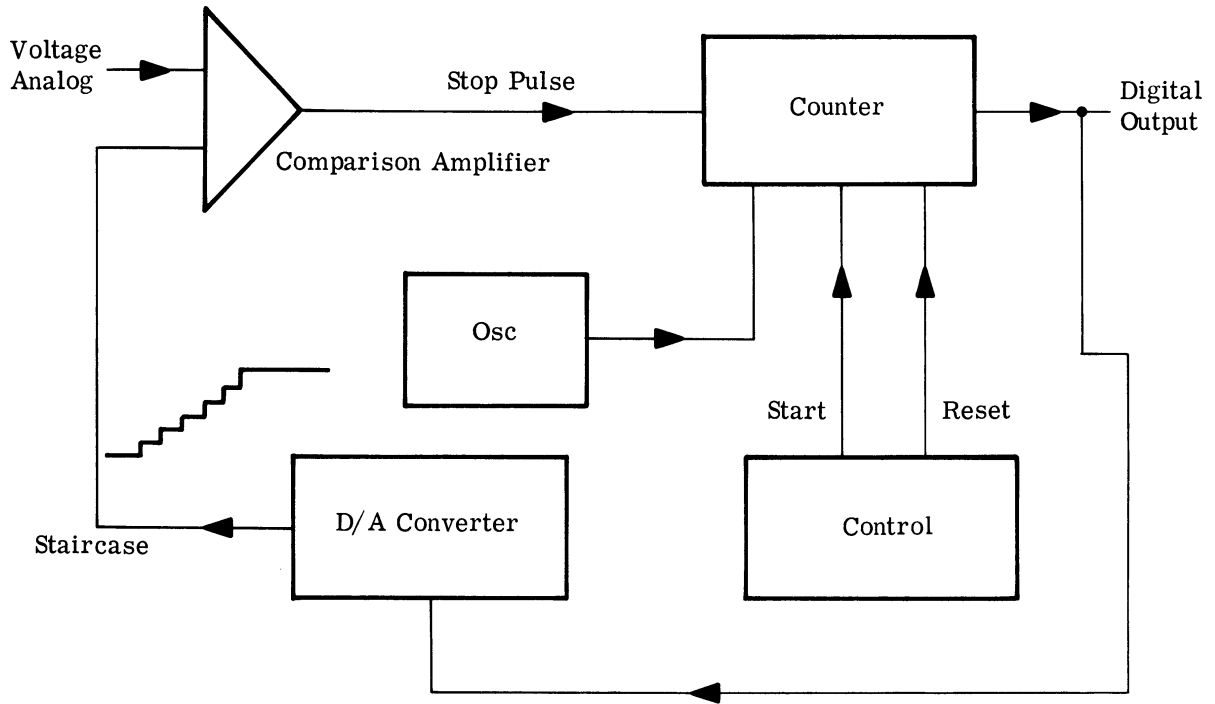
FIGURE 5-7. ELECTRICAL A/D CONVERTER USING A D/A CONVERTER AS A COMPARISON STANDARD
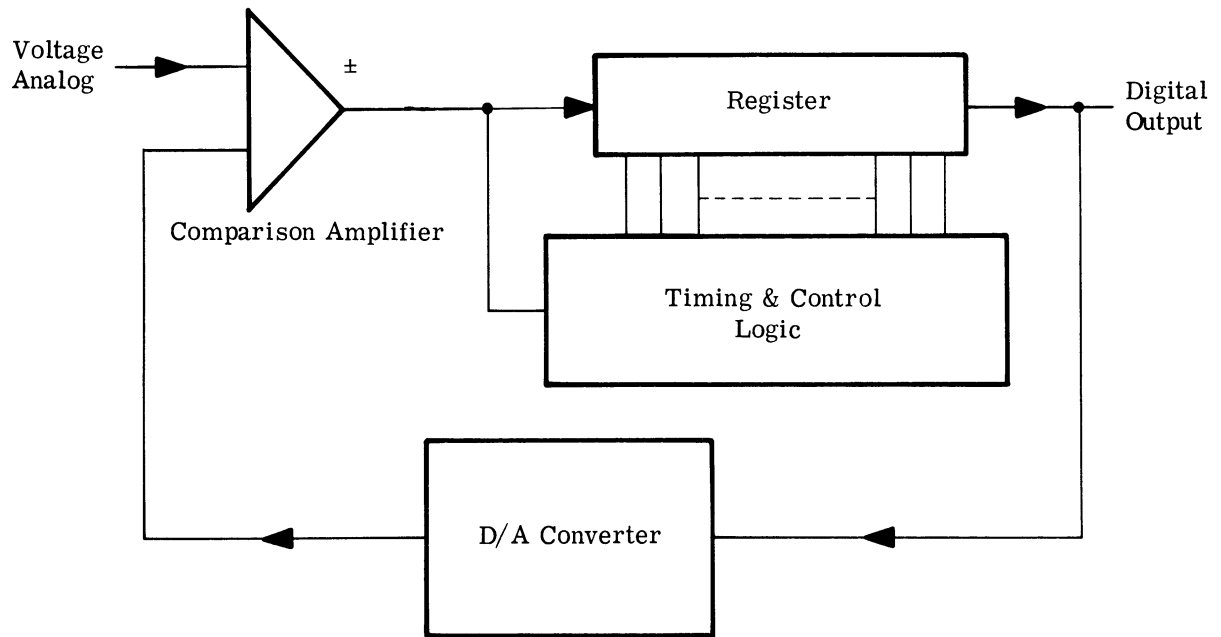
FIGURE 5-8. ELECTRICAL A/D CONVERTER USING THE SUCCESSIVE APPROXIMATION METHOD

of full-scale value, and it is either left "one" or replaced with "zero," again according to the output of the comparison amplifier. The process continues in this manner until every bit in the register has been examined. The voltage at the output of the D/A converter comes nearer and nearer to the voltage analog as the process continues. The principle advantage of the successive approximation method lies in the speed of conversion. Whereas the two methods just previously described require 2^n -oscillator or "clock" pulses for a complete conversion of n bits, the successive approximation method requires n + 1 clock pulses. To illustrate this capability, one company claims a conversion speed of 15 million 7-bit samples per second. With this, it is possible to digitize the complete output of a modern seismic observatory using a single, time-shared converter, with time to spare. What one then does with the data will be discussed later.

The next converter to be considered is the incremental interferometer type for directly digitizing mass motion. Gerrard [2] discussed one intriguing method of converting mass motion into digital output (see Figure 5-9). He postulated a quartz oscillator radiating 500-Mc acoustic waves into air. The waves impinged on the mass of an inertial seismometer and were reflected to the source radiator. As the mass moved, the reflected waves interfered with the radiator and changed the impedance that it saw. Because of very sharp resonance in the quartz oscillator, a radical change in loading was seen by the electronic driver. Radical changes in plate or collector current to the tube or transistor were observed and counted. Each incremental pulse represented the mass motion necessary to change the length of the path by one acoustic wavelength. In Gerrard's example, this distance was about 300 mμ. The author does not know if any further work was done with this idea, but, if it was, the results would certainly be of interest.
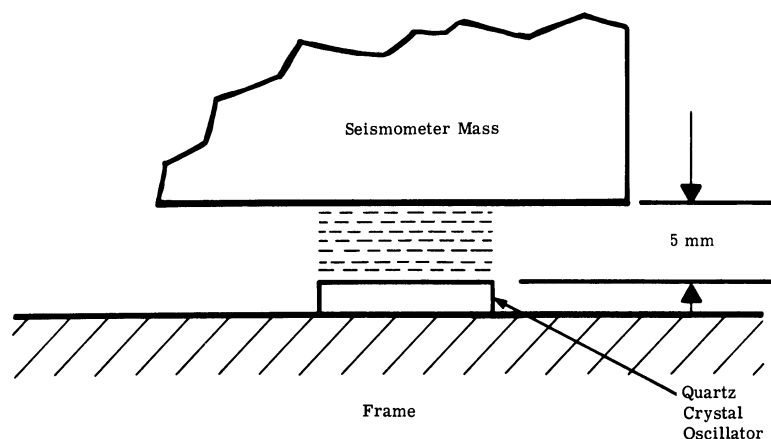
FIGURE 5-9. INCREMENTAL INTERFEROMETER TRANSDUCER USING
ACOUSTIC-WAVE INTERFERENCE

Another often proposed converter of the electrical type, diagrammed in Figure 5-10, uses a frequency analog (FM carrier) derived from mass motion. The simplicity of the method is appealing, and it has been used successfully in experimental long-period seismographs. There is, however, an accuracy limitation in this method caused by averaging the count over a finite counting period. As the counting period becomes short compared to the data frequency (1/30), the accuracy of a given sample approaches that obtained by a sample-and-hold amplifier. To obtain good resolution then, the carrier frequency must be quite high ($\times$ 30,000) compared to the data frequency. These problems are not insoluble, however, and the future may see greater use of the method, primarily because we can measure frequency with greater precision and ease than any other variable.

Frequency
Analog
→ Counter → Digital Output

Timing and Control
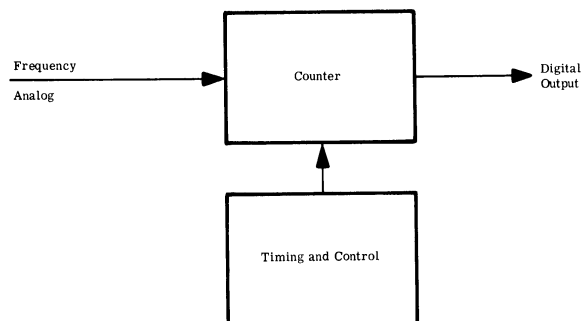
FIGURE 5-10.   ELECTRICAL A/D CONVERTER
USING A FREQUENCY ANALOG SIGNAL

CAPABILITIES OF VARIOUS DIGITIZING METHODS

At this point, the relative capability of the various methods presented can be discussed briefly. Under any given circumstance, one of the methods may be more expeditious than another, but, at the present time, the author believes the sample-and-hold, then conversion, method to be the least likely to cause data processing problems. Knowing the exact time the sample was taken and the accuracy with which it was converted is of indisputable value in data processing.

In any digital data collection system, there are three related parameters of interest: the dynamic range of the numbers, the resolution of the system, and the accuracy of the system. If we define dynamic range as measured from the long-term peak-to-peak noise in the data passband to the maximum peak-to-peak value a system is capable of handling, then this author has not observed a seismograph with a ratio much in excess of 10^4 or 80 db. The seismometer range may exceed this value by as much as 40 db, but the electronics following usually limit the

range anyway. The greatest range the author has seen claimed for voltage-to-digital converters is 2^{14}, or slightly over 80 db. Thus, digitizing an electrical analog with an 80-db range is possible if the full-scale amplitude of the analog is at least equal to the full-scale rating of the converter (usually 1 or 10 volts).

The resolution of a data collection system is limited by the value of the least significant digit or by noise, whichever is greater. The accuracy of a data collection system is probably not as important as most digital designers would be led to believe if asked to produce a 14-bit system. Under the best of circumstances, the absolute accuracy of seismographs measuring earth motion is probably such that errors exceeding 5% of full-scale value are common. Under ordinary circumstances, the error can easily become as great as 30%. Thus, the primary requirement should be for the linear error function to be well-behaved and smooth. An accumulated error of 1% of full-scale is probably insignificant if other factors are satisfactory.

For a moment, let us suppose that we wished to digitize on a continuous basis the entire analog output of WMSO. There are approximately 30 short-period and 20 long-period data channels. Using round numbers, let us assume 25 samples per second required for short-period signals and 1 sample per second for long-period signals. This yields a total of 770 samples per second for seismic data, excluding time data. Suppose we are satisfied with a full-scale range of 10 bits (60 db) for our numerical values because, if we are lucky, this will permit a sample to be sectioned into two characters on computer tape. If 556 characters per inch are used for packing density, approximately 3 inches of tape per second will be used, neglecting blocking, etc. This would require about 10 reels of computer tape per day. The odds are that we would not be this lucky or this efficient, and it would not be surprising if we used a reel per hour. Processing this amount of tape in a computer may be feasible, but it would require a highly sophisticated data processing system. The point, then, is that digital output requires digital recording if it is to be of use in a computer, and there is usually an elaborate editing procedure involved before even long-period data is presented for processing.

Thus, a search for high packing-density recorders is in progress. While magnetic tape recording is highly developed for both analog and digital data, several persons have suggested that photographic film may be a better recording medium for digital data. We have compared the two media and found that the fundamental limitations of minimum magnetizable particles of tape and minimum grain size of film are obscured by the practical limitations of recording and reproduction devices. For example, Eldridge and Baaba [3] recorded and reproduced a half-million bits to the square inch of tape by constructing a single-track tape head with a 1-mil track width, and spacing the tracks 2 mils apart across the tape. Lengthwise, they recorded 1000 bits to the inch. The single-track head was positioned across the tape with a

micrometer screw. Other experimenters [e.g., 4] have concluded that, to at least 90,000 cycles per inch, there is no fundamental limit to the resolution observed. Practically, however, tape width is controlled to only 4 mils (0.4% on 1-inch tape) because of mechanical design problems. This, compounded by guiding errors and the problems of constructing multitrack heads, makes it impractical to build a 500-track tape recorder-reproducer. The maximum number of tracks thought practical for digital recorders is 32 for 1-inch tape, though 64-track digital recorders might be constructed with difficulty.

Similarly, the fundamental limit for recording high density on film is related to grain size of the silver halide particles. While the author does not have information on experimental digital recording results, if any are available, a typical fine-grain film would probably permit packing densities on the order of 32,000 bits/mm^2 or 20 million bits/inch^2. Limitations of guiding, optical magnification and reduction, photocell size, etc., make film recorders with such packing densities impractical. Our considerations show that it should be possible to build a film recorder which would pack ten 12-bit words in parallel across 16-mm film (see Figure 5-11). Optical magnification of $\times$ 15 would produce a spot size of about 1 mm (0.04 inch). Reading would be accomplished with a commercially available light sensor, the dimensions of which are shown in Figure 5-11. The recorder would use about 1000 feet of 16-mm film per day. A similar computation for a practical high-density magnetic tape recorder shows that approximately 1300 feet (433 meters) of 1-inch (25 mm) tape would be used for recording the same 10-channel digital data. Having the capability of recording ten digital channels in parallel also permits some real economics in memory and switching circuits compared with multiple-channel
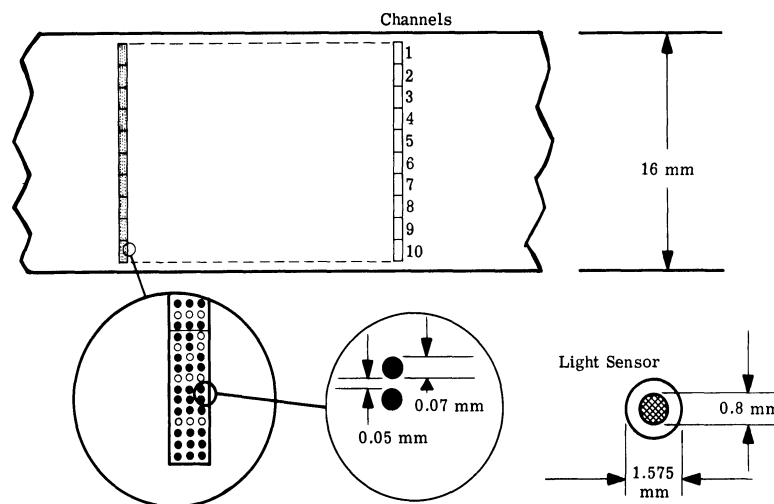
FIGURE 5-11. RECORDER WITH TEN PARALLEL 12-BIT DIGITAL
CHANNELS ON 16-mm FILM

tape recording done in a serial manner. There are a variety of exciting possibilities for editing and high-speed playback if one considers using a flying-spot scanner and photomultiplier tube for reading the film. Probably, flashing lights are practical for recording purposes.

Higher-density recording is possible, then, with either tape or film media. There is more activity with tape at the present time, probably because it is a "dry" process. Economics, rather than some inherent superiority, are likely to govern the choice of one over the other.

DEVELOPMENTS AT GEOTECH

Development of equipment at Geotech for providing digital outputs from seismographs has been in two areas. The first is part of a data collection system for studying earth background noise, using a 1604A type computer for processing. Figure 5-12 shows the main blocks of the data collection system that follow the seismometer-amplifier combination. Voltage analogs from various instruments are applied to voltage-controlled oscillators (VCO) operating on IRIG channels 1 to 7. A standard tone for tape speed compensation is mixed with the output of the VCO's, and the complex is recorded on one channel of an audio frequency magnetic tape recorder operating at 1.875 ips. A second channel is used for voice comments. About 4 hours
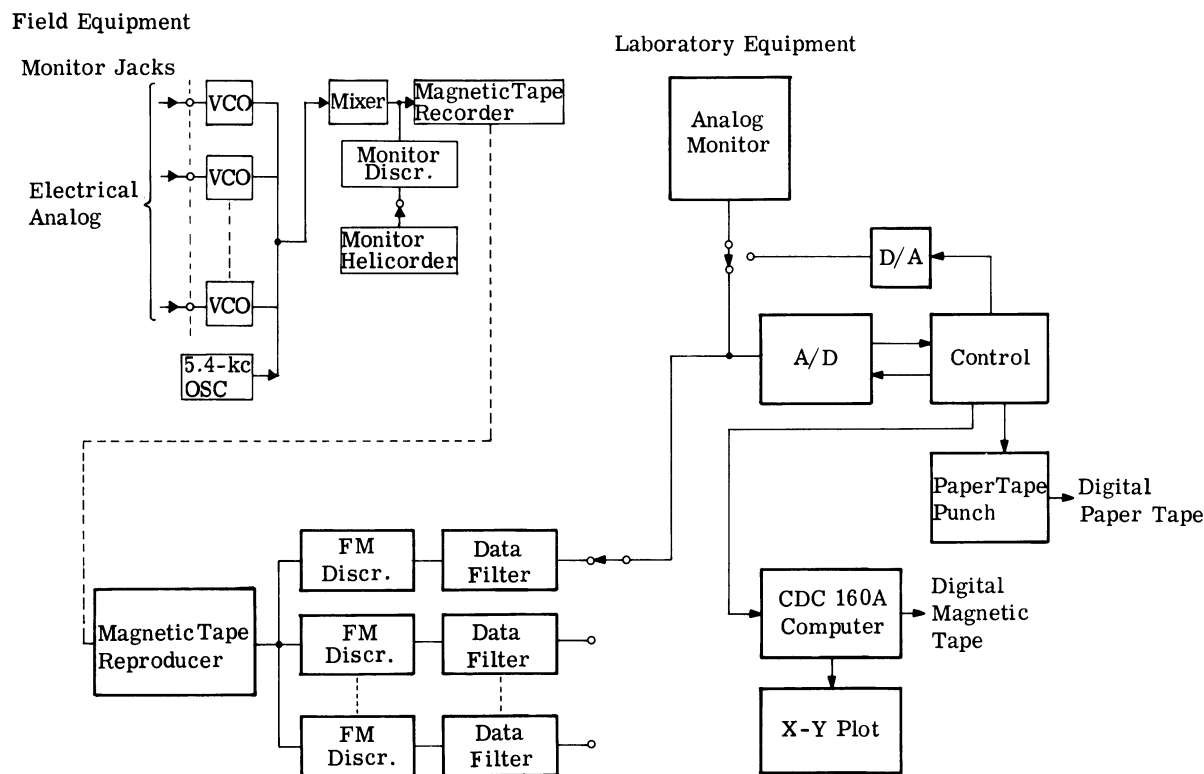
FIGURE 5-12. DIGITAL DATA COLLECTION SYSTEM AT GEOTECH

of recording time, using 7-inch reels of 1-mil × 1/4-inch tape, is provided, as are monitor circuits and a visible recorder.

Data taken in the field are brought into the laboratory and edited, and selected sections are digitized. If the section of data is short, it may be digitized and punched "off line" on paper tape at speeds of up to 100 characters per second. If long sections of data are to be digitized, they can be blocked in a CDC 160A computer and recorded on magnetic tape in an IBM compatible format. Error checking programs are used to verify the recorded data. The paper or magnetic tapes are then sent to a CDC 1604A computer for analysis. Several 160A program features are of interest. The data can be sent back through a D/A converter and checked visually on a Helicorder, a strip-chart recorder, or an X-Y recorder. The data can be checked to see that a maximum rate of change of amplitude has not been exceeded. Data can be smoothed, by use of a five-point average value, if a gross error is detected in any sample. The A/D and D/A converters and the tape punch are commercial items. The control logic for both on-line and off-line operation of the digitizer was built at Geotech, using digital modules developed on other programs. The A/D converter can digitize 10,000 samples per second, and it is possible to block and file these data on the computer's magnetic tape units at this same rate. LRSM data tapes and data from other sources can be digitized also. Part of this work was for a research project supported by the Advanced Research Projects Agency, and was monitored by the Air Force Office of Scientific Research under Contract AF 49(638)-1150.

The second area we have worked in is the development of digitizing equipment for field or seismic observatory use. We constructed a digitizer, using one of our long-period galvanometer-phototube amplifiers (PTA) and a code plate. The principles of operation are shown in Figure 5-13, which is the initial trial arrangement. A thin stripe of light shines on the code plate. The position of the stripe is controlled by the galvanometer mirror whose rotation is a function of the seismometer output. One special long-strip photocell is placed behind each significant digit. This arrangement did not work, because the special photocells had their own "code;" that is, they had imperfections which caused errors in the data. Figure 5-14 illustrates the method finally adopted. Here, an image of a lighted code plate is moved across a slit. Behind the slit are photocells which encode the galvanometer motion.

The long-period digitizer was an experimental device, and only an 8-bit range was provided. Enough difficulty was experienced in the development of the 8-bit model to discourage us from trying for better resolution. The 8-bit version works satisfactorily, however, and the method appears sound. Its primary advantage is that the long-period galvanometer can be used in a normal manner to construct any desired seismograph response curve. Figure 5-15 shows the complete instrument with cover removed.

Flash Tube
Mask with Slit
Lens
System

Common Conductor Grid (Vacuum Deposited)
Conductor Strip (Vacuum Deposited)
Photoconductive Layer
Gray Code Plate
Glass Support Plate
Slit Image

Output Leads
Each Channel
to Separate
Amplifier

Common Lead

Galvanometer Mirror
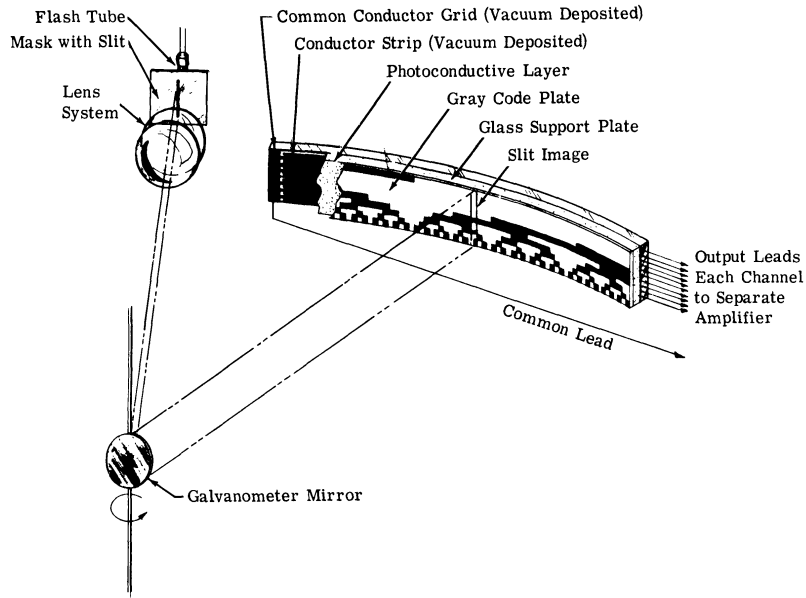
FIGURE 5-13. INITIAL DIGITIZER OPTICAL ARRANGEMENT

Lamp
Condenser Lens
Reflected Binary Code Mask

Lens

Photocell Leads
to Bridge Circuits

Galvanometer
Mirror

Slit and Miniature Photocells
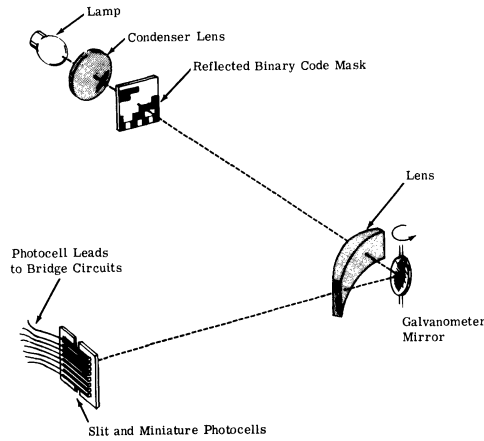
FIGURE 5-14. MODIFIED DIGITIZER OPTICAL
ARRANGEMENT

Code Mask

Lamp Source

Sequencing and Buffer
Storage Boards

Photocell
Amplifiers

Optical Slit
and Photocells
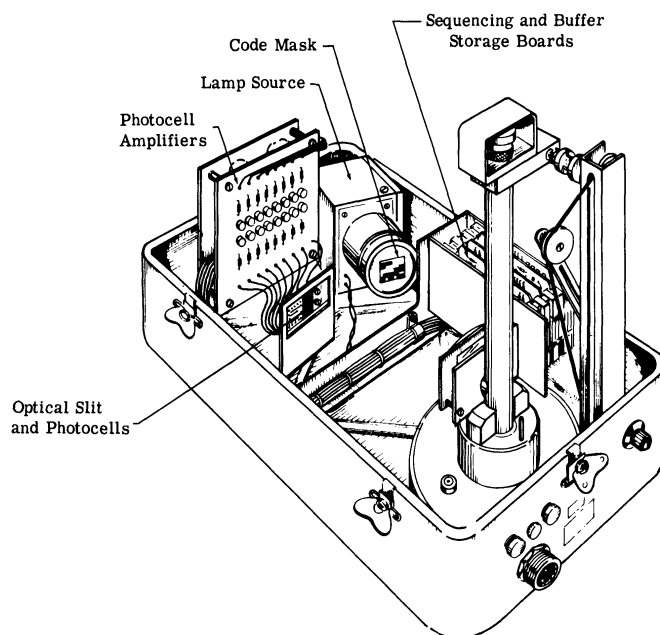
FIGURE 5-15. SKETCH OF THE MODIFIED DIGITIZER ASSEMBLY

Our latest effort is development of a low-power, short-period digitizer. It is being packaged in two different configurations. The first package is a completely self-contained PTA with digital electronics to provide a 12-bit output of up to 50 samples per second. The second package contains only the A/D converter electronics, for adding to the output of any suitable analog amplifier. Figure 5-16 is a block diagram of the complete amplifier-digitizer. The top part of the diagram is the low-level amplifier which can be adapted by using plug-in printed circuit cards to produce a voltage or frequency (FM) analog or a digital output. The bottom half of the diagram shows the A/D converter.

This method uses a precision frequency and a linear-ramp waveform for standards of comparison. Both outputs from a differential amplifier are sampled in negligible time with sample-and-hold circuits. The voltage analogs are held in the analog memories (capacitors) while conversion takes place. The output of the linear-ramp generator is applied to the two voltage comparators, and pulses are obtained from each when the ramp voltage crosses the stored voltage analogs. If the voltage analogs are unequal, the two pulses will occur at different instants, because the ramp is rising linearly with time. The time between pulses is then a linear function of the difference in potential between the two voltage analogs. The sequence of the pulses is a function of signal polarity. The counter gate is opened to the standard frequency in the time interval between pulses, giving a digital output proportional to the amplitude
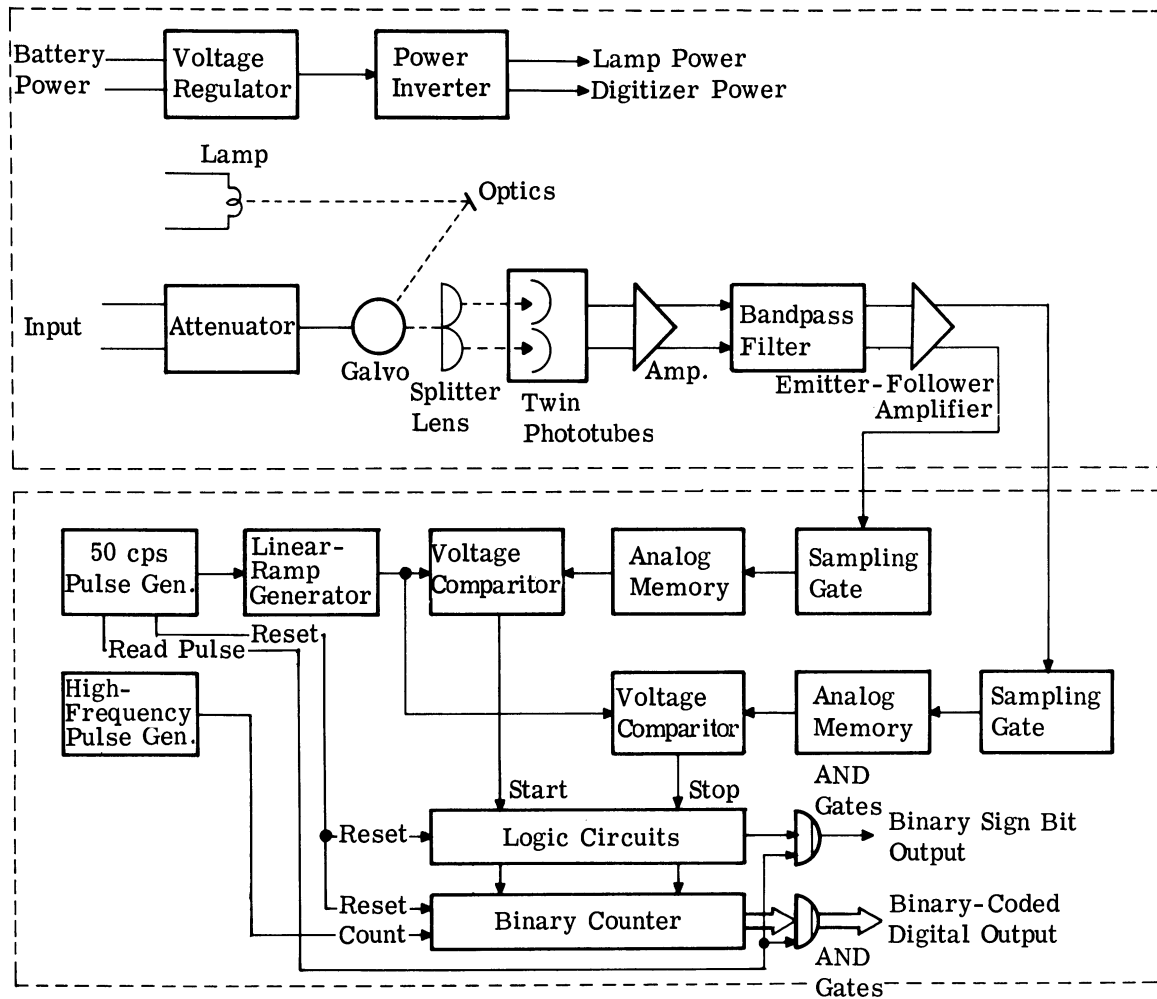
FIGURE 5-16. GEOTECH'S AMPLIFIER-DIGITIZER

of the original signal. The sign of the number is determined by the logic circuits' sensing of

the sequence. The output is pure binary code of 11 bits plus sign. The resolution is one part

in 2^{12} (4096), permitting a maximum dynamic range of 72 db (again on a p to p basis). The short-

period digitizer incorporated in a low-power phototube amplifier consumes less than 3 watts.

The D/A converter portion for use with an external amplifier has a power consumption less than

1 watt. These short-period digitizer developments are being performed under the technical

direction of the Air Force Technical Applications Center, with the overall supervision of the

Advanced Research Projects Agency in Project VELA UNIFORM (VT/072), Improved Seismo-

graph Program.

CONCLUSIONS

The information presented in this paper leads to the following conclusions:

(a) Earth motion and the instruments that measure it are not inherently digital.

(b) Converting from continuous mechanical motion to electrical digital signals is required to get earth motion into a digital computer.

(c) The maximum dynamic range currently available is about 2^{14} or 80 db on a p to p basis, and this is barely adequate for broadband seismic data.

(d) Digitizing broadband (long- and short-period) seismic data on a continuous basis creates a tremendous recording and storage problem.

(e) Within discernible limitations, it is possible to construct broadband digital seismographs as the need exists.

REFERENCES

1. M. L. Klein, F. K. Williams, and H. C. Morgan, "Analog-to-Digital Conversion," Instruments and Automation, 1956, Vol. 29, p. 915.

2. J. Gerrard, "The Need for Fundamental Research in Seismology," U. S. Dept. of State Rept. of the Panel on Seismic Improvement, Washington, D. C., 1959, Appendix 20, p. 209.

3. D. F. Eldridge and A. Baaba, The Effects of Track-Width in Magnetic Recording, The Ampex Corp., Redwood City, Calif., 1962.

4. J. J. Brophy, "High Density Magnetic Recording," IRE, Trans. PG on Audio, 1960, Vol. AU-8, No. 2.

SELECTED BIBLIOGRAPHY

Adams, W. M., and D. C. Allen, "Reading Seismograms with Digital Computers," Bull. Seism. Soc. Am., 1961, Vol. 51, pp. 61-67.

Ballen, S. B., and R. Broading, "Universal Computer Well Log," Oil Gas J., 1961, Vol. 59, pp. 92-96.

Bauman, D. M., et al., Character Recognition and Photomemory Storage Devices Feasibility Study, Sum. Rept. No. 2, Rept. No. RM-7692-3, Contr. Nonr 184141, Dynamic Analysis and Control Lab., Mass. Inst. of Tech., Cambridge, Mass., 1959.

Behrens, W. A., et al., Development of a Dovap Digitizer, Final Rept., Rept. No. LA-60-03, Contr. No. DA 29-040-ORD-1302 and DA-29-040-ORD-2013, Land-Air, Inc., Holloman, New Mex., 1960.

Benson, B. S., Analog-to-Digital Conversion Units, Lecture No. 8, Benson-Lehner Corp., Los Angeles, Calif., 1955.

Bower, G. G., Survey of Analog-Digital Converters, Natl. Bur. Std. (U.S.) Rept. No. 2755, Missile Development Div., Corona, Calif. 1963.

Bower, G. G., "Analog-to-Digital Converters: What Ones Are Available and How They Are Used," Control Engineering, 1957, Vol. 4, pp. 107-118.

Brain, A. E., et al., Graphical Data Processing Research Study and Experimental Investigation, Quart. Prog. Rept. No. 2, 1 July-30 Sept. 1960, Contr. No. DA 36-039-SC-78343, Proj. No. 3A99-22-001-2, Stanford Res. Inst., Menlo Park, Calif., 1960.

Brown, J. and D. Wagner, A Subsystem for the Digital Coding and Remote Display of Curved Lines, Rept. on Proj. Mich., Rept. No. 2900-219-T, Contr. No. DA 36-039-SC-78801, Inst. of Sci. and Tech., Univ. of Mich., Ann Arbor, Mich., 1960.

Bullard, E. C., "The Automatic Reduction of Geophysical Data," Geophys. J., 1960, Vol. 3, p. 237-243.

Burke, H. E., Jr., "A Survey of Analog-to-Digital Converters," IRE Proc., 1953, Vol. 41, pp. 1455-1462.

Burke, H. E., Jr., A Survey of Analog-to-Digital Converters: Review of Input and Output Equipment Used in Computing Systems, AIEE, New York, N. Y., pp. 98-105.

Burns, A. J., A Communication Link between an Analog and a Digital Computer, Res. Rept. No. RE-142, Grumman Aircraft Engineering Corp., Bethpage, N. Y., 1960.

Caldwell, S. H., Switching Circuits and Logical Design, John Wiley and Sons, Inc., New York, N. Y., 1958.

Cotton, R. V., Design and Development of Analog-to-Digital Converters, Interim Tech. Rept. No. 3, 15 Aug.-15 Nov. 1960, Research Rept. No. 2237-3, Contract No. AF 33(616)-6693, Philco Corp., Philadelphia, Pa., 1960.

Cotton, R. B., and A. F. Tillman, Design and Development of Analog-to-Digital Converters, Interim Tech. Rept. No. 4, 15 Nov. 1960-15 Feb. 1961, Res. Rept. No. 2237-4, Contract No. AF 33(616)-6693, Philco Corp., Philadelphia, Pa., 1961.

Dowling, D., Evaluation of an Inverse Fourier Transform on Digital Computers, Special Rept. No. 49, Army Signal Missile Support Agency, White Sands Missile Range, New Mex., 1961.

El Hakin, Y., Digital Processing of Photographically Recorded Cro Traces, Lawrence Radiation Lab. Eng. Note EE-696A, Lawrence Radiation Lab., Berkeley, Calif., 1960.

Engineering Research Associates, Inc. (staff), High-Speed Computing Devices, McGraw-Hill, Inc., New York, N. Y., 1950.

Feingold, S. K., "The Logic of V-Brush Analog-to-Digital Converters," ISA J., 1957, Vol. 4, pp. 66-68.

Fields, T. H., and R. W. Findley, "Accumulating Digitizer System," Rev. Sci. Instr., 1960, Vol. 31, pp. 1312-1317.

Fletcher, T. C., and N. C. Walker, "Analog Measurement and Conversion to Digits," ISA J. 1955, Vol. 2, pp. 341-345.

Flores, I., "Reflected Number Systems," IRE, Trans. on Electron. Computers, 1956, Vol. EC-5, pp. 79-81.

Grannemann, W. W., et al., "Pulse-Height-to-Digital Signal Converter," Electronics, 1960, Vol. 33, No. 2, pp. 58-60.

Hodes, L., Machine Processing of Line Drawings, Rept. No. 54G-0028, Contract No. AF 19(604)-7400, Lincoln Lab., Mass. Inst. of Tech., Lexington, Mass., 1961.

Hollitch, R. S., and A. K. Hawkes, Automatic Data Reduction, Rept. No. 54-519, Wright Air Development Center, Wright-Patterson AFB, Ohio, 1954.

Hoover, C. W., Jr., R. E. Staehler, and R. W. Ketchledge, "Fundamental Concepts in the Design of the Flying Spot Store," Bell System Tech. J., 1958, Vol. 37, pp. 1161-1194.

Humphrey, W. S., Jr., Switching Circuits with Computer Applications, McGraw-Hill, Inc., New York, N. Y., 1958.

James, H. M., N. B. Nichols, and R. S. Phillips, Theory of Servomechanisms, Radiation Lab. Ser. 25, McGraw-Hill, Inc., New York, N. Y., 1947.

Kessler, M. M., An Experimental Communication Center for Scientific and Technical Information, Rept. No. 4G-0002, Contract No. AF 19(604)-5200, Lincoln Lab., Mass. Inst. of Tech., Lexington, Mass., 1960.

Keister, W., A. E. Ritchie, and S. H. Washburn, The Design of Switching Circuits, Van Nostrand and Co., New York, N. Y., 1951.

Klein, M. L., F. K. Williams, and H. C. Morgan, "Digital-to-Analog Conversion," Instruments and Automation, 1956, Vol. 29, pp. 695-697.

_____"Practical Analog-Digital Converters," Instruments and Automation, 1956, Vol. 29, pp. 1109-1117.

_____"High-Speed Digital Conversion," Instruments and Automation, 1956, Vol. 29, pp. 1297-1302.

Kurtz, L., An Optimization Procedure for a Single-Link Unidirectional Digital Communication System in the Presence of Additive Gaussian Noise and for Detection Independent of Fading, Scientific Rept. Nos. 3 and 4, Contract Nos. AF 19(604)-6168, AFCRL TN 60-1101, and AFCRL TN 60-1116, NYU Coll. of Eng., New York, N. Y., 1960.

Lechter, S., Survey of Analog-to-Digital Converters, Applied Math. Lab. Research and Development Rept., Rept. No. 1257, U. S. Dept. of the Navy, Washington, D. C., 1958.

MacKay, R. S., "Nearest Count Indication in Counter Timers and Related Analog-Digital Converters," Rev. Sci. Instr., 1960, Vol. 31, pp. 1241-1242.

Melpar, Inc. (staff), Tape Converter (For Dynamic Tester T12), Projs. TW-301 and 5R13-02-063 (Sponsored by Frankford Arsenal, Philadelphia, Pa.), Rept. No. FCDD-339, Vols. 1 and 2, Melpar, Inc., Watertown, Mass., 1960.

Michael, G., Novel Graphical Input Device for Digital Computers, Lawrence Radiation Lab. Rept., Berkeley, Calif., 1960.

Ornstein, S. M., and R. J. Saliga, Wallops Island Preliminary Processing Computer Programs, Rept. No. 21G-0003, Revis. 2 (Supersedes Rept. No. 21G-0003, Revis. 1 AD-243 045), Contract No. AF 19(604)-7400, Lincoln Lab., Mass. Inst. of Tech., Lexington, Mass., 1961.

Palevsky, M., "Hybrid Analog-Digital Computing Systems," Instruments and Automation, 1957, Vol. 30, pp. 1877-1880.

Platzek, R. C., H. F. Lewis, and J. J. Mielke, "High Speed A/D Conversion with Semiconductors," Automatic Control, 1961, Vol. 15, pp. 37-41.

Pontarelli, D. A., and N. S. Kapany, Infrared Fiber Optics, Quarterly Rept. No. 6, Rept. No. ARF 1139-16, Contract No. AF 33(616)-6247, Armour Res. Foundation, Chicago, Ill., 1960.

Pontarelli, D. A., and N. S. Kapany, Infrared Fiber Optics, Quarterly Rept. No. 7, Rept. No. ARF 1139-19, Contract No. AF 33(616)-6247, Armour Res. Foundation, Chicago, Ill.

Richard, R. K., Digital Computer Components and Circuits, Van Nostrand and Co., New York, N. Y., 1957.

Rigby, S. "Analog-to-Digital Data Converter," Electronics, 1956, Vol. 29, No. 1, pp. 152-155.

Saunders, M. G., "Digital Conversion of Electroencephalograph Records," Electronics, 1960, Vol. 33, No. 5, pp. 78-79.

Stern, J., R. Greenstone, and J. H. Wright, Data Processing Devices and Systems, Natl. Bur. Std. (U.S.), Rept. No. 4310, Washington, D. C., 1955.

Susskind, A. K. (ed.), Notes on Analog-Digital Conversion Techniques, Technology Press of M. I. T. and John Wiley and Sons, Inc., New York, N. Y., 1957.

Towles, W. B., "Transistorized Analog-Digital Converter," Electronics, Vol. 31, No. 31, pp. 90-93.

Westinghouse Electric Corp. (staff), Research in Advanced Photoelectric Information Storage, Quarterly Rept. No. 6, 1 Sept.-30 Nov. 1960, Rept. No. DYD-45096, Contract No. AF 33(616)-6666, Westinghouse Electric Corp., Baltimore, Md., 1960.

6
BROADBAND DIGITAL RECORDING

Stewart W. Smith
California Institute of Technology

ABSTRACT

A direct digital recording seismograph system has been in continuous operation at Caltech for 2 years. The frequency band covered is 0.03 to 3.0 cps, and the dynamic range is 86 db. In principle, this single instrument could replace all of the existing seismograph systems recording at Pasadena. In practice, since the data retrieval and handling systems are geared for experimental work only, the digital seismograph does not replace any of the existing instruments, but it serves as a valuable addition for studies requiring digital analysis. The present system has been successfully used for surface-wave phase velocity measurements, experimental source mechanism studies using the spectrum of P and S waves, and experimental studies on the polarization of P and S waves. Projects now underway but not yet completed include automatic picking and classification of phases, and routine measurement of seismic energy. For any of the projects now underway or contemplated, a special purpose narrowband system would better meet the requirements than a general purpose broadband system, if a means of digitizing the data was easily available.

In seismic recording, the term broadband implies that the system response is more or less flat across the microseism frequency bands at 2 cps and 0.16 cps. Because of the large dynamic range required to reproduce natural seismic signals with a wide range of amplitudes, most broadband systems use digital recording. The Caltech digital seismograph system has been in continuous operation for two years and has yielded important information about the research use of a broadband system.

Briefly, the system consists of a matched set of Press-Ewing seismometers operated at a period of 24 seconds, a set of 4-digit BCD digital voltmeters, and a 16-track digital magnetic tape recorder. With the present configuration, at a sampling rate of 10 times per second per channel, the frequency band from 3 to 0.03 cps is adequately covered. At the time this system was planned, almost four years ago, no commercially available systems completely filled our requirements; so the system was designed and built in our laboratory from standard and modified components. One of the requirements was for 24-hour continuous recording, and another was a simple editing procedure. Events had to be located, verified, and transferred to IBM compatible library tapes properly labelled and indexed. Since the instrument was to be a research tool for a wide variety of problems, a rather complex indexing scheme was set up including origin time, depth of focus, location, and magnitude. For instance, if an individual were to study a particular seismic phase from a particular class of events, he would be able to automatically search for the proper data and put it into the computer for analysis.

Since a number of research projects were going on in various regions of the seismic spectrum, such as P waves at 5 cps and free oscillations at 0.0003 cps, a broadband system seemed clearly desirable. However, because of the nature of the natural spectrum of seismic waves in the earth, it turned out that almost all research projects were carried out within narrow frequency bands. All the projects together covered a tremendous range of frequencies, but, with few exceptions, there was little overlap between frequency bands for those projects that required data from a single instrument. To illustrate this, Table 6-I contains a list of projects that have actually made use of data from the digital seismograph, and the frequency bands that were of interest. In most cases other stations and other instruments were also used.

TABLE 6-I. CALTECH PROJECTS USING DATA FROM
THE DIGITAL SEISMOGRAPH

	Relevant Frequency Bands (cps)	
Earthquake Mechanism Studies		
Polarization of S waves	0.06	-0.16
Explosion — collapse mechanism	0.5	-3.0
Surface-wave equalization	0.03	0.06
Crust and Mantle Structure		
P traveltimes	0.5	3.0
Higher-mode surface-wave dispersion	0.02	0.16
Transmission coefficients	0.05	0.16
Free oscillations	0.001	0.003
Microseisms	0.2	0.12

Briefly, here are some of the attitudes about the system encountered. The long-period experimenters paid a heavy price in amount of computer time and tape required by the large volume of data resulting from the high sampling rate. For example, a 45-minute surface-wave train amounts to 80,000 data points, whereas the equivalent amount of long-period information from a station digitized by hand can be put on a few hundred cards. People working with short-period body waves found it necessary to prewhiten the spectrum before doing many operations because of the high spectral density near the 6-second microseism peak. Those working with higher-mode Love and Rayleigh waves found the response to be about optimum, as did those who were studying microseisms, although the dynamic range at normal gain settings was not adequate for the latter.

For each of the cases mentioned, there is a narrowband analog system well suited for the research being carried out, except for the difficulty of getting the data into a computer. Per-

haps eight different instruments are in current operation, most of which record on photographic paper. They each sample the seismic spectrum in a different region and at a different sensitivity. Most of these instruments were developed over years and arrived at their present configuration by trial and error. In addition to standard short- and long-period systems, they include a narrowband high-gain instrument sharply tuned at 14 to 20 seconds for crustal Rayleigh waves, low-sensitivity Wood-Anderson torsion seismometers for magnitude studies of local earthquakes, a Benioff strain seismometer with long-period galvonometers for mantle Love and Rayleigh waves, and a recording gravimeter for free oscillations. In all cases, if there were an easy way to get the data into a computer, these special purpose instruments would be superior to our single broadband digital system.

Until recently, essentially the only advantage of the digital system over special purpose instruments was the convenience of having the data directly in digits. This was an advantage because of the rather complicated editing procedures necessary to get the data off the source tapes and onto an indexed computer tape. We have made use of a special-purpose device with preset counters and a small core buffer and digital tape transport to pull off the desired section of data and write a gapped tape in IBM format. An important point is that the user had to know in advance, by examining analog records, what time intervals he needed. We now have operating the beginning of a system in which the source tapes can go directly into the computer. In fact, we do not in principle need the intermediate recording tape; we can go directly into the computer from the seismometer on a real-time basis, without excessive use of the main part of the computer. This important advance was made possible by the installation of three data channels in the IBM 7040-7090 system at Caltech, and by the development of a parallel programming system making it possible to record and process data in real time at the same time that the computer is processing other programs.

The addition of a computer to the digital seismograph makes a fundamental difference in the kinds of problems that can be handled. For example, we can now attack the problem of automating a seismic station. We are starting with easy-to-recognize earthquake signals, and applying simple phase picking and identification criteria. With experience, we hope to increase the complexity of the phase picking schemes until we can automatically pick the identify all but the most complicated events and very small events, which are better left to an array station with the capability for velocity discrimination. For example, Pacific events of moderate size are easily distinguished at Pasadena by long trains of oceanic Rayleigh waves. Particle motion and simple group-velocity dispersion measurements for these wavetrains will give a first approximation of the distance and direction of the earthquake, and thus indicate where one should look for other phases. Recognition and identification of P and S waves will be attempted by

angle of emergence and spectral ratio measurements. The criteria used will be arranged in a sequence which will be carried through only until it becomes clear in what category the earthquake falls. In addition to times of arrival of prominent seismic phases, the direction, distance, and energy flux will be estimated.

To conclude, then, two years of experience with an experimental broadband digital seismograph have shown that the most important feature of the system is the easy computer access to the data and not the broadband capability.

7
LIMITATIONS IN THE MEASUREMENT OF LOW-FREQUENCY
GROUND MOTION

R. A. Haubrich
University of California, San Diego

ABSTRACT

Below 40 millicycles per second the recorded seismic background is so low that considerable difficulty is encountered in its detection from both instrument and site noise. The measured coherence between instruments placed several kilometers apart is found to be low for these frequencies, though one would expect just the opposite for propagating seismic energy at points only a fraction of a wavelength apart. Recordings have been made which attempt to separate the different types of errors in the data and to evaluate the precision of measurements made in the field. In all cases it was found that recorded levels were well above theoretical thermal noise and measured amplifier noise.

Comparisons were made, using digital recording, between JM and Press-Ewing vertical seismometers, at frequencies below 1 cps. Measurements of coherence between 2 JM and between 2 Press-Ewing seismometers at the same site indicate that the JM seismometers detect normal seismic background accurately down to frequencies of about 80 millicycles per second. Below this frequency the JM records exhibit instrument noise; the two Press-Ewing records are coherent down to frequencies as low as 1 millicycle per second.

Coherence measurements between vertical ground motion and atmospheric pressure indicate that below 40 millicycles per second most of the ground motion is due to pressure. The seismic recorded have been corrected for pressure by using a linear least mean-square prediction filter. The corrected seismic records show a decrease in level of 10 db in the band 5 to 40 millicycles per second. The residual ground displacement amounts to about 1 μ rms in this band.

8
A SOLION SEISMOMETER

J. L. Collins and D. W. Evertson
Defense Research Laboratory
The University of Texas

INTRODUCTION

The solion seismometer utilizes a fluid mass coupled to a pressure sensitive transducer for the detection of seismic signals. The heart of the system is the solion full-wave linear pressure transducer, hereafter referred to as the solion. This is a hydroacoustic, electrochemical transducer which possesses characteristics well suited to applications in geophysics. The solion transducer has long-term stability, low power consumption, high sensitivity, and remote operating capabilities. These characteristics, along with an inherently large transduction power gain, derive from the simple nature of the solion. Although the solion seismometer has not been used extensively, solions have been used in other ways for about ten years, primarily in oceanographic and infrasonic transducers.

In this paper, the solion transducer and the basic principles that describe the solion action are discussed. Also included is a discussion of how the solion is joined with a fluid inertial mass system in an effort to enhance the acceleration sensitivity of the transducer. Because the solion seismometer is new, an empirical calibration has not yet been made. The sensitivity presented is based upon the measured pressure response of the solion and the predicted effects of the fluid mass system.

THE SOLION ELECTROCHEMICAL TRANSDUCER

GENERAL COMMENTS. The science of electrochemistry began around 1800 when Galvani noticed that if two dissimilar conducting materials were placed in contact with a freshly prepared frog's leg, the leg twitched as if alive. The solion utilizes some of the principles noticed in Galvani's experiment. It is an electrochemical device with very low power consumption, commonly known as a redox system. With a redox electrode the reaction occurring at the electrode is completely reversible. Furthermore, the electrodes are composed of an unattackable metal, usually platinum, which will not enter into the reaction itself. The electrochemical system consists of the electrode set immersed in a solution containing soluble forms of the same chemical in two different oxidation states. For the solion this is generally an iodine-iodide electrolyte system.

The name solion is derived from the phrase "ions in solution." Electric current is transferred by ion flow in a solution as opposed to electron or ion flow in a gas or solid. While the

redox electrochemical system is the one discussed in this paper, other solions may utilize different electrochemical principles such as electrokinetic transduction.

THE SOLION ELECTROCHEMICAL DIODE. Consideration of a solion diode will illustrate the basic characteristics of the solion, except for those effects due to hydroacoustic flow. Figure 8-1 is a schematic diagram of the basic electrochemical diode system. The diode consists of a pair of platinum electrodes sealed into an airtight chamber filled with a solution of iodine, potassium iodide, and water. One electrode, the anode has an effective surface ten times that of the other electrode, the cathode. The chamber is constructed of a chemically inert plastic material such as Kel-F. The external electrical circuit consists of a variable low-voltage d-c supply, a d-c milliampere meter, and a high-impedance d-c voltmeter.
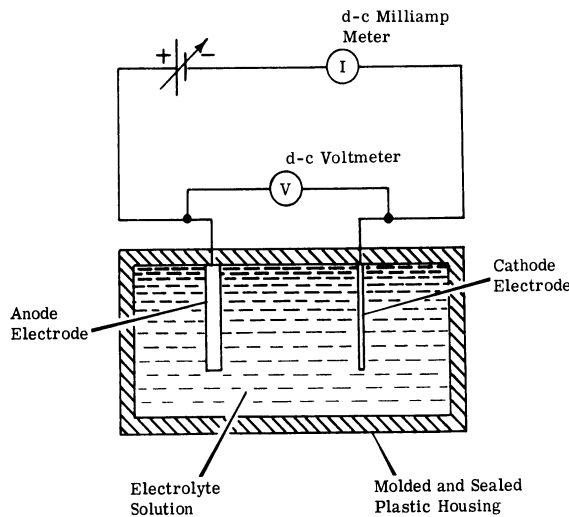
FIGURE 8-1. SCHEMATIC DIAGRAM OF THE
SOLION DIODE

With the circuit connected as shown in Figure 8-1, the voltage between the electrodes is increased, and the current through the cell is monitored. The voltage-current relationship is shown in the concentration polarization curve of Figure 8-2. Maximum voltage is about 0.9 volt d-c; any substantial increase above this will tend to cause hydrogen evolution at the cathode. This curve illustrates one of the basic features of the solion: the output current is independent of the applied voltage over the range 0.1 to 0.9 volt. Typical value for the slope of the plateau is approximately 1 MΩ. Over the region of the plateau, the limiting current is given by the following relationship:

$$i_d = \frac{AD}{\mathscr{L}} n\ FN \qquad\qquad (8\text{-}1)$$
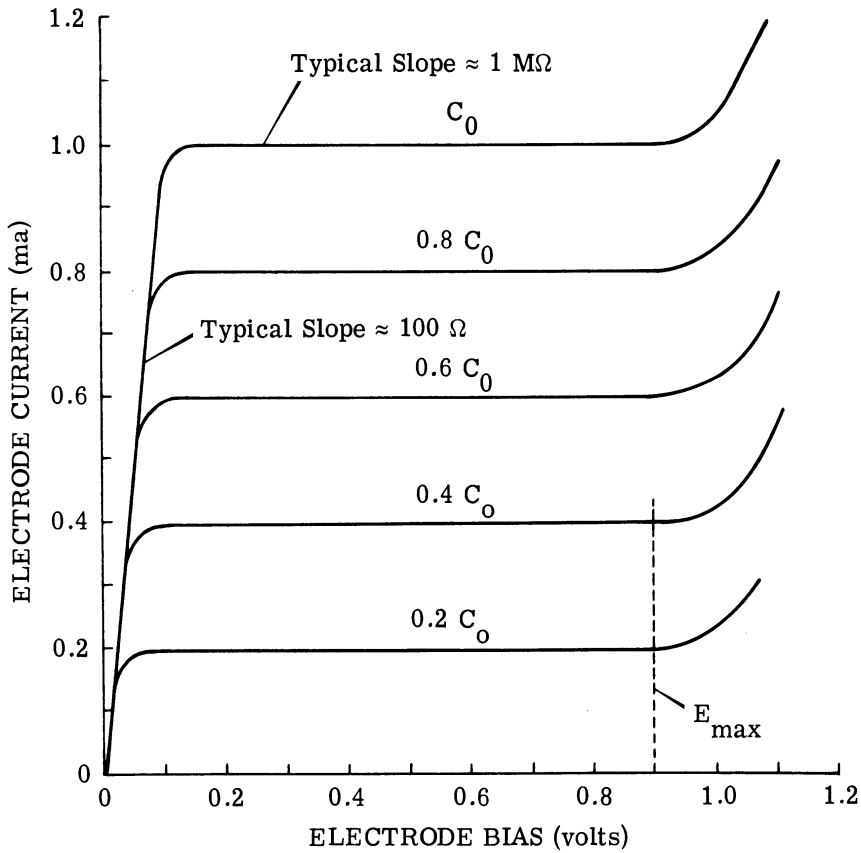
FIGURE 8-2. CONCENTRATION POLARIZATION CURVE FOR THE SOLION DIODE

where A is effective area of the cathode, N is iodine concentration of normality, $\mathcal{L}$ is effective thickness of the diffusion layer, n is 2 (number of electrons involved in the reaction), and F is the Faraday constant. The diffusion coefficient, D, is given by $D = KT/\sigma$, where T is absolute temperature in degrees Kelvin, σ is viscosity of the solution, and K is a constant for the particular system. Therefore, for a solion diode the limiting current is primarily determined by the cathode area (a cathodic controlled reaction), the iodine concentration, and the absolute temperature.

The electrochemical reactions occurring at the electrodes consist of reducing iodine at the cathode and onidizing iodide back to iodine at the anode. At the cathode $I_2 + 2e \rightarrow 2I^-$, and at the anode, $2I^- \rightarrow I_2 + 2e$. The electrode material itself has not entered into the reaction, and the completely reversible process can continue indefinitely. The shape of the "knee" of the curve can be adjusted by varying the potassium iodide concentration, but the shape illustrated in Figure 8-2 makes greatest use of the constant current feature. Still another unusual feature

of the solion is the "double" source impedance characteristic. Although the signal output appears to originate from a 1-MΩ source, the cell appears as a 100-Ω source to any 60-cps pickup that might appear in the external electrical circuit.

"Reverse" voltage characteristics of the diode are very similar to those shown by the curve of Figure 8-2. The anode and cathode leads are now interchanged with the cathode becoming an electrode of ten times the previous area. The polarization curve will have a similar shape, except that the limiting current will be approximately ten times the "forward" limiting current, strictly because of the increased area of the cathode. The front to back ratio is therefore primarily determined by the ratio of the electrode areas. Values in excess of 100:1 have been obtained.

THE EFFECTS OF HYDROACOUSTIC FLOW. The diode has been discussed to illustrate some of the basic principles of the electrochemical system utilized in the solion. The assumption was then made that hydraulic flow was absent. By proper design, the solion can be utilized as a hydraulic flow or pressure detector. Let us consider the design of a solion similar to that indicated in Figure 8-3. The rigid plastic body of the diode has been replaced by a cell of different design. The cathode element is now mounted in a solid web at the center of the plastic housing so that any fluid flow between chambers is possible only through the cathode electrodes. The electrolyte solution is constrained by compliant diaphragms which permit limited volume flow between chambers. Since the cathode structure tends to obstruct any flow of fluid between chambers, it is considered as an acoustic resistance, R, measured in acoustic ohms. Since the diaphragms are compliant, this
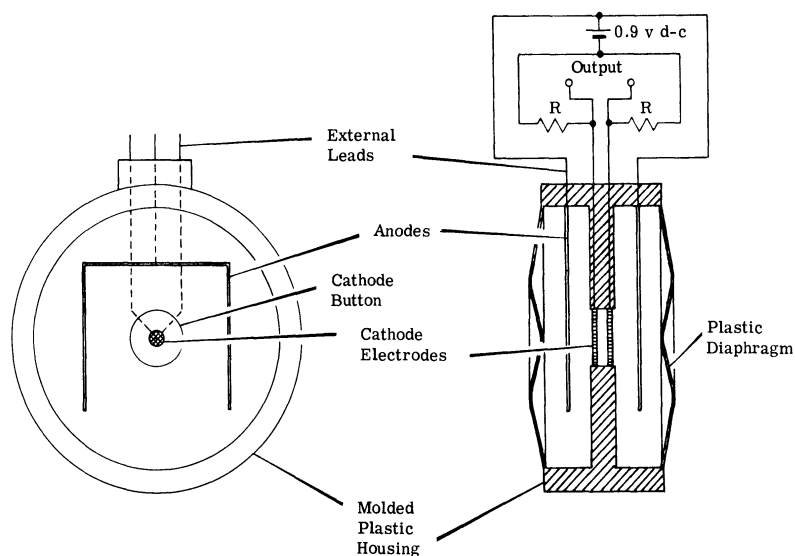

FIGURE 8-3. SCHEMATIC DIAGRAM OF A SOLION PRESSURE DETECTOR

effect is considered as an acoustic compliance, C, measured in acoustic farads. The product of the acoustic resistance and compliance determines the low-frequency response of the transducer.

If the flow detector is connected to the external electrical circuit shown in Figure 8-3, and if flow through the cathode elements is assumed to be zero, the individual cathodic currents will tend to a quasi-background current as the iodine ions near the cathodes are depleted. The background current is then determined by Equation 8-1. If the two cathode electrodes indicated in Figure 8-3 are identical, their background or "no-flow" currents will be identical. The differential output will then read zero or near zero volts, depending upon how nearly identical the cathodes actually are. The iodine ions contained in the volume in and around the cathodes are reduced to near zero, except for the small amount of iodine diffusing into the region.

Let us now assume that, with the cell connected to the external bias, a net differential pressure is developed between the compliant diaphragms. A net hydraulic flow of the electrolyte solution will commence from one chamber to the other chamber. The amount of volume flow is determined by the net differential pressure and the acoustic resistance through the cathodes:

$$\Delta p = R \frac{dv}{dt} \tag{8-2}$$

where Δp is the net differential pressure, R is the acoustic resistance of the cathodes, and dv/dt is the volume flow rate. The volume flow rate is related to the pressure by R and can be a linear or a nonlinear relationship, depending upon whether R is constant or some function of pressure. At low frequencies, pressure and volume flow rate are related by R, but at higher frequencies the relationship must become $|Z|$ so as to include the acoustic inertance of the fluid in the flow path. A linear flow detector has a useful upper frequency response in the 30- to 50-cps region.

As flow commences through the cathodes, electrolyte at the bulk ionine concentration is forced into the region of the cathodes. The output current is not limited to the diffusion currents of Equation 8-1, but increases in relationship to the number of iodine ions per unit time arriving at the cathode. If the cathodes behave as linear detector electrodes, all the iodine arriving at the cathodes is reduced. The linear detector cathode, therefore, furnishes an output current which is linearly proportional to the volume flow rate:

$$I = FN \frac{dv}{dt} \times 10^{-3} \tag{8-3}$$

where I is the electrical current in the external cathode circuit. Substitution for the volume flow rate from Equation 8-2 gives

$$I = FN \left(\frac{\Delta p}{R}\right) \times 10^{-3}$$

During the flow cycle discussed, the electrolyte passing through the "upstream" cathode has been depleted of its iodine ions, and only dilute electrolyte arrives at the "downstream" cathode. The latter has its small background current reduced even further since the dilute solution flowing through this cathode tends to overcome the iodine diffusing in from the bulk solution on the downstream side. The net effect is to cause an increase in the external electrical current associated with the upstream cathode, while the electrical current associated with the downstream cathode remains small or even decreases.

The resulting voltage developed across the two resistors in the external load is such that one output lead becomes positive with respect to the other and, in the case described, this differential voltage is proportional to the applied differential pressure and preserves the phase as well as the amplitude. A return to zero differential pressure lets the output differential voltage return to zero. A reversal of the pressure causes a reversal in the polarity of the output differential voltage. Output characteristics of a typical linear detector are illustrated by Figure 8-4. The load line has been adjusted so that at some hypothetical maximum pressure
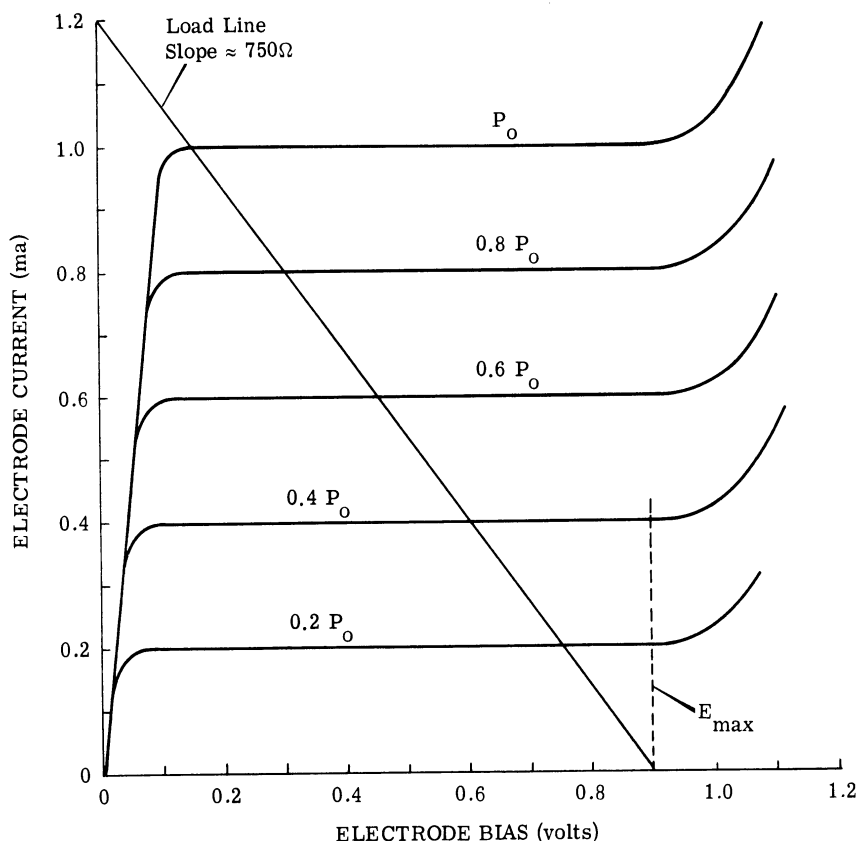
FIGURE 8-4. OUTPUT CHARACTERISTICS OF THE SOLION PRESSURE
DETECTOR

the voltage between the cathode and anode is always greater than 0.1 volt. Therefore, the solion always operates in the proper region as a constant current device. For a typical solion linear detector operating in the linear region, it is interesting to note the volume flow sensitivity. If an iodine concentrate of 1.0 normal iodine is used, it can be seen from Equation 8-3 that a flow of 10^{-6} cc/sec will produce an output current of 100 μa, which offers an extremely sensitive flow detection capability.

Comment should be made on one other characteristic of the linear flow detector. If an excessive differential pressure is applied to the transducer, the flow rate exceeds the linear ion-reduction capacity of the cathode. This does not cause the output current to "clip," but cause it to increase as the square root of the flow above the linear range. The flow signal is not lost, but simply modified. In this manner pressures far in excess of the linear range can be monitored and even measured with proper corrections of the output signal.

Linear flow detector transducers have been built with a wide variety of parameters, which are given in Table 8-I. Although a wide range of values is indicated, all combinations of extremes are not obtainable in a single detector. To reiterate before proceeding on to the seismic detector, some of the unusual characteristics of the solion are (1) low power consumption, (2) remote operation capabilities, (3) high sensitivity, (4) low pressure threshold capabilities,

TABLE 8-I. RANGE OF PARAMETERS FOR SOLION
PRESSURE DETECTORS

Parameter	Range of Values
Cathode Acoustic Resistance	10^4-10^7 acoustic ohms
Current Sensitivity	0-300 $\mu a/d/cm^2$
Pressure Threshold	0.01-100 d/cm^2
Frequency Range	0.0001-30 cps
Dynamic Pressure Range	1:1-30,000:1
Background Power Consumption	10-1800 μw
Maximum Signal Output Power	up to 27 mw
Operating Temperature	-10-+30°C
Maximum Temperature Coefficient of Sensitivity	+2.5%/°C
Maximum Size Diameter	3.0 in.
Thickness	0.75 in.
Maximum Weight	8.2 oz

(5) very low frequency response, (6) broadband response at low frequencies, (7) a reasonable temperature coefficient that can be corrected with thermistors, (8) excellent stability and reliability, (9) surprisingly rugged construction, except for the possibility of diaphragm puncture, and (10) a true differential, constant current output.

THE SEISMIC DETECTOR

The construction of a solion linear detector is such that an acceleration of the detector body parallel to its axis of symmetry will cause a flow of electrolyte through the cathode orifice. Since the electrolyte flow produces an electric current, the solion is in itself acceleration-sensitive. Coupling the solion with a long column of liquid, as is shown in Figure 8-5, is one method of magnifying the acceleration sensitivity of the transducer. If the column is accelerated, the pressure on the solion is directly proportional to the length of the column, the density of the liquid, and the component of acceleration along the column.

To relate pressure drop to acceleration, let us consider a cylindrical element of liquid in which flow is assumed to be absent. This is a valid assumption, since fluid flow through the orifice is extremely small (on the order of 10^{-6} cc/sec). Let L = length (not necessarily small), ρ = mass density, S = cross section area, A = acceleration, and ΔP = change in pressure across the element length. Then the net force along the element is $\Delta P(S)$. From Newton's Second Law, the force on a discrete object is equal to its mass times its acceleration; therefore,

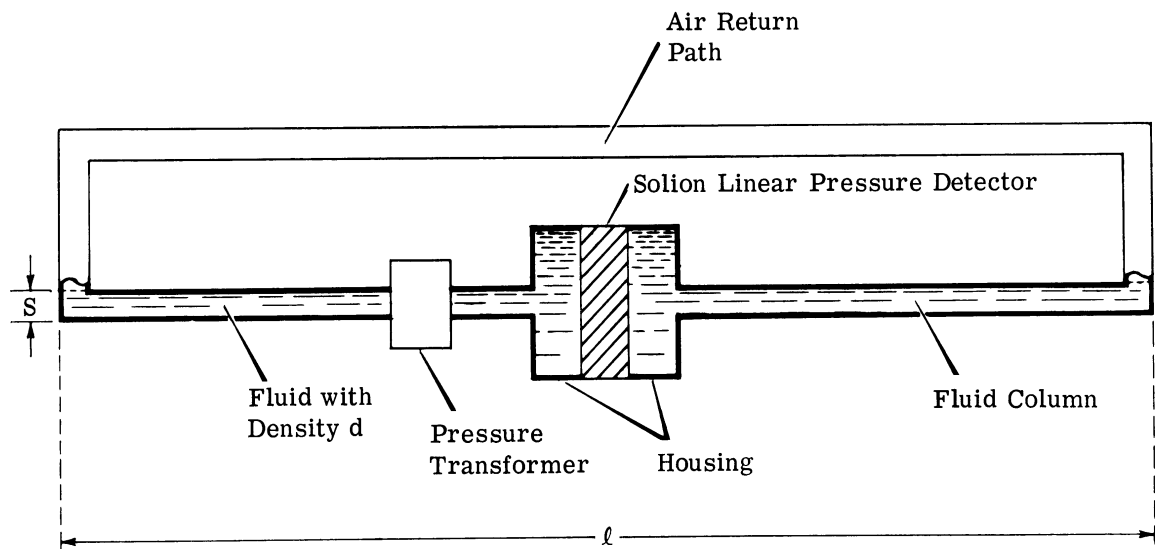$$\Delta P(S) = (LS\rho)(A), \text{ or } \Delta P = L\rho A$$

FIGURE 8-5. SCHEMATIC DIAGRAM OF THE SOLION SEISMOMETER

Let us now consider a single-frequency simple harmonic displacement of the element along its axis, $x = a \sin \omega t$, where a = amplitude and ω = circular frequency. Differentiating x twice gives the acceleration

$$\frac{d^2 x}{dt^2} = -a\omega^2 \sin \omega t$$

The acceleration amplitude then is $a\omega^2$. The change in pressure across the cylindrical element is, therefore, $\Delta P = -L\rho a\omega^2 \sin \omega t$, and the peak pressure amplitude is then $L\rho a\omega^2$.

Figure 8-5 shows an air-filled tube connecting the extremities of a fluid column. The fluid column is separated into two parts by a solion at the column's midpoint. If the column is accelerated, the solion exerts a force on the liquid which accelerates it. The liquid also exerts an opposite differential force on the solion which is measured as pressure. There would likewise be a pressure drop across an element of air, but the difference in density between air and any liquid makes this consideration negligible.

In terms of period T, the expression for pressure amplitude becomes

$$(\Delta P) = L\rho a \frac{4\pi^2}{T^2}$$

The current solion pressure threshold is about $0.05 \ d/cm^2$. Substitution of this value into the above relation, along with a suitable length and liquid density, gives an acceleration detection threshold in terms of amplitude and period. Mercury was used as the liquid in a 5-meter-long device shown in Figure 8-6. A solion transducer used in the seismometer is shown in Figure 8-7. The enlarged insert of Figure 8-6 is a close-up of the housing used to mount the solion transducer. With these parameters, the amplitude detection threshold is

$$a = \frac{\Delta P(10^4)}{L\rho 4\pi^2} T^2 = \frac{0.05}{(500)(13.6)(4\pi^2)} T^2$$

If a is measured in microns ($1 \ \mu = 10^{-4} \ cm$),

$$a = \frac{(.05)(10^4)}{(500)(13.6)(4\pi^2)} T^2 = .001862 \ T^2$$

Examples of values of a for values of T are given in Table 8-II. For a pressure threshold of $0.05 \ d/cm^2$, the acceleration threshold can be expressed in acceleration units:

$$\Delta P = L\rho A, \text{ or } A = \frac{\Delta P}{L\rho} = \frac{0.05}{(500)(13.6)} \ cm/sec^2$$

$$= 7.35 \times 10^{-6} \ cm/sec^2 \text{ or } 7.50 \times 10^{-9} \ g$$

101
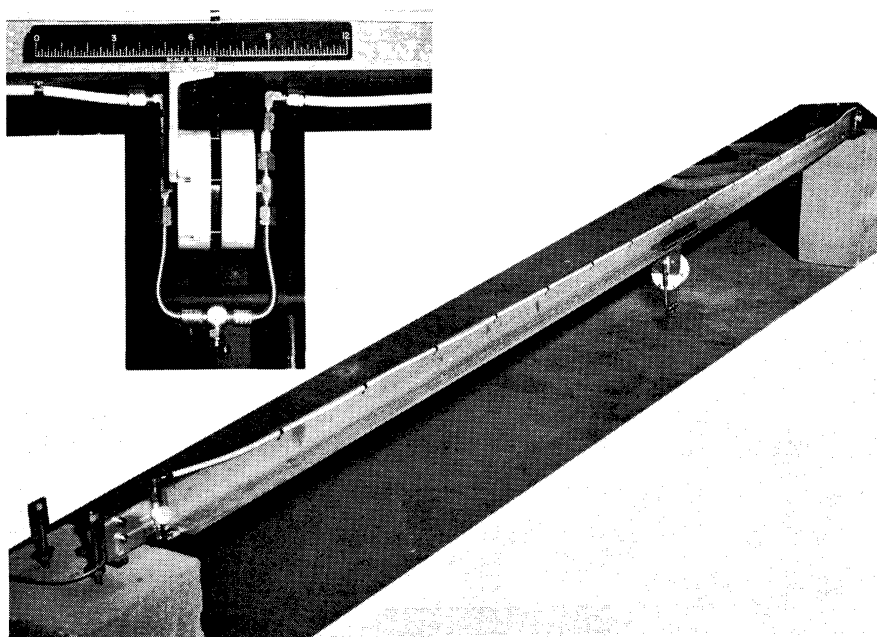
FIGURE 8-6. THE EXPERIMENTAL SOLION SEISMOMETER
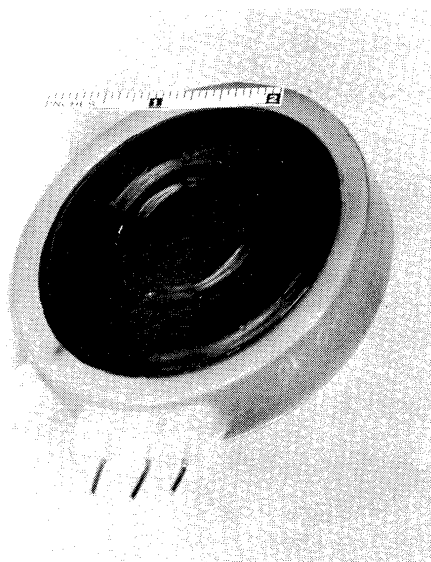
FIGURE 8-7. SOLION PRESSURE
DETECTOR USED IN THE EXPERI-
MENTAL SEISMOMETER

TABLE 8-II. EXEMPLARY a VALUES FOR
SOME VALUES OF T

T (sec)	a (μ)	a (Å)
0.1	1.862×10^{-5}	0.1862
1.0	1.862×10^{-3}	18.62
10.0	1.862×10^{-1}	1862
100	18.62	----
1000	1862	----

The practical application of the solion seismometer requires that certain characteristics of the solion transducer be considered for maximum utilization. The primary problem is to provide an electrical load circuit that will allow the solion to operate in its constant current region. An ideal load circuit is shown in Figure 8-8. The transistor's emitter-base junction presents a low impedance load to the solion constant current generator, while the sensitivity of the circuit is determined by the values of the transistor's collector load resistors. The differential nature of the system is preserved, while maximum use is made of the solion characteristics. A "free" voltage gain of about 25 volts is provided by the transistor load circuits. An example of possible sensitivity would be as follows: assuming a solion sensitivity of 50 μa/d/cm^2, a pressure threshold of 0.05 d/cm^2, and a transistor load of 10 kΩ, the current output at threshold would be 2.5 μa. Assuming a transistor current gain of one, the voltage signal developed across
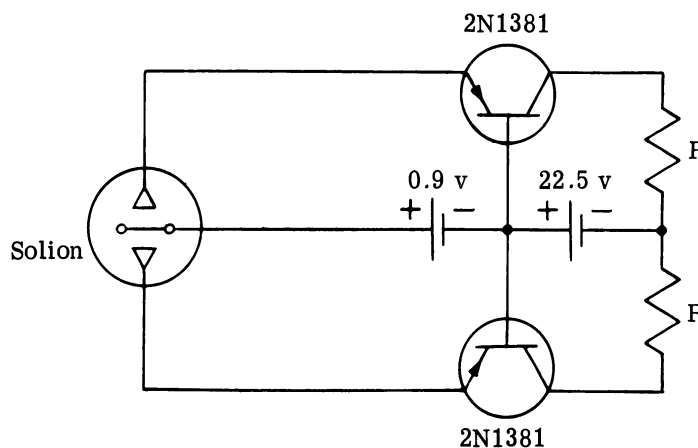
FIGURE 8-8. A PRACTICAL TRANSISTOR LOAD CIRCUIT FOR
THE SOLION

the 10-kΩ load would be 25 mv, a very usable threshold level. For the above described seis-

mometer (L = 5 meters, ρ = 13.6, pressure threshold = 0.05 d/cm^2), the voltage sensitivity of

the system would be on the order of 3×10^3 v/cm/sec^2 or about 300 mv/μ/sec^2. Indications

are that the lowest usable pressure level is determined by the external electronic noise. Noise

effects such as Brownian motion, barometric pressure, and thermal excitation have not been

considered as yet.

A proposed overall system design is indicated in the block diagram in Figure 8-9. Appro-

priate amplifier, recording, and monitoring systems are shown only in block form. The pro-

cedure of analysis is to prewhiten the data by narrowband filtering, then convert the filtered

outputs into digital form and perform the actual analysis with a digital computer. This method

of analysis provides the speed and accuracy of digital and computer techniques. Several vari-

ations and refinements of the original system are planned.
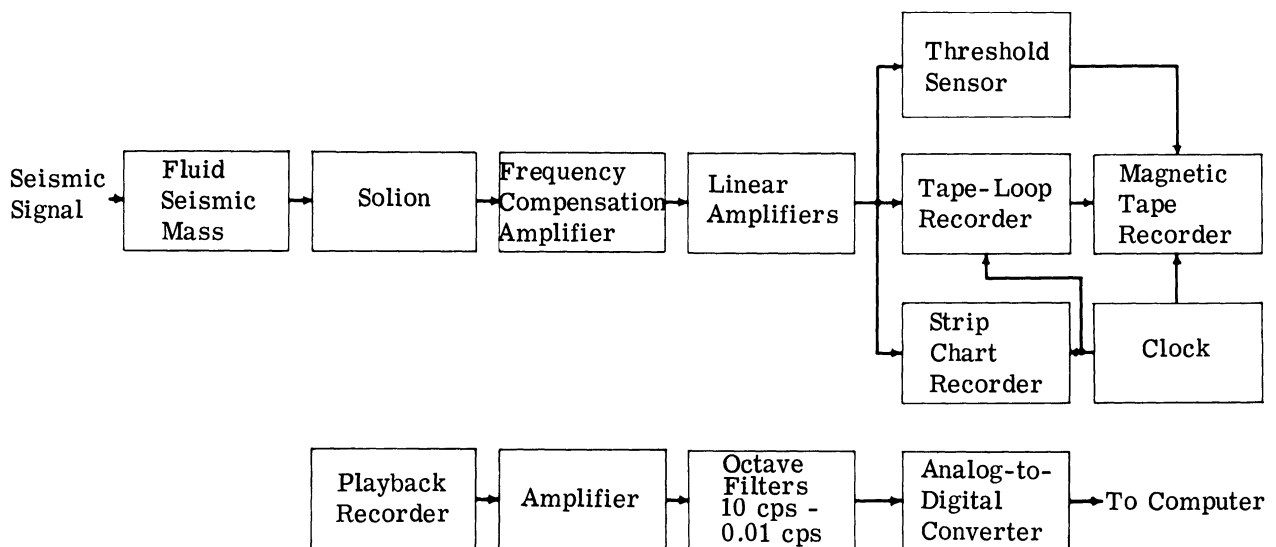
FIGURE 8-9 PROPOSED SEISMOGRAPH SYSTEM

(1) A system in which the axis of sensitivity is vertical will be designed and built. Such a

system would necessarily be a little more intricate than a horizontal solion seismometer.

(2) Effort will be made to reduce the physical size of the seismometer, which could be

achieved by increasing solion sensitivity or possibly by incorporating a "pressure transformer"

into the system,

(3) A miniature solion seismometer with reduced sensitivity might be useful. A self-con-

tained system using the electrolyte as the inertial mass, and having no diaphragms, could be

made quite small. It is conceivable that this configuration could be made either acceleration sensitive or displacement sensitive, depending upon solion orifice resistance and the provided system compliance.

The literature indicates that typical microseisms occur with amplitudes from a fraction of a micron up to 10 μ in the period range 2 to 10 seconds. Since the solion has a useful period range of 0.1 second to several hundred seconds, it should be possible for a solion system to measure microseismic activity accurately.

9
BROADBAND SEISMOGRAPHS

Eugene Herrin
Dallas Seismological Observatory
Southern Methodist University

ABSTRACT

The broadband seismograph in operation at the Dallas Seismological Observatory has a velocity response approximately flat over periods from 1 second to 90 seconds. Recording is in digital form on paper tape or magnetic tape, with a true dynamic range of greater than 60 db. Power spectra of the system noise and the background seismic noise without correction for system response have been determined. There are plans for constructing a three-component system with built-in editing features. Also in operation is a short-period, multicomponent system with a flat velocity response within 3 db from 1 to 10 cps, and with FM multiplex recording on 1/4-inch tape. Data from this system are digitized later for computer analysis.

DISTRIBUTION LIST

Advanced Research Projects Agency
The Pentagon
Washington 25, D. C.

ATTN: Dr. Charles C. Bates

Advanced Research Projects Agency
The Pentagon
Washington 25, D. C.

ATTN: Mr. Russell Beard

Advanced Research Projects Agency
The Pentagon
Washington 25, D. C.

ATTN: Mr. R. Black

Advanced Research Projects Agency
The Pentagon
Washington 25, D. C.

ATTN: Mr. William Bolton

Advanced Research Projects Agency
The Pentagon
Washington 25, D. C.

ATTN: Mr. D. Clements

Advanced Research Projects Agency
The Pentagon
Washington 25, D. C.

ATTN: Dr. Robert Frosch

Advanced Research Projects Agency
The Pentagon
Washington 25, D. C.

ATTN: Lt. Col. Robert Harris

Advanced Research Projects Agency
The Pentagon
Washington 25, D. C.

ATTN: Dr. Robert L. Sproull

Advanced Research Projects Agency
The Pentagon
Washington 25, D. C.

ATTN: TIO

Aerospace Corporation
P. O. Box 95085
Los Angeles 45, California (2)

ATTN: Mr. Carlton M. Beyer

Aerospace Corporation
2400 East El Segundo Boulevard
El Segundo, California

ATTN: Dr. Byron P. Leonard

Air Force, U. S. Headquarters
Aeronautical Chart & Information Center
Second and Arsenal
St. Louis 18, Missouri

ATTN: ACDEG-4

Air Force Office of Aerospace Research
Headquarters
Washington 25, D. C. (2)

ATTN: Major Philip J. Crossman (RROS)

Air Force Aerospace Research
Headquarters
Washington 25, D. C. (2)

ATTN: Lt. Col. James A. Fava (RROS)

Air Force Cambridge Research Laboratories
Electronic Systems Division
L. G. Hanscom Field
Bedford, Massachusetts

ATTN: Project Officer
System 477-L (ESH)

Air Force Cambridge Research Laboratories
Headquarters
L. G. Hanscom Field
Bedford, Massachusetts (5)

ATTN: Major Robert A. Gray
USAF

Air Force, Department of
Office of the Assistant Secretary of the Air Force
(Research and Development)
Washington 25, D. C.

ATTN: Mr. Franklin J. Ross

Air Force, Department of
Office of the Deputy Chief of Staff
Development
Washington 25, D. C.

ATTN: Lt. Col. G. T. Grottle
AFDSD/MS

Air Force Office of Aerospace Research
Commander
Tempo D
6th and Constitution Ave., S.W.
Washington 25, D. C.

Air Force Office of Scientific Research
Executive Director
Washington 25, D. C.

ATTN: SRG

Air Force Office of Scientific Research
Washington 25, D. C. (4)

ATTN: SRPG
Mr. William J. Best

Air Force Systems Command
Andrews Air Force Base
Washington 25, D. C. (15)

Air Force Systems Command
Andrews Air Force Base
Washington 25, D. C.

ATTN: Major J. C. Stokes, USAF

HQ USAF (AFTAC)
VELA Seismological Center
Washington, D. C. 20333 (5)

ATTN: TD-1, Lt. Col. Ridenour

University of Alaska
Geophysical Institute
College, Alaska

ATTN: Dr. Edward Berg

Alberta, University of
Calgary Campus
Calgary, Alberta, Canada

ATTN: Prof. K. Vozoff

Allied Research Associates, Inc.
43 Leon Street
Boston, Massachusetts

American Geological Institute
2101 Constitution Ave., N.W.
Washington, D. C.

ATTN: Linn Hoover

American Geological Institute
1444 N. Street, N. W.
Washington, D. C. 20005

ATTN: Editor, Geoscience Abstracts

ALPENS
10 Rue Claude Bernard
Paris V, France

ATTN: Prof. Y. Rocard

American University
Department of Earth Science
Washington, D. C., 20016

ATTN: Professor Paul Bauer

Arctic Institute of North America
3458 Redpath Street
Montreal 25, P. Q., Canada

ATTN: Mr. John C. Reed
Executive Director

Arms Control and Disarmament Agency
Project CLOUD GAP
Washington 25, D. C.

ATTN: Capt. E. M. Cappola

Arms Control and Disarmament Agency
Science and Technology Bureau
Room 5486, State Department
Washington 25, D. C.

ATTN: Dr. H. R. Meyers

Army
Signal Research and Development Laboratory, U. S.
Fort Monmouth, New Jersey

ATTN: Commanding Officer

Army, Department of the
Office of the Chief
Research and Development
OCS
Washington 25, D. C.

ATTN: Brig. Gen. David C. Lewis

Army Engineer Research and Development
Laboratories, U. S.
Fort Belvoir, Virginia

ATTN: Mine Detection Branch

Army Research Office
CM Duke Station
Durham, North Carolina

Atlantic Refining Company
4500 West Mockingbird Lane
Dallas, Texas

ATTN: Helen McKenzie
Librarian

Atomic Energy Commission, U. S.
Albuquerque Operations Office
P. O. Box 5400
Albuquerque, New Mexico

ATTN: Mr. R. E. Miller

Atomic Energy Commission, U. S.
Director
Division of Military Applications
Washington 25, D. C. (2)

ATTN: Brig. Gen. Delmar L. Crowson

Atomic Energy Commission, U. S.
Division of Military Applications
Chairman
Washington 25, D. C.

ATTN: Mr. Don Gale

Atomic Energy Commission
Division of Peaceful Nuclear Explosions
Chairman
Washington 25, D. C.

ATTN: Mr. John Kelly

Atomic Energy Commission
General Managers Office
Washington 25, D. C. (2)

ATTN: Mr. Allan M. Labowitz

Atomic Energy Commission
Technical Information Service Extension
Oakridge, Tennessee (2)

ATTN: Hugh Voress

Atomic Energy Establishment Trombay
Nuclear Physics Division
Seismology Section
Room No. 2 Apsara
Trombay, Bombay 74, India

Barringer, Limited
145 Belfield Road
Rexdale, Toronto, Canada

Roland F. Beers, Inc.
P. O. Box 23
Alexandria, Virginia

ATTN: Roland F. Beers

Bell Telephone Laboratories
Murray Hill, New Jersey

ATTN: Dr. Bruce P. Bogert

Bell Telephone Laboratories
Room 1A-218
Murray Hill, New Jersey

ATTN: Dr. John W. Tukey

Bell Telephone Laboratories
Whippany, New Jersey

ATTN: C. M. Brandaver
        Command Systems Dept.

Bell Telephone Laboratories, Inc.
Whippany, Laboratory
Whippany, New Jersey

ATTN: C. F. Weibusch

Blue Mountains Seismological Observatory
The Geotechnical Corporation
Baker, Oregon

ATTN: Station Manager

Group Captain John Rowlands, RAF
Atomic Coordinating Office
Room 427
British Defence Staffs
British Embassy
3100 Massachusetts Avenue, N.W.
Washington 8, D. C. (5)

British Petroleum Company Ltd.
Exploration Division
BP Research Center
Chertsey Road
Sunbury-on-Thames, Middlesex, England

ATTN: Manager

Observatoire de Geophysique
College Jean-de-Brebeuf
3200 Chemin Ste-Catherine
Montreal 26, Canada

ATTN: Prof. M. Buist, S.J.
        Director

Professor Dr. Hans Closs
Bundesanstalt fur Bodenforschung
Wiesenstrasse 1, Hanover 3
West Germany

Bureau of Mines, U. S.
Applied Physics Research Laboratory
College Park, Maryland

ATTN: Dr. Leonard Obert

Bureau of Ships, U. S.
Department of the Navy
Washington 25, D. C.

ATTN: Code 689D

Bureau of Ships, U. S.
Code 689D
Washington 25, D. C.

ATTN: Mr. Gambino

California Institute of Technology
Seismological Laboratory
220 North San Rafael Avenue
Pasadena, California

ATTN: Dr. Hugo Benioff

California Institute of Technology
Division of Engineering
Pasadena, California

ATTN: Dr. George W. Housner

California Institute of Technology
Seismological Laboratory
220 North San Rafael Avenue
Pasadena, California

ATTN: Dr. Frank Press

California Institute of Technology
Seismological Laboratory
220 N. San Rafael Avenue
Pasadena, California

ATTN: Dr. L. Knopoff

California Research Corporation
200 Bush Street
San Francisco, California

ATTN: Mr. R. S. Faull

California Research Laboratory
P. O. Box 446
La Habra, California

ATTN: Dr. A. Riley, Jr.

California, University of
Lawrence Radiation Laboratory
Livermore, California (2)

ATTN: Donald L. Springer
        Dr. Charles E. Violet

California, University of
Lawrence Radiation Laboratory
Livermore, California

ATTN: Dr. Kenneth M. Watson

California, University of
Seismograph Station
Berkeley, California 94720

ATTN: Prof. P. Byerly
        Dr. C. Lomnitz

California, University of
Lawrence Radiation Laboratory
Technical Information Division
P. O. Box 808
Livermore, California

ATTN: Clovis G. Craig

California, University of
La Jolla Laboratories
La Jolla, California

ATTN: Dr. Walter Munk

Seismological Laboratory
USC&GS, Sandia Base
Albuquerque, N. Mexico

Cambridge University
Department of Geodesy & Geophysics
Madingley Rise, Madingley Road
Cambridge, England (2)

ATTN: Sir Edward Bullard
        Dr. Maurice Hill

Canadian Defense Research Staff
2450 Massachusetts Avenue, N.W.
Washington 8, D. C. (5)

ATTN: Dr. C. E. Hubley

Carnegie Institution of Washington
Department of Terrestrial Magnetism
5241 Broadbranch Road, N.W.
Washington 15, D. C.

ATTN: Dr. John J. Steinhart

Century Geophysical Corporation
P. O. Box C
Admiral Station
Tulsa 15, Oklahoma

ATTN: Lewellyn Thomas

Commerce, Department of
Coast & Geodetic Survey, U. S.
Geophysics Division
Washington 25, D. C.

ATTN: Dr. Dean S. Carder

Commerce, Department of
Coast & Geodetic Survey, U. S.
Geophysics Division
Washington 25, D. C.

ATTN: Mr. J. Jordan

Commerce, Department of
Coast & Geodetic Survey, U. S.
Geophysics Division
Washington 25, D. C.

ATTN: Mr. Leonard Murphy

Commerce, Department of
Coast & Geodetic Survey, U. S.
Camp Mercury, Nevada

ATTN: T. H. Pierce

Commerce, Department of
Seismological Data Center
U. S. Coast and Geodetic Survey
Washington 25, D. C. (2)

ATTN: Director

Commerce, Department of
Coast & Geodetic Survey, U. S.
Seismological Laboratory
Sandia Base
Albuquerque, New Mexico

ATTN: Technical Director

Commerce, Department of
National Bureau of Standards, U. S.
Washington 25, D. C.

ATTN: Mr. Harry Matheson

Continental Oil Company
P. O. Drawer 293
Ponca City, Oklahoma

ATTN: Dr. John M. Crawford

Cornell University
Research and Advanced Studies
303 Day Hall
Ithaca, New York

ATTN: Dr. Frank A. Long
        Vice President

Cumberland Plateau Seismological Observatory
McMinnville, Tennessee

ATTN: Station Manager

Defense Atomic Support Agency
Department of Defense
Chief
Washington 25, D. C.

ATTN: Major J. Dickson

Defense Atomic Support Agency
Field Command
Sandia Base
Albuquerque, New Mexico

ATTN: Col. Conrad R. Peterson

Defense Atomic Support Agency
Headquarters
Washington 25, D. C.

ATTN: John G. Lewis

Defense Atomic Support Agency
Weapons Effects and Tests
Headquarters
Field Command
Sandia Base
Albuquerque, New Mexico

ATTN: FCWT
VELA UNIFORM Programs Officer

Defense, Department of
Office of the Assistant Secretary of Defense
for International Security Affairs
Washington, D. C.

ATTN: Mr. John McNaughton
Room 3E989

Defense, Department of
Office of the Assistant to the Secretary of
Defense of Atomic Energy
Washington 25, D. C.

ATTN: Col. Philip L. Hooper

Defense Documentation Center
Cameron Station
Alexandria, Virginia (20)

Defense, Department of
Office of the Director of Defense
Research & Engineering
The Pentagon
Washington 25, D. C.

ATTN: Director, Office of Atomic Programs

Director of Research and Development
Office of the Secretary of the Army
Washington 25, D. C.

ATTN: Lt. Col. William D. Sydnor

Dresser Electronics
SIE Division
P. O. Box 22187
Houston 27, Texas (2)

ATTN: Mrs. Mildred Beaman
Librarian

Dresser Electronics
SIE Division
P. O. Box 22187
Houston 27, Texas

ATTN: Mr. Howard A. Bond
Vice-Pres., Military Engineering

Dupont Company
Eastern Laboratory
Gibbstown, New Jersey

ATTN: Mr. A. B. Andrews
Explosives Department

Edgerton, Germeshausen, and Grier, Inc.
Director of Research
160 Brookline Drive
Boston, Massachusetts

ATTN: Clyde Dobbie

Edgerton, Germanshausen, and Grier, Inc.
160 Brookline Drive
Boston, Massachusetts

ATTN: Dr. Raymond C. O'Rourke

Edgerton, Germeshausen, and Grier, Inc.
160 Brookline Avenue
Boston, Massachusetts

ATTN: F. T. Strabala

Electro-Mechanics Company
P. O. Box 802
Austin 64, Texas

ATTN: Dr. Fred H. Morris

Engineer Research and Development Laboratory
Mines Detection Branch
Fort Belvoir, Virginia

ATTN: Mr. S. E. Dwornik

Engineering-Physics Company
5515 Randolph Street
Rockville, Maryland

ATTN: Mr. Vincent Cushing

The Superintendent
The Observatory
Eskdalemuir
Langholm, Dumfriesshire, Scotland

Ford Motor Company
2000 Rotunda Drive
Dearborn, Michigan

ATTN: Dr. Michael Ference

General Atronics Corporation
1200 East Mermaid Lane
Philadelphia, Pennsylvania 19118

ATTN: Mr. Joseph T. Underwood, III

General Dynamics Corporation
Electric Boat Division
Groton, Connecticut

ATTN: Mr. J. V. Harrington

General Electric Company
735 State Street
Santa Barbara, California

ATTN: Mr. Finn Dyolf Bronner
Defense Electronics Division

Geophysical and Polar Research Center
6021 South Highland Road
Madison 6, Wisconsin

ATTN: Director

Geophysical Service, Inc.
P. O. Box 35084
Dallas 35, Texas

ATTN: Dr. Saunders

Georgia Institute of Technology
Engineering Experiment Station
Atlanta, Georgia

ATTN: Mr. Frederick Bellinger, Chief
Materials Sciences Division

Georgia Institute of Technology
Engineering Experimental Station
Atlanta, Georgia

ATTN: Mr. John E. Husted
Research Scientist, Head

Geosciences, Inc.
P. O. Box 175
Lexington 73, Massachusetts

ATTN: Dr. Thomas Cantwell

Geotechnical Corporation
WMO
P. O. Box 2071
Lawton, Oklahoma (2)

ATTN: Station Director

Geotechnical Corporation
3401 Shiloh Road
P. O. Box 28277
Dallas 28, Texas (19)

ATTN: Dr. W. Heroy, Jr.

Graduate Research Center
P. O. Box 8478
Dallas 5, Texas

ATTN: Dr. A. L. Hales

Gravity Meter Exploration Co.
3621 W. Alabama Avenue
Houston 27, Texas

ATTN: Dr. Nelson Steeland

Gulf Research and Development Co.
Geophysical Research Division
P. O. Box 2038
Pittsburgh 30, Pennsylvania

ATTN: Dr. T. J. O'Donnell
Director

Harvard University
Department of Geology
Cambridge, Massachusetts

ATTN: Prof. L. Don Leet

Hawaii, University of
Hawaii Institute of Geophysics
Honolulu 14, Hawaii (2)

ATTN: Dr. Doak Cox, Prof. Woolard
Department of Earth Sciences

Hudson Laboratories of Columbia University
145 Palisade Street
Dobbs Ferry, New York

ATTN: Mr. Kenneth T. Morse

Hughes Aircraft Company
Communications Division
P. O. Box 90902
Airport Station
Los Angeles 45, California

Humble Oil and Research Labs.
Geophysics Department
P. O. Box 2180
Houston 1, Texas

ATTN: Dr. Lynn Howell

Illinois, University of
Department of Mining
Urbana, Illinois

ATTN: Dr. Adrian Scheidegger

Interior, Department of
Bureau of Mines, U. S.
Washington 25, D. C. (5)

ATTN: James Hill

Interior, Department of
Branch of Crustal Studies
U. S. Geological Survey
7580 W. 16th Street
Lakewood 15, Colorado

ATTN: Dr. George Keller

Interior, Department of
Branch of Crustal Studies
U. S. Geological Survey
7580 W. 16th Street
Lakewood 15, Colorado (5)

ATTN: Louis C. Pakiser

Interior, Department of
Geological Survey
Denver Federal Center
Denver 25, Colorado

ATTN: Dr. H. Roach

Interior, Department of
Office of the Science Advisor to the Secretary
Washington 25, D. C.

ATTN: Dr. Calhoun

Interior, Department of
U. S. Geological Survey
Room 4215, GSA Building
Washington 25, D. C. (2)

ATTN: Dr. William Thurston
Dr. Wayne Hall

Interior, Department of
Geological Survey
Branch of Military Geology
Washington 25, D. C. (3)

ATTN: Mrs. Mildred P. White

Institute for Defense Analyses
1666 Connecticut Avenue, N. W.
Washington 9, D. C.

ATTN: Classified Library

Institute for Defense Analyses
Research and Engineering Support Division
1666 Connecticut Avenue, N. W.
Washington, D. C.

ATTN: Mr. Al. Rubenstein

Instituto Geografico
y Catastral
General Ibanez 3
Madrid, Spain

ATTN: Dr. José M. Munuera

Isotopes, Inc.
123 Woodland Avenue
Westwood, New Jersey

ATTN: Dr. Bruno E. Sables

Itek Corporation
1450 Page Mill Road
Palo Alto, California

ATTN: Mr. Ed Lantz

Itek Laboratories
Lexington 73, Massachusetts

ATTN: Mr. Robert Fleming

Jersey Production Research Company
1133 North Lewis Avenue
Tulsa 10, Oklahoma

ATTN: Mr. Dan Skelton

Jersey Production Research Company
1133 North Lewis Avenue
Tulsa 10, Oklahoma

ATTN: Mr. F. K. Levin

John Carroll University
Cleveland 18, Ohio

ATTN: Rev. H. F. Birkenhauer, S.J.

John Carroll University
Cleveland 18, Ohio

ATTN: Dr. Edward Walter

Jordskelstasjonen
University of Bergen
Bergen, Norway

VIA: Office of the Economic Counselor
U. S. Embassy
Drammesveien, Oslo, Norway

LaCoste and Romberg
Austin, Texas

ATTN: Mr. Lucian J. B. LaCoste

Lamont Geological Observatory
Columbia University
Palisades, New York

ATTN: Dr. Maurice Ewing

Lamont Geological Observatory
Columbia University
Palisades, New York

ATTN: Dr. K. L. Hunkins

Lamont Geological Observatory
Columbia University
Palisades, New York (2)

ATTN: Library

Lamont Geological Observatory
Columbia University
Palisades, New York

ATTN: Dr. Jack E. Oliver

Lebel, Jean
CLES
6 Avenue Daniel Leseur
Paris 7a, France

Los Alamos Scientific Laboratory
Los Alamos, New Mexico

ATTN: Dr. Conrad L. Longmire

Mandrel Industries, Inc.
Electro-Technical Labs Division
5234 Glenmont Drive
P. O. Box 363060
Houston 36, Texas

ATTN: Dr. R. N. Ostreim

Mandrel Industries, Inc.
Research Division
1025 S. Shepard
Houston 19, Texas

ATTN: Dr. Lewis M. Mott-Smith

Massachusetts Institute of Technology
Department of Electrical Engineering
Cambridge, Massachusetts

ATTN: Prof. J. Ruina

Massachusetts Institute of Technology
Lincoln Laboratory
Lexington 73, Massachusetts

ATTN: Dr. Paul Green

Massachusetts Institute of Technology
Lincoln Laboratory
Lexington 73, Massachusetts

ATTN: Librarian

Massachusetts Institute of Technology
Department of Earth Sciences
Cambridge 39, Massachusetts

ATTN: Prof. S. M. Simpson

Melpar, Inc.
Technical Information Center
3000 Arlington Boulevard
Falls Church, Virginia

ATTN: P. D. Vachon

Melpar, Inc.
Applied Science Division
11 Galen Street
Watertown 72, Massachusetts

ATTN: Mrs. Lorrine Nazzaro
Librarian

Meteorological Office (M. O. 14)
London Road, Bracknell
Berkshire, England

ATTN: The Director-General

Minnesota, University of
Institute of Technology
School of Mines and Metallurgy
Minneapolis 14, Minnesota

ATTN: Prof. Harold M. Mooney
Geophysics

Minneapolis-Honeywell Company
Heiland Division
Denver, Colorado

ATTN: Mr. Vohn Paul
Director of Magnetic Tape Division

The MITRE Corporation
Box 208
Bedford, Massachusetts 01730

ATTN: R. B. Smaller

MOHOLE Project
National Academy of Sciences
2101 Constitution Avenue, N.W.
Washington 25, D. C.

ATTN: Executive Secretary

National Bureau of Standards
Boulder Laboratories
Boulder, Colorado

ATTN: Mrs. Victoria S. Baker, Librarian

National Engineering Science Company
1711 South Fair Oaks Avenue
Pasadena, California

ATTN: Dr. N. D. Baratynski

National Engineering Science Company
1711 South Fair Oaks
Pasadena, California

ATTN: Dr. J. F. Hook

National Science Foundation
1951 Constitution Avenue, N.W.
Washington, D. C.

ATTN: Dr. Roy E. Hanson

National Science Foundation
Office of Antarctic Programs
1951 Constitution Avenue, N.W.
Washington 25, D. C.

ATTN: Information Officer

Director
National Security Agency
Fort George G. Meade, Maryland

ATTN: C3/TDL (Room 2C087)
Miss Jean Creswell

U. S. Naval Radiological Defense Laboratory
San Francisco 24, California

ATTN: Mr. E. R. Bowman
Head, Library Branch

U. S. Naval Radiological Defense Laboratory
San Francisco 24, California

ATTN: Mr. Ken Sinclair

Naval Research Laboratory
Washington 25, D. C.

ATTN: The Librarian

Navy Department
Bureau of Ships
Washington 25, D. C.

ATTN: Code 362 B

Navy, Department of
Office of the Deputy Chief of Naval Operations
(Development)
Washington 25, D. C.

ATTN: Mr. W. Magnitizky
Op-07T

Navy, Director of
Office of the Deputy Chief of Naval Operations
(Development)
Op-75
Washington 25, D. C.

Navy, Department of
Office of Naval Research
Washington 25, D. C. (5)

ATTN: James W. Winchester
        Code 418

Navy Electronics Laboratory, U. S.
Director
San Diego 52, California

ATTN: Code 2350

Navy Electronics Laboratory, U. S.
Point Loma Laboratory
San Diego, California

ATTN: Charles Johnson

Director
Navy Electronics Laboratory
San Diego 52, California

ATTN: Mr. T. McMillian

Navy Oceanographic Office, U. S.
The Hydrographer
Washington 25, D. C.

Navy Radiological Defense Lab., U. S.
Director
San Francisco 24, California

ATTN: Dr. Eugene Cooper

Navy Radiological Defense Laboratory
Hunters Point
Building 815
San Francisco, California

ATTN: Dr. L. Gevantman

New Mexico, University of
Albuquerque, New Mexico

ATTN: Dr. H. L. Walter
        Director of Research

North American Aviation (S+ID)
12214 Lakewood Boulevard
Downey, California (3)

ATTN: Mr. Robert Fowler
        Dept. 197-330

ATTN: D. T. Hodder
ATTN: Mr. Rauol Choate

Nortronics
Geophysics Research Group
77 A Street
Needham Heights 94, Massachusetts

ATTN: Mr. Paul R. Miles

Osservatorio Geoficico Sperimentale
Viale R. Gessi
Trieste, Italy

ATTN: Prof. C. Morcelli

The Ohio State University Research Foundation
1314 Kinnear Road
Columbus 12, Ohio

ATTN: Dr. Robert C. Stephenson
        Executive Director

Oklahoma, The University of
Research Institute
Norman, Oklahoma

ATTN: Dr. Norman Ricker

Oregon State University
Department of Oceanography
Corvallis, Oregon

ATTN: Dr. P. Dehlinger

Oregon State University
Department of Oceanography
Corvallis, Oregon

ATTN: Dr. Joe Berg

Pennsylvania State University
University Park, Pennsylvania

ATTN: Dr. B. F. Howell, Jr.

PETTY Geophysical Engineering Co.
P. O. Drawer 2061
San Antiono 6, Texas

ATTN: J. O. Parr, Jr.

Phillips Petroleum Company
Bartelsville, Oklahoma

ATTN: Mr. Harold L. Mendenhall
        District Geophysicist

Planetary Sciences, Inc.
501 Washington Street
P. O. Box 561
Santa Clara, California

ATTN: Dr. William Adams

Prengle, Dukler, and Crump, Inc.
5417 Crawford Street
Houston 4, Texas

ATTN: Dr. Clark Goodman

Princeton University
Physics Department
Princeton, New Jersey

ATTN: Dr. Val L. Fitch

Pure Oil Company
Research Laboratories
Crystal Lake, Illinois

ATTN: Dr. Ira Cram, Jr.

Radio Corporation of America
David Sarnoff Research Center
Princeton, New Jersey

ATTN: Dr. D. S. McCoy

Rand Corporation, The
1700 Main Street
Santa Monica, California

ATTN: Dr. Richard Latter

Raytheon Company
Missile and Systems Division
Bedford, Massachusetts

ATTN: Mr. C. C. Abt

Rensselaer Polytechnic Institute
Troy, New York

ATTN: Mr. R. B. Finch
        Director of Research

Rensselaer Polytechnic Institute
Troy, New York

ATTN: Dr. Samuel Katz

Research Institute of National Defense
Stockholm 80, Sweden

ATTN: Dr. Ulf A. Ericsson

VIA: Office of the Science Attache
        U. S. Embassy
        Stockholm, Sweden

University of Rhode Island
Kingston, Rhode Island

ATTN: Professor Kane

Rice University
Houston 1, Texas

ATTN: Prof. J. Cl. DeBremaecker
        Dept. of Geology

Sandia Corporation
Division 7000
Sandia Base
Albuquerque, New Mexico

ATTN: Mr. G. A. Fowler

Sandia Corporation
Sandia Base
Albuquerque, New Mexico

ATTN: William R. Perret

Saskatchewan, University of
Saskatoon
Saskatchewan, Canada

ATTN: Dr. James Mawdsley

Seismic Data Center
P. O. Box 334
Alexandria, Virginia (6)

ATTN: Dr. Van Nostrand

Seismograph Service Corporation
P. O. Box 1590
Tulsa, Oklahoma

ATTN: Dr. James E. Hawkins

Seismological Laboratory
Uppsala, Sweden

ATTN: Dr. Markus Båth

Shell Development Lab.
P. O. Box 481
Houston 1, Texas

ATTN: Dr. Sidney Kaufman

Sinclair Research Inc.
P. O. Box 3006, Whittier Station
Tulsa, Oklahoma

ATTN: Mr. John Bemrose

South Carolina, University of
Columbia, South Carolina

ATTN: Professor O. Scheutte
        Head, Dept. of Physics

Southern Methodist University
Department of Geology
Dallas, Texas

ATTN: Dr. Eugene T. Herrin

Southwest Research Institute
8500 Culebra Road
San Antonio 5, Texas

Special Assistant to the President for
        Science and Technology
Office of the Executive Office Building
The White House
Washington 25, D. C.

ATTN: Mr. Spurgeon M. Keeny, Jr.

Sperry Rand Research Center
Sudbury, Massachusetts

ATTN: Mr. Alan Steeves
        Librarian

W. F. Sprengnether Instrument Co., Inc.
4567 Swan Avenue
St. Louis 10, Missouri

ATTN: Mr. R. F. Hautly

Stanford Research Institute
Menlo Park, California

ATTN: Dr. Allen Peterson

Stanford Research Institute
Menlo Park, California

ATTN: L. M. Swift

Stanford University
Department of Geophysics
Stanford, California

ATTN: Prof. George F. Thompson

Stanford Research Institute
Building 108
Menlo Park, California

ATTN: Dr. Robert B. Vaile, Jr.
      Director, Physics Division

Stanford Research Institute
Menlo Park, California

ATTN: Mr. E. C. Wood
      Manager, Geophysics Dept.

State, Department of
Arms Control and Disarmament Agency
Washington 25, D. C. (2)

ATTN: Bureau of International Relations

State, Department of
Arms Control and Disarmament Agency
Washington 25, D. C.

ATTN: Research Reference Staff

State, Department of
Office of International Scientific Affairs
Washington 25, D. C.

ATTN: Dr. A. Rollefson

St. Louis University
The Institute of Technology
3621 Olive Street
St. Louis 8, Missouri

ATTN: Dr. Carl Kisslinger

St. Louis University
Department of Geophysics
3621 Olive Street
St. Louis 8, Missouri

ATTN: Dr. William Stauder, S.J.

Strategic Air Command
(OAWS)
Headquarters
Offutt Air Force Base, Nebraska (2)

Sydney, University of
Department of Mathematics
Sydney, Australia

ATTN: Dr. Keith Bullen

Tenneco Oil and Gas Co.
P. O. Box 18
Houston 1, Texas

ATTN: Lynn Ervin

Texaco, Inc.
Research and Technical Department
P. O. Box 509
Beacon, New York

ATTN: Dr. L. C. Roess

Texas, University of
Defense Research Laboratories
P. O. Box 8029
Austin 12, Texas

ATTN: Mr. Joe Collins

Texas, University of
Austin 12, Texas

ATTN: Prof. W. T. Muehlberger
      Dept. of Geology

Tonto Forest Seismological Observatory
P. O. Box 337
Payson, Arizona

ATTN: Mr. Allen M. Rugg, Jr.

Toronto, University of
Department of Physics
Toronto 5, Canada

ATTN: Prof. J. T. Wilson

Texas Instruments, Inc.
Science Services Division
6000 Lemmon Avenue
P. O. Box 5621
Dallas, Texas 75222 (7)

ATTN: R. A. Arnett

Uinta Basin Seismological Observatory
Vernal, Utah

ATTN: Station Manager

United ElectroDynamics, Inc.
DATDC
300 N. Washington
Alexandria, Virginia

ATTN: E. A. Flinn

United ElectroDynamics, Inc.
DATDC
300 N. Washington
Alexandria, Virginia

ATTN: Mr. J. Griffin

United ElectroDynamics, Inc.
DATDC
300 N. Washington
Alexandria, Virginia

ATTN: Ted Winston

United Kingdom Atomic Energy Authority
Blacknest Brimpton, Near Reading
Berkshire, England

ATTN: Dr. Eric Carpenter

Virginia Polytechnic Institute
Department of Geology
Blacksburg, Virginia

ATTN: Professor Charles Sears

University of Utah
Department of Geophysics
Mines Building
Salt Lake City, Utah

ATTN: Professor Kenneth L. Cook

University of Wisconsin
Geophysical and Polar Research Center
6021 South Highland Road
Madison 6, Wisconsin

ATTN: Director

University of Witwatersrand
Bernard Price Institute of Geophysical Research
Johannesburg, South Africa

ATTN: Director

U. S. Geological Survey
345 Middlefield Road
Menlo Park, California

ATTN: Librarian

U. S. Geological Survey
Assistant Chief Geologist for Engineering Geology
GSA Building
Washington 25, D. C.

ATTN: V. R. Wilmarth

U. S. Geological Survey
Branch of Astrogeology
Box 1906
Flagstaff, Arizona 86002

ATTN: Dr. Joel S. Watkins

Waterways Experiment Station
Jackson, Mississippi

ATTN: Mr. James Polatty

Waterways Experiment Station, U. S.
Vicksburg, Mississippi

ATTN: Librarian

Weizmann Institute of Science
Post Office Box 26
Rehovoth, Israel

ATTN: Prof. C. L. Pekeris

Western Geophysical Corporation
933 N. LaBrea Street
Los Angeles 38, California

ATTN: Mr. Carl H. Savit

Weston Observatory
Weston 93, Massachusetts

ATTN: Rev. Daniel Linehan, S.J.

Xavier University
Cincinnati, Ohio

ATTN: Rev. E. A. Bradley, S.J.

AD   Div. 2/10

Inst. of Science and Technology, U. of Mich., Ann Arbor
WASHINGTON CONFERENCE PROCEEDINGS: A RE-
VIEW OF BROADBAND SEISMOGRAPHS TO INCLUDE
DIGITAL SEISMOGRAPHS. Report of VESIAC. Oct. 64.
107 p. incl. tables, figs., refs.
(Report No. 4410-77-X)
(Contract SD-78)   Unclassified Report

This report publishes a collection of papers presented
at a VESIAC Special Study Conference, held 18-19 No-
vember 1963, on recent developments in wideband seis-
mic recording. Emphasis is placed on advances in digi-
tal recording and problems related to digital record-
ing systems. A related report is included on a pres-
sure-sensitive transducer, known as the "Solion
Transducer," applicable to hydroacoustic sensing.
                                            (over)

UNCLASSIFIED

I.   VESIAC
II. Advanced Research Proj-
       ects Agency
III. Contract SD-78

Defense
Documentation Center
UNCLASSIFIED

AD   Div. 2/10

Inst. of Science and Technology, U. of Mich., Ann Arbor
WASHINGTON CONFERENCE PROCEEDINGS: A RE-
VIEW OF BROADBAND SEISMOGRAPHS TO INCLUDE
DIGITAL SEISMOGRAPHS. Report of VESIAC. Oct. 64.
107 p. incl. tables, figs., refs.
(Report No. 4410-77-X)
(Contract SD-78)   Unclassified Report

This report publishes a collection of papers presented
at a VESIAC Special Study Conference, held 18-19 No-
vember 1963, on recent developments in wideband seis-
mic recording. Emphasis is placed on advances in digi-
tal recording and problems related to digital record-
ing systems. A related report is included on a pres-
sure-sensitive transducer, known as the "Solion
Transducer," applicable to hydroacoustic sensing.
                                            (over)

UNCLASSIFIED

I.   VESIAC
II. Advanced Research Proj-
       ects Agency
III. Contract SD-78

Defense
Documentation Center
UNCLASSIFIED

AD   Div. 2/10

Inst. of Science and Technology, U. of Mich., Ann Arbor
WASHINGTON CONFERENCE PROCEEDINGS: A RE-
VIEW OF BROADBAND SEISMOGRAPHS TO INCLUDE
DIGITAL SEISMOGRAPHS. Report of VESIAC. Oct. 64.
107 p. incl. tables, figs., refs.
(Report No. 4410-77-X)
(Contract SD-78)   Unclassified Report

This report publishes a collection of papers presented
at a VESIAC Special Study Conference, held 18-19 No-
vember 1963, on recent developments in wideband seis-
mic recording. Emphasis is placed on advances in digi-
tal recording and problems related to digital record-
ing systems. A related report is included on a pres-
sure-sensitive transducer, known as the "Solion
Transducer," applicable to hydroacoustic sensing.
                                            (over)

UNCLASSIFIED

I.   VESIAC
II. Advanced Research Proj-
       ects Agency
III. Contract SD-78

Defense
Documentation Center
UNCLASSIFIED

AD   Div. 2/10

Inst. of Science and Technology, U. of Mich., Ann Arbor
WASHINGTON CONFERENCE PROCEEDINGS: A RE-
VIEW OF BROADBAND SEISMOGRAPHS TO INCLUDE
DIGITAL SEISMOGRAPHS. Report of VESIAC. Oct. 64.
107 p. incl. tables, figs., refs.
(Report No. 4410-77-X)
(Contract SD-78)   Unclassified Report

This report publishes a collection of papers presented
at a VESIAC Special Study Conference, held 18-19 No-
vember 1963, on recent developments in wideband seis-
mic recording. Emphasis is placed on advances in digi-
tal recording and problems related to digital record-
ing systems. A related report is included on a pres-
sure-sensitive transducer, known as the "Solion
Transducer," applicable to hydroacoustic sensing.
                                            (over)

UNCLASSIFIED

I.   VESIAC
II. Advanced Research Proj-
       ects Agency
III. Contract SD-78

Defense
Documentation Center
UNCLASSIFIED

AD

UNCLASSIFIED

DESCRIPTORS

Seismographs
Recording systems
Seismic waves
Computers and data
systems

UNCLASSIFIED

AD

UNCLASSIFIED

DESCRIPTORS

Seismographs
Recording systems
Seismic waves
Computers and data
systems

UNCLASSIFIED

+

AD

UNCLASSIFIED

DESCRIPTORS

Seismographs
Recording systems
Seismic waves
Computers and data
systems

UNCLASSIFIED

AD

UNCLASSIFIED

DESCRIPTORS

Seismographs
Recording systems
Seismic waves
Computers and data
systems

UNCLASSIFIED

AD   Div. 2/10   UNCLASSIFIED

Inst. of Science and Technology, U. of Mich., Ann Arbor   I.   VESIAC
WASHINGTON CONFERENCE PROCEEDINGS: A RE-   II. Advanced Research Proj-
VIEW OF BROADBAND SEISMOGRAPHS TO INCLUDE   ects Agency
DIGITAL SEISMOGRAPHS. Report of VESIAC. Oct. 64.   III. Contract SD-78
107 p. incl. tables, figs., refs.
(Report No. 4410-77-X)
(Contract SD-78)   Unclassified Report

This report publishes a collection of papers presented
at a VESIAC Special Study Conference, held 18-19 No-
vember 1963, on recent developments in wideband seis-
mic recording. Emphasis is placed on advances in digi-
tal recording and problems related to digital record-
ing systems. A related report is included on a pres-
sure-sensitive transducer, known as the "Solion
Transducer," applicable to hydroacoustic sensing.
                                              (over)

                        Defense
                 Documentation Center
                   UNCLASSIFIED

AD   Div. 2/10   UNCLASSIFIED

Inst. of Science and Technology, U. of Mich., Ann Arbor   I.   VESIAC
WASHINGTON CONFERENCE PROCEEDINGS: A RE-   II. Advanced Research Proj-
VIEW OF BROADBAND SEISMOGRAPHS TO INCLUDE   ects Agency
DIGITAL SEISMOGRAPHS. Report of VESIAC. Oct. 64.   III. Contract SD-78
107 p. incl. tables, figs., refs.
(Report No. 4410-77-X)
(Contract SD-78)   Unclassified Report

This report publishes a collection of papers presented
at a VESIAC Special Study Conference, held 18-19 No-
vember 1963, on recent developments in wideband seis-
mic recording. Emphasis is placed on advances in digi-
tal recording and problems related to digital record-
ing systems. A related report is included on a pres-
sure-sensitive transducer, known as the "Solion
Transducer," applicable to hydroacoustic sensing.
                                              (over)

                        Defense
                 Documentation Center
                   UNCLASSIFIED

AD   Div. 2/10   UNCLASSIFIED

Inst. of Science and Technology, U. of Mich., Ann Arbor   I.   VESIAC
WASHINGTON CONFERENCE PROCEEDINGS: A RE-   II. Advanced Research Proj-
VIEW OF BROADBAND SEISMOGRAPHS TO INCLUDE   ects Agency
DIGITAL SEISMOGRAPHS. Report of VESIAC. Oct. 64.   III. Contract SD-78
107 p. incl. tables, figs., refs.
(Report No. 4410-77-X)
(Contract SD-78)   Unclassified Report

This report publishes a collection of papers presented
at a VESIAC Special Study Conference, held 18-19 No-
vember 1963, on recent developments in wideband seis-
mic recording. Emphasis is placed on advances in digi-
tal recording and problems related to digital record-
ing systems. A related report is included on a pres-
sure-sensitive transducer, known as the "Solion
Transducer," applicable to hydroacoustic sensing.
                                              (over)

                        Defense
                 Documentation Center
                   UNCLASSIFIED

AD   Div. 2/10   UNCLASSIFIED

Inst. of Science and Technology, U. of Mich., Ann Arbor   I.   VESIAC
WASHINGTON CONFERENCE PROCEEDINGS: A RE-   II. Advanced Research Proj-
VIEW OF BROADBAND SEISMOGRAPHS TO INCLUDE   ects Agency
DIGITAL SEISMOGRAPHS. Report of VESIAC. Oct. 64.   III. Contract SD-78
107 p. incl. tables, figs., refs.
(Report No. 4410-77-X)
(Contract SD-78)   Unclassified Report

This report publishes a collection of papers presented
at a VESIAC Special Study Conference, held 18-19 No-
vember 1963, on recent developments in wideband seis-
mic recording. Emphasis is placed on advances in digi-
tal recording and problems related to digital record-
ing systems. A related report is included on a pres-
sure-sensitive transducer, known as the "Solion
Transducer," applicable to hydroacoustic sensing.
                                              (over)

                        Defense
                 Documentation Center
                   UNCLASSIFIED

AD

UNCLASSIFIED

DESCRIPTORS

Seismographs
Recording systems
Seismic waves
Computers and data
    systems

UNCLASSIFIED

+

AD

UNCLASSIFIED

DESCRIPTORS

Seismographs
Recording systems
Seismic waves
Computers and data
    systems

UNCLASSIFIED

AD

UNCLASSIFIED

DESCRIPTORS

Seismographs
Recording systems
Seismic waves
Computers and data
    systems

UNCLASSIFIED

AD

UNCLASSIFIED

DESCRIPTORS

Seismographs
Recording systems
Seismic waves
Computers and data
    systems

UNCLASSIFIED